Fabrication of Quantum Dot Encoded Silica Beads for High-throughput Screening Applications

By

Gerson Aguirre

A Dissertation Submitted to the Graduate Faculty in Chemistry in Partial Fulfillment of the Requirement for the Degree of Doctor of Philosophy

THE CITY UNIVERSITY OF NEW YORK

2011

This manuscript has been read and accepted for the Graduate Faculty in Chemistry in satisfaction of the dissertation requirement for the degree of Doctor of Philosophy.

_____	_____
Date	Prof. Alex Couzis (Mentor)
_____	_____
Date	Prof. Mahesh Lakshman Executive Officer
	Prof. Charles Maldarelli (Co-Mentor) _____
	Prof. Ilona Kretzschmar _____
	Prof. Charles Drain _____
	Prof. Lane Gilchrist _____
	Supervisory Committee

THE CITY UNIVERSITY OF NEW YORK

ABSTRACT

Fabrication of Quantum Dot Encoded Silica Beads for High-throughput Screening Applications

By

Gerson Aguirre

Advisors: Professors Alex Couzis and Charles Maldarelli

Department of Chemical Engineering

City College of City University of New York

The focus of this research is on the development of optically barcoded silica gel microbeads, synthesized to be used in high throughput screening platforms, using suspension methods for bead synthesis developed specifically for rapid gelation. In suspension methods for particle manufacture, precursor droplets are first formed in a continuous phase immiscible with the droplet phase. The droplets are then solidified into particles. Silica is chosen as the bead material because it can very easily be functionalized to anchor probe molecules which is necessary to function as a capture element in high throughput screening applications. The optical code embedded into the microbeads consists of the spectral signature (the emission spectrum) of a collection of luminescent

species. In particular, for this study, multicolor semiconductor nanocrystals or quantum dots (QDs) are used. Each type of QD emits electromagnetic waves at a set wavelength (color), and sets of QDs will be incorporated in differing quantities to form the code. The encoding QDs are dispersed in the pre-gel droplet phase, and are surface functionalized so as not to partition in the continuous phase. In this way, the QDs are effectively trapped in the droplets as they gel to microbeads, which allows for a quantitative loading necessary for optical coding.

In this study, the suspension process for encoded silica bead production is implemented using a batch stirring method for forming the emulsion, and a flow-focusing microfluidic device. The later is used to generate uniformally sized droplets of the pre-gel phase, thus insuring a monodisperse size distribution that is useful for high throughput screening platforms. The gelation of the silica precursor droplets uses an amine catalyst as an accelerant, and thus eliminates the post-production necessary in existing methodologies for obtaining silica beads.

Confocal laser scanning microscopy (CLSM) is used to record the spatial distribution of the nanocrystal fluorescence in the beads and the emission spectra (the barcode). Two colors of QDs were used to create a prototype barcode, and Forster Resonance Energy Transfer (FRET) between these colors was used in addition to the spatial distribution of the fluorescence to infer the aggregation of the nanocrystals in their new silica gel environment. A comparison of the photoluminescence (PL) profiles of the barcoded silica beads demonstrate that indeed resonant energy transfer is occurring, and the crystals do aggregate. FRET shifts in the PL profiles can be attributed to poor dispersability issues in the precursor solution and can in some instances- due to extent of

unfavorable conditions for the surface molecules of QDs with the solvent- limit our ability to generate a full compliment of barcodes. Untimely ionization of catalyst, and degree of which, and poor solvability of hydrophylically surface functionalized nanocrystals leads to their poor performance as entrapped luminescing signals.

Contents

List of Tables

List of Figures

Chapter 1

Introduction

The impetus for this thesis originates primarily in the pharmaceutical and medical diagnostics/life sciences communities, both of which require platforms for screening the binding interactions of many biomolecules at one time against other molecules (high throughput screening). In the pharmaceutical industry, different variants of a potential drug molecule designed to bind to a particular receptor to exert its therapeutic effect are developed by combinatorial chemistry protocols. These candidates then need to be assayed against the intended receptor to identify which variant is the most effective at binding to the receptor. A platform for displaying the cell surface membrane receptors to other biomolecules, e.g. glycoprotein receptors, antigens, protein membranes, etc. is necessary to identify a lead candidate. In medical diagnostics, diseases are often diagnosed by identifying markers in the blood stream; assaying a blood sample with molecules that each bind to only one of these markers and identifying which markers are bound allows a screening for several diseases at once.

To fulfill the needs of high-throughput screening, protein microarrays have very rapidly become an area of active and emerging technology (for reviews see Walter et al.[2], Kodadek[3], Lal et al.[4], and Yeo[5]. In the usual design, different proteins or binding partners are printed by fluidic dispensing from a robotic spotter into designated positions (spots) to form a spatially indexed array of capture molecules. The array is covered with an analyte solution containing potential binding targets. After allowing binding events to proceed, the surface is washed and analyzed to identify the conjugation of targets to the surface displayed capture elements. The identification is undertaken by a spatially

resolved assay; usually targets are labeled with a fluorophore whose signature fluorescence is detected at the positions where the printed capture molecule has bound the target. Robotic fluid handling prints spots with sizes of the order of 100 μm – 1 mm in diameter, with the spots separated by similar dimensions and arrayed on an active area of 1 cm x 1cm. Hence the active area contains upwards of thousands of capture elements, so a single assay can interrogate thousands of receptor-ligand interactions at once, with the added advantage that a minimal amount of target analyte is used (approximately one milliliter to cover the 1 cm x 1 cm active area). Hence the microarray design and efficiency are developed specifically for high throughput analysis and they make use of minimum material while still generating large amounts of information about their system. Protein chip designs are mainly used for high efficiency and additionally high sensitivity of a protein analysis by fluidic spotting techniques; the means by which they have become such a powerful detection device has to do with parallel determination (multiplexing) screening of thousands if not millions of interactions by automated means. The delivery system however limits their use as shearing may damage the proteins, at the delivery stage, or loss of activity and molecular shape at the solid-phase ligand binding site by anchoring the proteins to a substrate. Another limitation is the solubility and immobilization of membrane proteins like antibodies that comprise a huge percentage of the proteome in which the important aim is to quantify the detection of proteins in different conditions.

Microbead-based screening platforms are a potentially revolutionary format for high throughput assaying. In this platform, the drug candidates or molecules that bind to the disease-identifying markers (the “probes”) are conjugated to micron-sized beads. A

necessary component for successful multiplexed screening lies on the ability to allow the beads to display a high-density area for receptors to become active. These beads are encoded to identify the probe on the bead surface. The beads are incubated in an analyte solution of a blood sample of potential markers, or a receptor for a drug candidate (the "targets"). Identifying the binding of the targets to the probes on the beads is usually undertaken by pre-labeling the targets, usually with unique fluorescent labels. After incubation, the beads are flowed through a flow cytometer or arrayed and tethered on a surface of functionalized wells that are of the same length scale, and their fluorescence measured to identify hits or binding events. These wells are etched in a silicon wafer in a square grid pattern. The label on the beads that have bound targets is then read to identify the probe on the bead. If the bead is labeled with a spectral code consisting of fluorescing species that emit a unique spectrum, the label can be read with the same fluorescence detection spectrometer used to identify the binding events.

The key to the technology is the fabrication of the spectrally labeled microbeads. These are required to have three key properties: (1) the beads should be approximately 10-100 microns in size to miniaturize the screening, and to be compatible with flow cytometers and wafer micro-arrays. The size distribution of the beads should be very narrow so that the spectral label is not distorted. (2) The beads should be encoded with a scheme that allows for a large encoding capacity. (3) The beads should be made of a material that allows for easy probe conjugation. (4) The encoding fluorophores should be incorporated in the synthesis step, where the crystals become permanently embedded in the fabric of the structure, and the spectral label is steadfast. The fabrication of beads

with the above properties has proved to be very difficult, and is the primary impediment to the advancement of this high throughput bead based screening technology.

This thesis develops synthesis routes to fabricate beads that meet all of these requirements. Silica is chosen as the bead material because it can very easily be functionalized to anchor probe molecules. Semi-conductor quantum dots (QDs) are embedded into the beads in order to encode the beads with a spectral label for using the beads for high throughput screening applications. While current technologies for spectral encoding have used organic fluorophores, QDs are employed in this study because of their significant advantages over organic fluorophores for spectral encoding purposes. QDs are more luminous than organic fluorophores. In addition, their narrow and symmetrical emission spectrum is a function of their size (quantum confinement effect found mainly in CdSe/ZnS core shell QDs) so that by varying the size a large number of crystals with unique emission spectra can be fabricated. Combinations of QDs with different sizes can be used to form an encoding label with high encoding capacity for a set of colors (c) and a set of intensities (i). The use of ten intensity levels and six colors can theoretically give the ability to code 1 million protein sequences or other biological macromolecule.

The synthesis routes developed in this thesis are based on an emulsion/suspension procedure in which liquid droplets containing a silica precursor, tetra-alkoxysilane, as a starting material is dispersed as an emulsion in a continuous phase that is immiscible with the droplet phase. A gelation process is then implemented to condense the droplets into silica microbeads. The known chemistry of gelation of the tetra-alkoxysilane precursor to silica is a two-step process of hydrolysis to form silanols, and siloxane bridging of the

silanols to gel the silanols. Hydrolysis is accelerated under acid conditions, while siloxane bridging is accelerated under basic conditions. Optimal control of the pH during the process allows for a rapid synthesis of silica from the alkoxide precursor. The quantum dots are embedded in the beads by initially dispersing them in the precursor liquid. The QDs used are surface functionalized so that they are readily dispersed in the droplet liquid and do not disperse into the continuous phase of the emulsion which is immiscible with the droplet phase. This insures that the spectral label derived from the composition of the QDs in each bead is the same for each bead fabricated, a necessary requirement for using the QD encapsulated beads for labeling. The fact that the emulsion/suspension route easily facilitates the incorporation of the quantum dots in the microbeads in a way that insures that the concentration of the QDs is the same in each bead is what makes this route attractive for the synthesis of encoded beads.

This thesis studies two synthesis routes:

In the first synthesis route, the emulsion is created by the batch stirring of the precursor droplets with dispersed QDs into a continuous phase. The droplets are a neat hydrophobic solution of a tetra-alkoxysilane precursor, and the continuous phase is an aqueous solution. The dispersed QDs are functionalized with a hydrophobic surface coat so they can be dispersed in the neat hydrophobic tetra-alkoxysilane solution, and do not disperse in the aqueous solution. The droplets gel by transport of water into the tetra-alkoxysilane droplets, which hydrolyzes the silane to silanols. The silanols then bridge by formation of siloxane linkages to gel the droplet. To accelerate the gelation, a novel chemistry is used in which octylamine, dissolved in the droplet phase alongside the tetra-alkoxysilane, is used as a basic catalyst to increase the pH after hydrolysis and accelerate

the gelation process. Encoded silica particles in the size range of 10-100 μm are made with a wide size distribution due to the wide size distribution realized in the formation of the emulsion. Both hollow and completely gelled particles are made. A prototype code is constructed by embedding quantum dots with two colors at a prescribed ratio and concentration. A study of the photoluminescence (PL) spectra of the two color QD encoded silica beads using confocal fluorescence microscopy demonstrated that the spectral code can easily be read from the beads. Comparing the PL spectrum in the bead with a reference spectrum in which the nanocrystals are in a known unaggregated state indicated significant Forster Resonance Energy Transfer (FRET) between the two QDs. This energy transfer is caused by aggregation of the nanoparticles during the gelation, and this is confirmed by the spatial distribution of the fluorescence in the bead as recorded by the confocal microscope.

The manufacture of *monodsiperse* silica particles (requisite for the use of the encoded microbeads for screening applications) using the batch stirring for forming the emulsion is a difficult task since this process produces droplets with a very non-uniform size distribution. To solve this problem, in the second synthesis route, a microfluidics method is used to create the precursor droplets. In this route, the precursor droplets are a pre-hydrolyzed acidic aqueous/alcohol solution of the tetra-alkoxysilane which is subsequently gelled to a silica microbead. The precursor solution also contains a triblock polymer to template the silica into a gel with a prescribed mesoporous structure. In a microfluidics cell, an emulsion, consisting of a train of micron-sized droplets of the prehydrolyzed precursor in a continuous mineral oil phase (immiscible with the aqueous/alcohol solution) is formed by pinch-off of the precursor at a flow-focusing

orifice. The pinch-off process is very reproducible, and hence the droplets are uniformly sized. The QDs are again incorporated into the droplet phase, but are surface functionalized with a polyethylene oxide surface coat to make them dispersable in the aqueous/alcohol solution. To gel the pre-cursor droplets, the concept of using the octylamine as an accelerant to raise the pH and increase the gelation rate is again used. A fluidic cell is developed in which, after the train of droplets is formed, the train contacts a stream of the octyl amine solution which flows as a film along the walls of the channel with the main mineral oil/ droplet stream flowing in the center of the channel. The octylamine is allowed to diffuse from this film into the mineral oil and in turn into the pre-cursor droplets. The octylamine acts as an accelerant, as it raises the pH of the droplet and catalyzes the gelation of the precursor. The collected gel-like droplets, which emerge from the microfluidic cell, are then further gelled by treatment with concentrated base. Without the accelerant, the droplets emerging from the cell are too fluid like and coalesce during collection. The result are smooth spherical silica particles whose size range can be adjusted precisely in the 10-100 micron range by changing flow rates of the precursor and the continuous phase at the orifice. The catalyst also has the added advantage that the gel-like particles during the final step do not shrink, but retain a spherical smooth shape, ideal for the screening applications. A second microfluidic flow regime is also described in which the droplets directly contact the side wall amine stream, and immediately gel the particles without need for post gelation using base. These particles are however more crenated.

As with the first route, a prototype QD spectral code is formed by embedding QDs with two colors (for the smooth particles). The photoluminescence emission

spectrum of the QDs indicates significant aggregation of the nanocrystals in the silica matrix, as reflected by significant resonance energy transfer relative to the spectrum recorded in the precursor solution. This is attributed to aggregation of the nanocrystals in the triblock copolymer solution prior to its introduction into the microfluicdic cell.

An outline of this thesis is as follows: In Chapter 2, a background review is presented of the luminescence properties of quantum dots, and the methods which have been use to date to embed these nanocrystals in microbeads for encoding purposes for use in high throughput screening applications. Chapter 3 describes the synthesis of the silica beads using the batch emulsion/suspension method and Chapter 4 describes the synthesis using microfluidics.

Chapter 2

Background

The focus of this research is on synthesizing optically encoded silica gel microbeads, to be used in high throughput screening platforms[6, 7], using suspension methods developed specifically for rapid gelation[8]. In general, suspension methods for microbead manufacture form emulsions of liquid droplets of a pre-gel in an immiscible phase, and then gel the droplets to form the beads[9-28]. The optical code embedded into the microbeads consists of the spectral signature of a collection of luminescent species, in particular, for this study multicolor semiconductor nanocrystals or quantum dots (QDs)[29-41]. The encoding QDs are dispersed in the pre-gel phase, and are surface functionalized[29, 42-45] so as not to partition in the continuous phase. In this way, the QDs are effectively trapped in the microbeads, which allows for a quantitative loading necessary for optical coding. The method studied in this thesis uses an amine catalyst as an accelerant[27, 46-49], and thus eliminates the post-production necessary in existing methodologies for obtaining silica beads. The emulsion/suspension process is implemented using a batch stirring method for forming the emulsion (Chapter 3), and a flow-flocusing microfluidic device (Chapter 4). The later is used to generate uniformally sized droplets of the pre-gel phase, thus insuring a monodisperse size distribution which is useful for high throughput screening platforms[50].

This background chapter begins (2.1) by reviewing the luminescence spectral characteristics of quantum dots, and the features that make these nanocrystals ideal for spectral encoding. The following section (2.2) reviews the methods that have been developed to incorporate QDs into microbeads, and the final section (2.3) reviews the

microfluidic production of microbeads and the incorporation of nanoparticles in the beads.

2.1 Quantum Dot Spectral Encoding

2.1.1 The Concept of Spectral Encoding of Microbeads

In microbead based assays (Fig 2.1), as a general rule, the ability to identify each individual free-standing microbead requires a labeling system for uniqueness of the thousands of beads that will be required as part of an assay, as the microbeads are to be separately identified in the same environment[30, 51]. It becomes an impossible task if they are of the same size (preferably within a narrow micron size range) since their physical size cannot be used to distinguish them. Thus the bottleneck of the technology is how to encode the microbeads effectively. The encoding methods appearing in the past years such as optical encoding, electronic encoding, graphical encoding and physical encoding have their own advantages and disadvantages respectively. Among the proposed encoding schemes, microbeads with an embedded spectral signatures (such as the fluorescence of quantum dots (QDs)) (Fig 2.2) have been made the focus of attention due to their greater stability, repeatability and their ability to accomplish high-through detection easily[6, 36-39, 52]. In addition, photoluminescence spectral barcoding has emerged as a favorite of many researchers as it has presented itself as reliable and effective for this purpose. The paradigm for spectral encoding is to embed species in the microbeads that luminesce at different wavelengths (colors) usually in the visible spectrum[32, 35, 53, 54] (figs 2.3,4). By varying the number of colors (c), and for each color the concentration (*i* concentrations), a spectral barcode can be developed which is read by exciting the luminescent species with light, and recording the emission spectrum. An encoding

capacity of i^c is obtained and the spectral signature of the beads are read optically and a software that deconvolutes each color from the total spectrum is necessary.

The coding uniformity is mainly determined by the intrinsic variation in bead size[38]. It has been reported previously that ratiometric measurements are considerably more reliable than absolute intensities because the ratio values are often not affected by simultaneous drifts or fluctuations[55] in the individual signals caused by the instrument-fluctuations are enormously amplified in diffusion measurements due to the variation in the excitation intensity the chromophore is subjected to as it diffuses through various regions of the focal volume. The ratiometric method[55], in effect, provides a way to normalize the data with respect to many of these fluctuations. Therefore, the use of ratios for bead decoding could help in the development of advanced devices and algorithms that can read the doped beads at high accuracies and speeds.

2.1.2 The Photochemistry of Quantum Dots and Their Use For Spectral Labeling.

Photoluminscensce encoding has relied upon the use of organic chromophores, which have a rather broad spectral signature as well as some other drawbacks that have placed a limit on the number of degrees of freedom required to satisfactorily make a high-throughput system for assaying. Considering these drawbacks, a more attractive strategy has been presented and that is the use of luminescent semiconducting nanocrystals or quantum dots (QDs). These inorganic chromophores have a narrow spectral signature, resistance against photobleaching, and simultaneous excitation of multiple fluorescence colors, and blinking is not a nuisance when tracking the signature[56-58]. In addition, their maximum emission wavelength can be tuned by their size, making them ideal to develop an encoding scheme with high capacity.

In 1982 experiments on chemically synthesized "quantum crystallites," of semiconductors, sometimes called "quantum dots", were first published in which it was observed that the optical spectra are quite sensitive to size[59]. Over the past decade, highly reproducible organometalic synthesis routes have been developed for making high quality semiconductor colloidal nanocrystals as solution-grown, nanometre-sized, inorganic particles. In these synthesis routes, the nanocrystals are enclosed in a shell and stabilized by a hydrophobic layer of surfactants attached to their surface. The purpose of the shell is to protect the nanocrystal from oxidation, and to confine exciton energy (see below). The coat, mainly TOPO (trioctylphosphine oxide) and HMA (hexadecylamine) that allows the QDs to be solubilized in an apolar solvent and remain dispersed[60].

The origin of the size dependence of their optical properties, at the center of their interest in encoding, is a quantum mechanical effect. Semiconductor nanocrystallites whose radii are smaller than the bulk exciton Bohr radius which has a characteristic length at least twice as long as its bulk counterpart, constitute a class of materials intermediate between molecular and bulk forms of matter (fig 2.5). Semiconductors whose excitons are confined in all three spatial coordinates leads to an increase in the effective band gap of the material with decreasing crystallite size. A 35-40 Å diameter CdSe crystallite, for example, containing some 1500 atoms exhibits a series of discrete excited states with a lowest excited state at 530 nm and Bragg X-ray scattering measurements indicate that these nanocrystals have the same unit cell and structure as their corresponding bulk material. The bandgap energy that determines the energy (and hence color) of the fluorescent light is inversely proportional to the size of the quantum dot.

There are to-date two types of quantum dots: types I and II, differing in whether they have a contravariant or covariant band layout[61]. This classification is defined by how the energy differs between the core and the shell that make up the nanocrystal composite. Type I have a shell of higher band gap material, thus trapping the electron-hole pair in the core while type II have material of lower bandgap, and can be made to capture either one of the components of an exciton. The material conjugation for these semiconducting nanocrystals are II-VI, III-V, or IV-VI atoms. The modeling behavior of the electronic wavefunctions determines which one of these behaviors the QD will have, depending on the atomic make up of the crystal[62]. Additionally, the series of discrete excited states is modeled by a Gaussian distribution and gives a narrow, symmetric emission. When mixed with QDs differing in bandgap energy, they can provide a large number of tunable photoluminescent tags each with its own distinctive spectral signatures that is ideal for a barcoding scheme. Their symmetric spectra and narrow distribution where the full-width half maximum, FWHM is only about 20-30 nm, and the single absorption of a UV wavelength commonality with the addition of concentration mixing allows a high barcoding capacity.

Semiconducting QD's of II-VI materials that have core-shell-capping use organic amphiphilic moieties extensively to stabilize these colloids in non-polar solvents and to maintain their properties through chemisorption, which are fundamentally what makes them such an attractive material for diverse uses. The organic moiety is chosen so as to maintain a 'balance' of bonding strength between its chemical groups with an affinity for either ion of the semiconducting material through metal coordination chemistry in the given solvent. This balancing helps to control size: If too strong, the crystal will not

grow. On the other hand, if too weak the crystal will grow uncontrollably[57]. The balance is dependent on concentration by sterically barring new material deposition on crystal- and most importantly the nature of the chemical group with the chosen chalconide moiety. The most widely used groups of amphiphilic species are phosphates, phosphines, carboxyls, thiols, and amines. Very few, other than TOPO, have been used to synthesize in-situ the colloids. Instead what has been predominantly done is cap exchange of varying organic moieties (see below). Most of these organic molecules are labile especially amines, and multiple exchanges reduces the PL QY of the nanoparticles[41, 42, 44, 54, 58].

The very high surface to volume ratio of these particles gives them their high reactivity since there are many 'dangling' bonds that create states within the bandgap, (also known as trapping emission states). These states at the edge of the crystal surface act as radiative exciton recombinant centers that may lead to non-radiative emission leading to quantum efficiency losses and are undesirable for certain applications, mainly ones requiring high efficiency luminescence (fig 2.4). This problem is for the most part solved by growing a shell which allows an increase in band gap thus confining the charge carriers and preventing the creation of surface states isolating the conduction band, i.e. widening the HOMO LUMO gap but at the same time decreasing the size of the material and results in quantum size effects, and partly by the environment that the bonding group creates at the bonding sites with the semiconducting material.

2.1.3 Surface Functionalizing Quantum Dots

Since QD's are not thermodynamically stable these chemical groups also prevent the QD's from aggregating. This instability is prevented by the capping agent that contains, depending on the type of groups in the chain and solvent type, a certain

hydrodynamic radius which is used to overcome the van der Waals attractive forces-lowering surface energy which is dependent on temperature and dielectric properties of the media. Depending on the type of solvent stearic stabilization by either hydrophobic alkyl or hydrophilic charges on chain is achieved. The ease with which some of the developed coating methods allow for modulation of the chemical nature of these QD's[63] and still maintain their photophysical abilities is a topic of interest and research.

Transfer of these luminescent materials into water or into polar media is a prerequisite, particularly for biological applications and in the context of this study, in inserting microbeads into polar bead matrices. Several phase-transfer protocols have been proposed and tested which rely on the adsorption of water-soluble ligands that can displace the native hydrophobic ligands. These transfer agents include sulfanylalkanoic acids polymeric silanes, and polymeric coatings such as polyethylene glycol (PEG) and polyacrylic acid derivatives. These passivation layers afford materials which remain stable for weeks and sometimes months, but the photostabilty of the QDs is drastically reduced in oxygenated aqueous solutions. Oxygen acts as a photoelectron scavenger, and catalyzes photoanodic dissolution of chalcogenide semiconductor particles in water. In principle, ZnS or ZnSe shells should effectively inhibit photocorrosion, but this photostability is difficult to achieve routinely because of charge-carrier tunneling into the shell or inhomogeneity of the deposited shell layer. These charge-carriers change the PL of the QDs profoundly if their interaction with the dielectric behavior of the external phase changes their wavefunctions.

An alternative process is to deposit other layers capable of impeding electron, proton, and oxygen diffusion to the QD surface. One such material is amorphous silica.

There are several advantages to encapsulating QDs in silica shells. First, silica is chemically inert and does not affect the chemical or biological reactions except physical blocking of the surface. Second, the silica shell is optically transparent, so that the optical coding will not be shielded. Finally, and most obviously, the shell prevents the leakage of QDs during reactions. A silica shell should also minimize fluorescence quenching by surface adsorbates or redox-active molecules. Consequently, such surface-coated particles could have widespread uses in optical and optoelectronic applications where photostability is critical for device longevity. Furthermore such surfaces are biocompatible and can be easily functionalized for bioconjugation purposes. Although the potential advantages of silica coating have been described for metal and semiconductor nanoparticles, the only existing routes rely on the core nanocrystals already being in a polar environment such as ethanol or water. The organically capped QDs are usually degraded in these polar media before coating can be effected. Consequently, a method is needed for encapsulating nanocrystals of luminescent semiconductors (or other materials) that are only soluble in nonpolar media.

A material and process must be conceived that conceals the QDs in a hydrophobic vestibule eliminating fluorescence deviations. However, since the QDs are hydrophobically capped and silica matrix is hydrophilic, Nann and Mulvany[64] chose to coat the surface of single QDs with silica following a Stober synthesis method. In this work, the surface of the QDs, therefore, had to be exchanged for more polar ligands to enable transfer into ethanol or any other polar solvent where the coating can take place. The first step was to cap exchange the organic molecules, which are usually TOPO or HAD, and the QDs were solvated in THF. A second requirement for the surface is to

provide nucleation sites for the controlled growth of a homogeneous silica coat. This is accomplished by using a bifunctional molecule- one that is going to coordinate with Zn or S on the core of the nanocrystal and the other end will catalyze the silanol groups in the solution. Careful observation of the chemistry of organosilane molecules led them to choose 3-sulfanylpropyl trimethoxysilane (MPS) as it prevents self-ionization and competing nucleation sites when in excess. Through an extensive analysis of the optimal quantities of the reacting products a protocol was chosen that lead to a homogenous coating but were limited obviously to the concentration of QDs as consistent with the necessary concentrations for primary nuclei for seeding. The results show that the photoluminescence of the QDs does not change from solution to encapsulation in the silica matrix. From their results, no conclusions could be obtained on which of the mechanisms is operative, either the inverse layer by the surfactant or the ligand exchange.

2.1.4 Resonance Energy Transfer Between Quantum Dots

Studies of the emission spectra and lifetimes of QDs of different sizes in close-packed assemblies formed as evaporated thin films or monolayers and multilayers[65, 66] show a quenching of the luminescence and lifetime of smaller QDs accompanied by an enhancement of the luminescence and lifetimes of the larger QDs. These measurements indicate then when nanocrystals are within the Foster radius of each other, a nonradiative resonance energy transfer (RET) between QDs arising from coupling between the transition dipoles in the excited donor (QDs with a smaller size) and the ground state acceptor (QDs with a larger size) takes place (Fig 2.6)[67].

This resonance energy transfer that occurs when nanoparticles are within the Forster[68] radius of each other is important to the issue of the spectral encoding of

microbeads. If the nanocrystals are aggregated in the bead, than resonance energy could cause problems such as spectral broadening, self-quenching, and wavelength shifting. More than a handful of experiments have been carried out in order to determine the extent of the behavior of the Silica matrix[52, 64, 69, 70] onto the spatial and opto-electronic properties of these nano clusters. In addition, synthesis of silica particles by emulsification techniques, diffusion of QDs by swelling particles, and seeding of QDs on the surfaces of particles by surface functionalization, are used as a tool and with the use of FRET (Foster Resonance Energy Transfer) were used to prove that this scheme was excellent as a tool for identifying and recording changes in subpopulations in a mixture and would lead to less ambiguity of the effects of interaction due to spatial restrictions. Deniz et al.[55] developed the technique called single-pair FRET (spFRET) to allocate the ratiometric scheme a placement as a viable tool for free diffusing molecules. This was necessitated by the inability to develop a process that eliminated polydispersity that creates subpopulations and the need for ratiometric loading of chromophores in the beads. When intensity decoding is based only on absolute concentrations but with varying quantities of QDs then the barcode can become non-unique. Specifically, when loading has same fraction of chromophores but the molar ratios are different then ratiometrically they are the same but not in regards to absolute intensity. The ability to produce monodispersed particles extends an extra degree of freedom in creating a full fledge barcode.

A further question is whether the quantum dots exist as dispersed single particles or as aggregates in the nanopores. Aggregation could cause problems such as spectral broadening, self-quenching, and wavelength shifting. More than a handful of experiments

have been carried out in order to determine the extent of the behavior of the Silica matrix onto the spatial and opto-electronic properties of these nano clusters. In addition, synthesis of silica particles by emulsification techniques, diffusion of QDs by swelling particles, and seeding of QDs on the surfaces of particles by surface functionalization, are used as a tool and with the use of FRET (Foster Resonance Energy Transfer) were used to prove that this scheme was excellent as a tool for identifying and recording changes in subpopulations in a mixture and would lead to less ambiguity of the effects of interaction due to spatial restrictions. Deniz et al. developed the technique called single-pair FRET (spFRET) to allocate the ratiometric a placement as a viable tool for free diffusing molecules. This was necessitated by the inability to develop a process that eliminated polydispersity that creates subpopulations and the need for ratiometric loading of chromophores in the beads. When intensity decoding is based only on absolute concentrations but with varying quantities of QDs then the barcode can become non-unique. Specifically, when loading has same fraction of chromophores but the molar ratios are different then ratiometrically they are the same but not in regards to absolute intensity. The ability to produce monodispersed particles extends an extra degree of freedom in creating a full fledge barcode.

2.2 Embedding QDs in Microbeads

Many latex type materials have been used for the technique of embedding organically capped QDs in pre-polymerized beads. Key steps in preparing quantum dot-encoded beads include the synthesis of highly monodisperse beads with suitable pore structures and the formulation of solvent conditions that strongly favor the partitioning of quantum dots from the solution into the pores and conceals the QDs in a hydrophobic

vestibule eliminating fluorescence deviations and the retention of the loaded QDs inside of the yet to be polymerized particles to retain the intended code. This behavior can be controlled by using the proper attractive forces between the type of organically terminated coating on the surface of the QDs and the type of material it will be incorporated into-nominally relying in strong hydrophobic forces. Many materials have been utilized to achieve this end. These have required both the ease of bead manufacturing and a high solvency of the QDs in these monomer droplets. These would be oil-in-water emulsions where the emulsified monomer serves only as a reservoir of the monomer supplying the radical-containing micelles and polymer particles by diffusion through the aqueous phase.

The principle methods for incorporating QDs into microbeads include: (i) embedding the nanocrystals into preformed microbeads, (ii) incorporation of QDs in shells around preformed particles and (iii) in situ polymerization or gelation of microbeads with the nanocrystals. These methods are reviewed below, in which focus is given to the fabrication of encorporating QDs in silica beads.

2.2.1 Encapsulation in Preformed Microbeads

The procedure involved in embedding QDs into preformed beads involves partitioning the QDs into the bead from a solvent in which the beads and QDs are both dispersed. In one of the first studies on encapsulation in preformed beads, Nie[36-38] developed a technique were he vortexed a pre-loaded solution of QDs in butanol or chloroform to diffuse them into the pores of the silica beads. Initially this process did not provide the intended results- to be used as a barcode. This was due to the fact that he was providing a designated space for the QDs to move into but not restricting them into a multiplexed

system. His argument for the improper engineering of the barcode relied on the non-uniformity of the silica matrix and the monodispersity of the beads. He then followed his logic by producing mesoscopic pores in polystyrene beads by burning off the poregen. He argues that the monodispersity and extended porous environment of the beads and he proved that "this comparison indicates that the observed signal variations are mainly determined by the intrinsic bead uniformity, not by doping statistics or measurement errors. This high level of doping uniformity achieved with porous beads allows the use of both absolute intensities and relative intensity ratios for coding. In contrast, QD-doped porous silica beads have been reported to exhibit intensity variations as large as 50% and are useful only for ratiometric coding." The caveat here is that none of these processes for the beads require in-situ synthesis of the chromophores inside the pre-polymerized beads. Thus, the chemical difficulties are eliminated but the physical constraints that need to be imposed to eliminate any fluctuations in the reading of code are still persistent. Cao et al.[40] also attempted to create a barcode scheme along these same techniques. They opted to use the same pore-functionalizing scheme but instead a controlled sulfonation reaction was undertaken to carboxylate the pore volumes post loading. The carboxylation was necessary to allow the modified beads with –COOH for the (i) immobilization of biomolecules and to (ii) increase the porosity of the beads more efficaciously than by swelling, thereby improving the coding ability.

2.2.2 Incorporating Quantum Dots in Shells Around Preformed Particles

Rather than impregnating QDs into beads, shells containing QDs can be placed around the beads as undertaken by Graf et al.[71] In this process the QDs were coated, instead of cap exchanged, with PVP (Polyvinyl pirrolidone)[72] and then seeded to an

amine terminated silica bead that was subsequently coated with silica following a lengthy protocol to stabilize and 'decorate' the silica bead perimeter with the QDs. PVP is an amphiphilic polymer that is soluble in water and many nonaqueous solvents. This behavior arises from the presence of a highly polar amide group within the pyrrolidone ring and apolar methylene and methine groups in the ring and along its backbone. Graf et al. used an alternative way based on an adsorption of the amphiphilic polymer PVP on their nanoparticles. Due to its amphiphilic character, it can be simply adsorbed on many different surfaces, especially on various colloidal particles such as metal, oxide, and polymer particles. Here Graf et al. determined that the photoluminescence of the single and 'nano-decorated' silica beads remains unchanged but that the quantum yield is considerably lower.

Growth of concentric shells around seeded particles and decorated by QDs was developed by Caruso et al.[73, 74] where a layer-by-layer (LBL[33]) envelop of polyelectrolytes, taking advantage of electrostatic forces, of alternating charges and polar soluble QDs are sequentially deposited on the surface and then Su et al.[40] took it one step further and used two different emitting QDs. The obvious restrictions when using shells, that Bawendi[53] used and was extended to the LBL technique, to contain QDs limit the ability to create a barcode, and the loci for these ideas lies on placing the QDs in particles that have already been synthesized or that are layered.

2.2.3 Suspension Polymerization and Microgel Formation

Vincent[75] proposed to use the suspension microgel approach to sequester the nanoparticles inside polystyrene as well as suspension polymerization, in which the components of the final bead product are mixed in together (monomer, initiator and QDs)

and then dispersed in an immiscible liquid[11, 17, 19-21]. Soon after the polymerization is commenced by activation of the solubilized initiator, and owing to its hydrophobic nature, it makes for the perfect stable environment for the QDs to remain dispersed. Others have used similar tactics whereby the QDs themselves have been functionalized with, for example, vinyl-terminated groups to promote polymerization with styrene[70]. All these techniques revolve around the ability to solvate the QDs in a favorable environment to maintain both spacing and quantitative accounting of the load. A limiting factor is partitioning of the QDs inside these beads due to differing polymerization kinetics and partial solubility of organic material in external phase that leads to inhomogeneities which forces the QDs into pockets or polydispersity, thus spatially diminishing their pitch-to-pitch length and effecting FRET amongst the subpopulations[39, 65, 66].

Hollow particle synthesis is an active research field due to its many industrial, biological and chemical activities including as molecular sieves due to its porosity. Many methods include layer-by-layer[73, 74] templating techniques, emulsion droplets, and others use template-assisted synthesis such as latex, colloidal particles to vesicles, structure-directing technique which uses extreme amounts of surfactants, silica even gold nanoparticles. Templating techniques are more effective given the ease with which hollow particles can be obtained. These methods require the removal of the templating agent by acid burning or calcinations of the organic material that can be detrimental if a sensitive material needs to be preserved and more importantly to retain its intended function. This technique can be rather simple but it suffers from the many short falls that the previous ones have. Specially, the hollow nature of the beads distorts the emission spectra as the QDs are trapped in a limited boundary layer of the material and thus

disallowing for proper barcode read out and separation through the most popular method of flow cytometry.

Emulsification processes have also been used to sequester QDs by the use of the hydrophobic micelle area. A reverse micelle (water in oil) was used by Koole et al[76], and it operates inversely from a microemulsion, where a ligand exchange mechanism is found to be responsible for the transfer of the hydrophobic QDs into the aqueous phase. On the basis of these results, they were able to control the position of the QD from centered to off-center and eventually to the surface of the silica sphere. Furthermore, they found that the ligand exchange is also responsible for the luminescence quenching that is generally observed when QDs are incorporated in silica as was noted by Graf et al as well. Multiple QDs per silica can be achieved by increasing the QD concentration, which implies the possibility of co-localizing different types of nanocrystals in silica at a tuneable distance. Even though this process is an in-situ process this becomes a rather onerous obstacle if the fluorescent signal loses quantum yield and with the addition of limited number of QDs capable of being loaded into the reverse micelle. Hence, a process for generation of silica particles with both multiple QDs with high concentration and a monodispersed population to be able to be separated by flow cytometry needed to be developed. After all, throughput is principally limited by the number of compartments in the array, especially, if indexing numbers in the range of 10^5-10^6 are needed. Most of these methods are either expensive or time-consuming, or they produce particles with insufficient control over their size distribution and morphology, as well as precise control of shell thickness.

2.3 Microfluidic Fabrication of Microbeads

Microfluidics presents itself as the leading technological candidate to meet the above both mission statements for a high-throughput and robust platform required by the vast amounts of information in many fields, especially proteomics. It is based on the science and technology of systems that process or manipulate small amounts of fluids, using channels with dimensions of tens to hundreds of micrometres. Microfluidic devices are capable of generating highly uniform droplets of order 10–100 μm in size with a frequency of thousands of droplets per minute. Precise control over droplet formation arises from confinement of injected droplets within complex, low Reynolds number flows generated in microscale geometries. One of the most effective geometries for this purpose is a flow-focusing junction, in which droplets form in elongation-dominated flows that are squeezed through an orifice- microfluidic flow-focusing device (MFFD). The manipulation of multiphase flows is another strength of microfluidic systems. They enable the generation and manipulation of monodisperse bubbles or droplets of a dispersed gas or liquid phase in a continuous liquid stream; these dispersions suggest new routes to the production of polymer particles, emulsions and foams. Droplets can also serve as compartments in which to study fast organic reactions as well as inorganic- one of the most important one for this specific work is gelation of silanol groups that compose the entire bead.

Anna's[1, 77] original work on flow focusing junctions for droplet production has elucidated many of the underlying physical behaviors that dominate in this geometry. By formulating scaling arguments to define dimensionless variables which capture all the parameters that control the droplet breakup process, including the flow rates and the viscosities ratios of the two immiscible fluids, the interfacial tension between the fluids

and the numerous dimensions in the flow focusing device, Anna determined the effects that define the regime in which the droplet production lies and helps the designation of the particle size for specific tasks. In her work with surfactants and their effect on droplet production Anna was able to prove that 'controlling the surfactant bulk concentration of a soluble nonionic surfactant in the neighborhood of the critical micelle concentration, along with the capillary number and the ratio of the internal and external flow rates, [they] observe several distinct modes of droplet breakup.' Monodispersed droplet generation is the major most attractive benefit of microfluidics for this particular project but the ability to anoint each droplet as its own reactor for the given designated chemistry, which is to encapsulate the QDs in a silica matrix, is the greatest advantaged of this system.

Most attempts at *in situ* gelation of particles when in the microfluidic cell for ease of handling are done by UV polymerization. A paper by Kumacheva and Whitesides[78] used MFFD and by changing the aspect ratio of the channels and immiscible liquids to produce diverse shapes and by controllable breakup of the liquid, embedded nanoparticles into the droplets that were polymerized by induced thermal solidification and UV initiated batch photopolymerization. This work exemplifies the extensive range of the types and shapes that MFFD can offer with the added control of tight polydispersity. Composition of droplets and variety of materials was later more confirmed with the extensive work that Kumacheva showed that multiple immiscible liquids could be used to create multi core-shell particles[79] by changing the flow rates of one of the liquids while keeping the others constant. This work used two different types of surfactant, oil soluble sorbitan monooleate (SPAN 80) and water soluble sodium

dodecyl sulfate (SDS) and found that SDS concentrations above 0.2wt% affected the dispersity of the droplets but SPAN 80 did not. The droplet behavior study was done by comparing the wetting and stability of droplets in PDMS and PU (polyurethane) cells as phase inversion is a situation when the dispersed phase has a high affinity to the cell walls[80]. In another paper[63] it was found that the stability of microfluidic emulsification depends critically on the preferential wetting of the walls of the microfluidic device by the continuous phase. Surface chemistry of the microchannels proved to be an efficient method for screening of the device for proper emulsification of droplets.

Multifunctional acrylates[81-84] were used and found that they are an alternative to increasing photopolymerization rate can increase cross-linked particles. Extending on this work a mixture of Janus particles and three-phase particles[85] of an organosilane as one liquid with a mixture of acrylates as the second phase also were produced. This was followed by biopolymer hydrogel[86] material of sodium alginate and κ-carrageenan where diffusion-controlled ionic cross-linking of the biopolymers was achieved in-situ by controlling the residence time of the particles and the concentration of the cross-linker in the continuous phase. Crenation followed by onset of diffusion of the cross-linking agent Ca^{2+} and was determined by the amount of corrugation seen on the surface of the particles. And this work also showed the ability to encapsulate rather large particles (10 μm) in the microgels.

This process though extremely useful in maintaining particles dispersed suffers from the obvious set back that the innate nature of the particles is the organic material. This type of material does not generate the best type of biofunctional platform without much ado post processing- '[n]o stabilization against coalescence or Ostwald ripening of

monomer droplets is required because their collisions in the microfluidic device are suppressed and the time prior to monomer polymerization is on the order of seconds.' However, the ideal material for said endeavours has to be metal oxides and principally silica; and handling silica gel droplets is quite a challenge, as they tend to form continuous films without proper liquid evaporation. In the case of a colloid, the volume fraction of particles (or particle density) may be so low that a significant amount of fluid may need to be removed initially for the gel-like properties to be recognized as has been recognized by previous successful productions.

Weitz's work in microfluidics is very extensive and he was able to make silica particles in microfluidics by a 'reverse emulsion' process[87]. The aqueous phase constituted of a solution of prehydrolized silica, ethanol, and a catalyst that promotes a faster hydrolysis kinetic rate than condensation, and by keeping the solution close to pH 2, the isoelectric point of silica (fig 2.7), it gave the ability to pump the solution in a microfluidc cell. The external phase was hexadecane and this oil was chosen as one that would allow the ease of evaporating the ethanolic solution out of the droplets to finalize the processing of the droplets into beads. This was done by placing the sample in a vacuum oven and heated for several hours and then calcined as the last step before being placed in an SEM. At these conditions ethanol is the only one of the liquids that will be extracted. The untimely evaporation of ethanol from the droplets into the external phase causes the problem most other gelation processes face, agglomeration of particles. The evaporation of ethanol accelerates gelation of the silica material and improper handling leads to this catastrophic behavior. Even careful handling leads to a low percentage of particles to remain dispersed and, hence, retaining their usefulness as platforms for

coacervates. Also it was revised that an extended interface is created, between the droplet and the continuous phase when the diffusion of ethanol is promoted by heating. This can lead to rather odd shaped particles.

Lee et al.[88] however extended this protocol to include a more viscous oil to prevent the aggregation of particles by using mineral oil. Ethanol is much less soluble in mineral oil than in hexadecane, so it prevents the agglomeration of the droplets but does not affect the induction of the extended interface but Le et al proved that with the use of a surfactant with the proper HLB and solubility in ethanol will prevent the interface from extending. This is a rather ingenious approach but then particles need to still be heated for a long period of time in order to drive the ethanol out and gelation to onset. The emulsified droplets are still very liquid like when they leave the microfluidic cell, and the post droplet production process is what determines the final quality of them.

A combination of synthesis of silica and in-cell polymerization has to be achieved in order to fulfill the premise of both monodispersity attained by microfluidics and gelation- an aerogel is made by the so called "sol-gel process"[89]. During this process, organic compounds containing silica undergo a chemical reaction producing silicon oxide (SiO2). This mixture is a liquid at the beginning of the reaction, and becomes more and more viscous as the reaction proceeds. When the reaction is finished, the solution looses its fluidity and the whole reacting mixture turns into a gel- 'it represents the point where the last link is formed in the chain of bonds that constitutes the spanning cluster' Brinker (book pg 358[90]). This gel consists of a three-dimensional network of silicon oxide filled with the solvent. During the special drying procedure, which leads to polymerization and increase of the network connectivity, the solvent is extracted from the gel body leaving

the silicon oxide network filled with air. This process is a result of condensation reactions and the product is called aerogel. Aerogels can be synthesized not only from silicon oxide (silica aerogels), but also from different organic, inorganic substances and a mixture of both, for example, titanium oxide, aluminium oxide, carbon etc.

With this in mind Ducree[91] used an ionotropic gelation method to gel chitosan particles. These gel microbeads were fabricated by extruding chitosan solutions through a polymeric micronozzle using a centrifugal platform that used a force ranging from 93 to 452g, and the mixing took place via two different channels one for the chitosan solution an the other the continuous oil flow that provided the shearing force. Though this technology cannot be ascribed to the microfluidic based synthesis it does adrress a major issue with gelling materials. Here the gelling mechanism is diffusion limited as the cross-linking agent is placed in the external phase and induces gelation as it diffuses into the aqueous bead. Ducree's process elucidates one of the main obstacles in microengineering particles in confined flows, as these require intimate contact between the two fluids that are to both generate the droplets and activate a gelation mechanism in them. Residence time of both liquids at the point of contact is usually short enough, as both phases are continuously refreshed, that diffusion kinetics of most molecules will seem rather slow. However the prospect of generating droplets and extending a rather measurable gelation condition to the beads minimizing post collection processing is a laudable and desirable goal. It facilitates handling of the emulsion and reduces the need for expensive equipment and consumption of time. Hence, in a PDMS channel where the bottom of the channel is in constant contact with both solutions aggregation of the condensed material is a constant obstacle to the extended production of the emulsion if the reactivity is quite

rapid. Thus a downstream introduction of the catalyst is necessary for concomitant rapid gelation and extended droplet production.

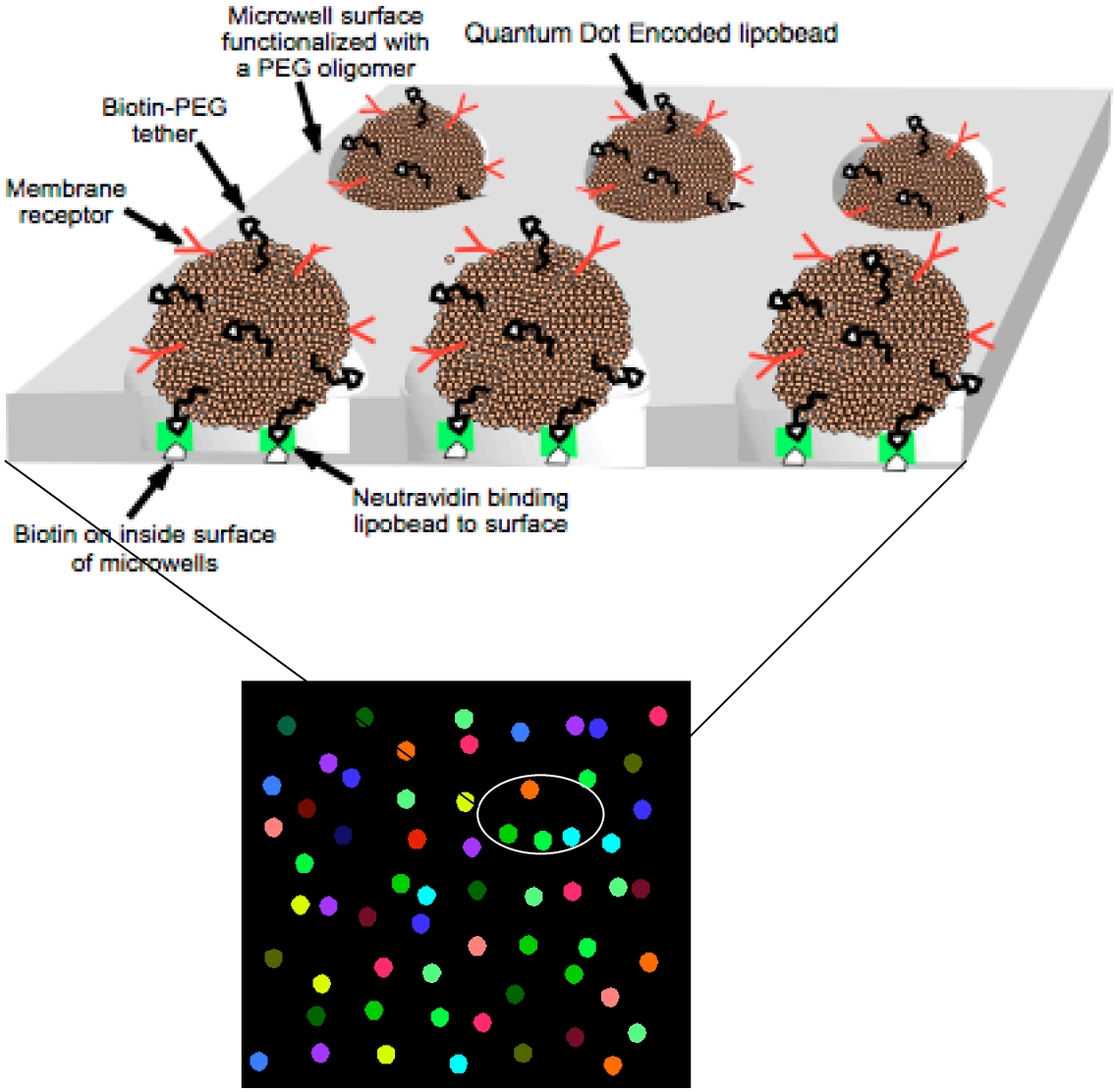

Fig 2.1. Rendition of a Lab-on-a-chip schematic as motivation for design of this project. Top part, zoom in, of schematic describes the lipobeads necessary as a membrane receptor in microwells. Bottom part of image is chromatic readout of how indexing of the wells would result in multiplexing system.

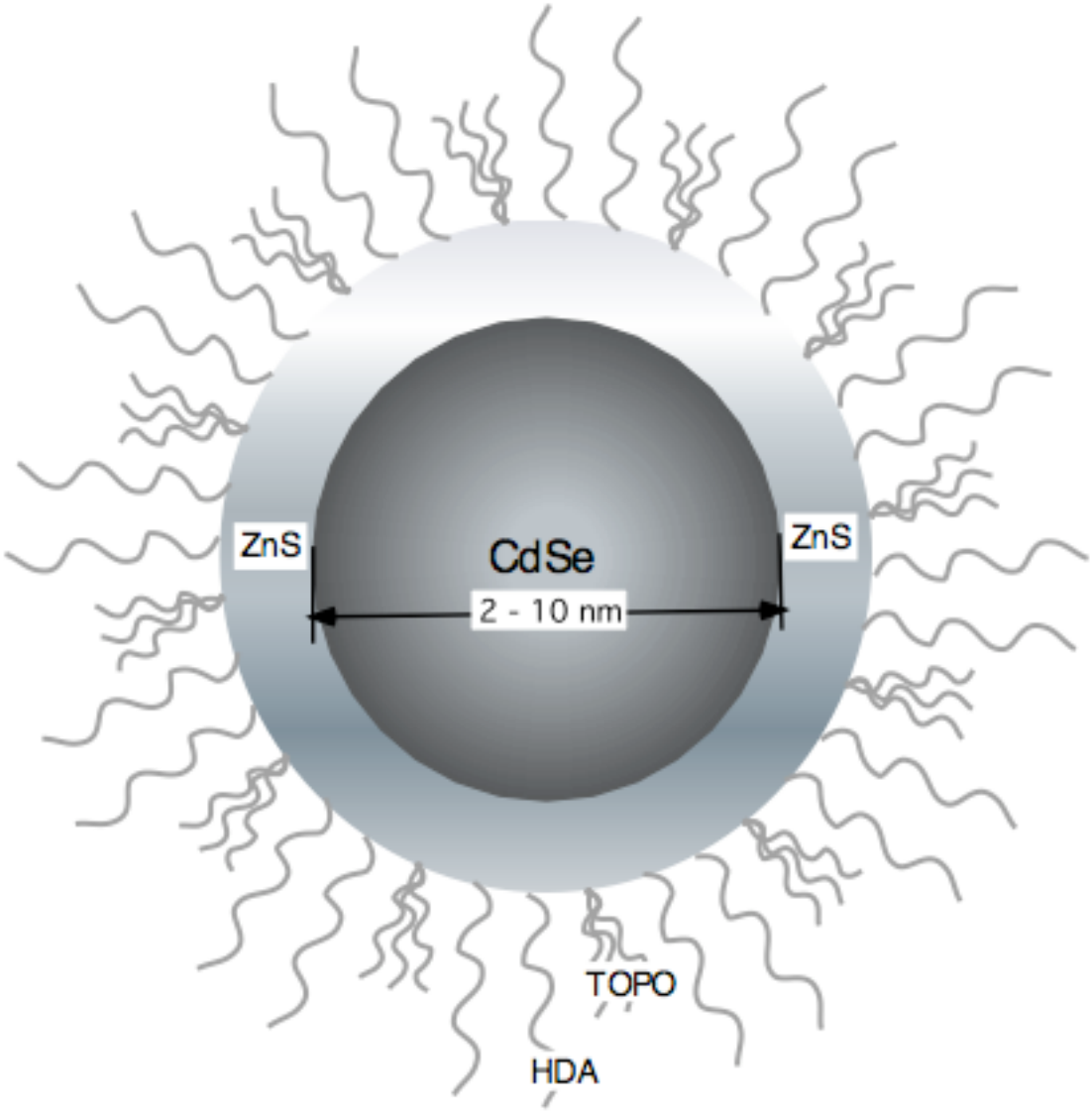

Fig 2.2. Drawing schematic representation of composition of core/shell (CdSe/ZnS) with long alkyl chain capping (TOPO, HDA) Quantum Dot.

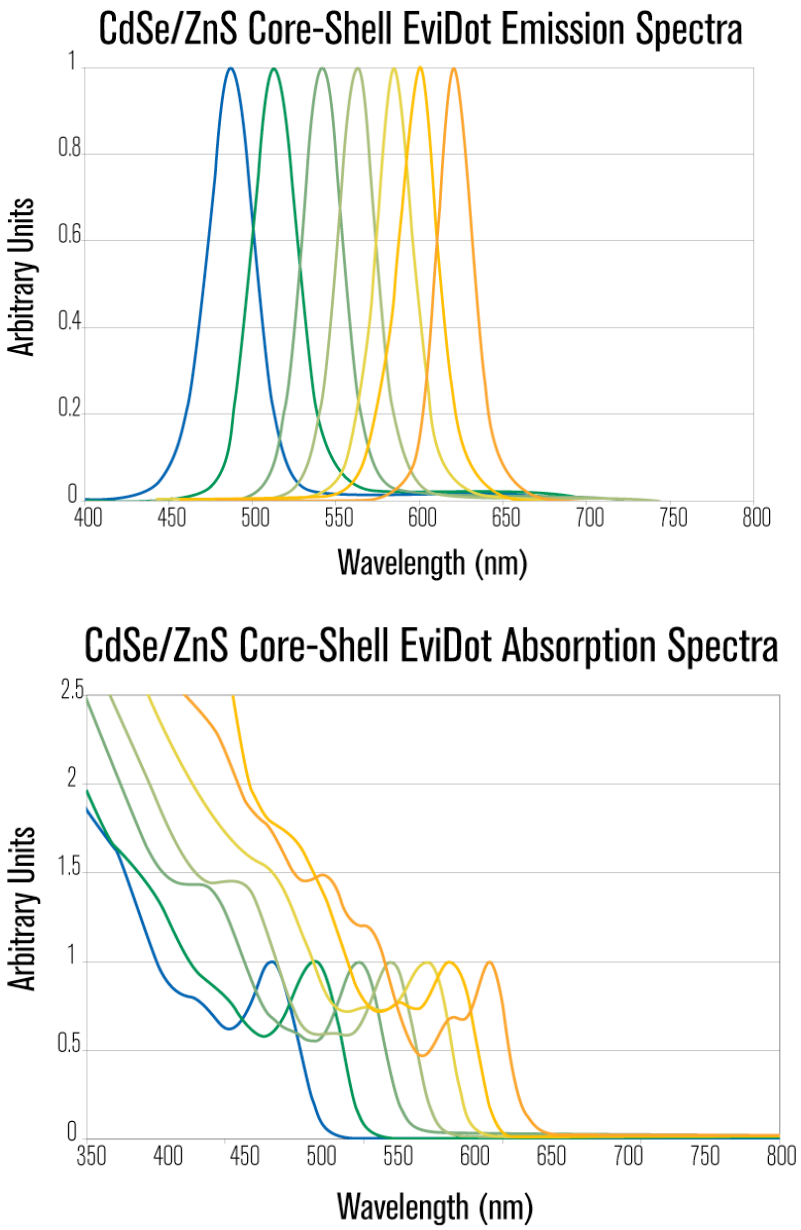

Fig 2.3 (Top graph) Normalized absorption spectra of semiconductingnanocrystals to equal absorption intensities at the first excitation wavelength. (Bottom graph) Absorption of same Quantum Dots. This graph shows the importance of exciting all nanocrystals with same single wavelength source.

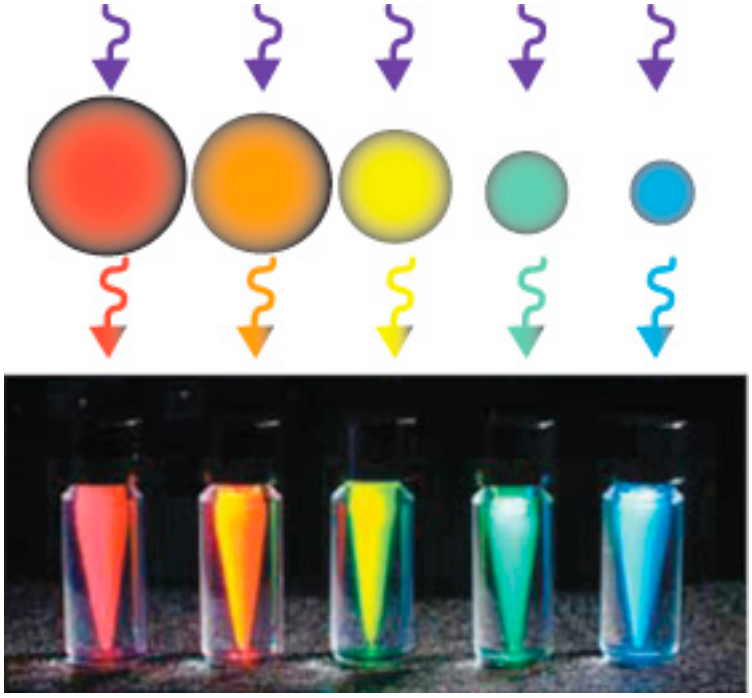

Fig 2.4 Colloidal Nanocrystal Quantum Dots. Here are five different sized QDs represented by the different colors respective of their crystal size (decreasing crystal radius from left to right emphasizing the quantum confinement effect) that have been excited by a UV-lamp.

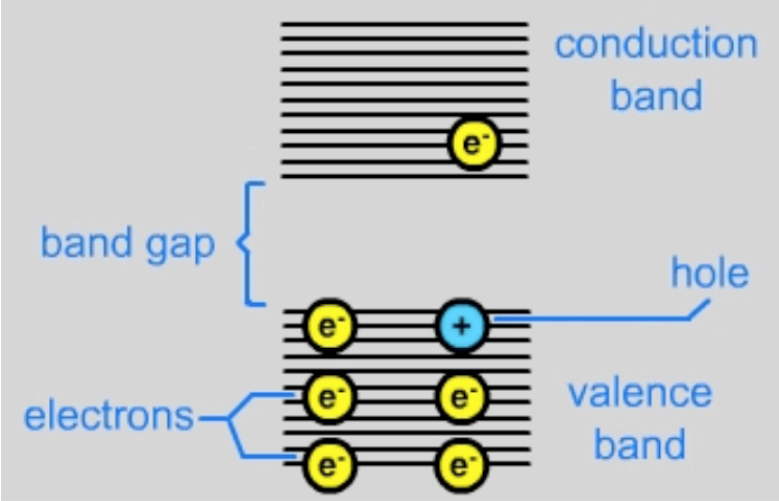

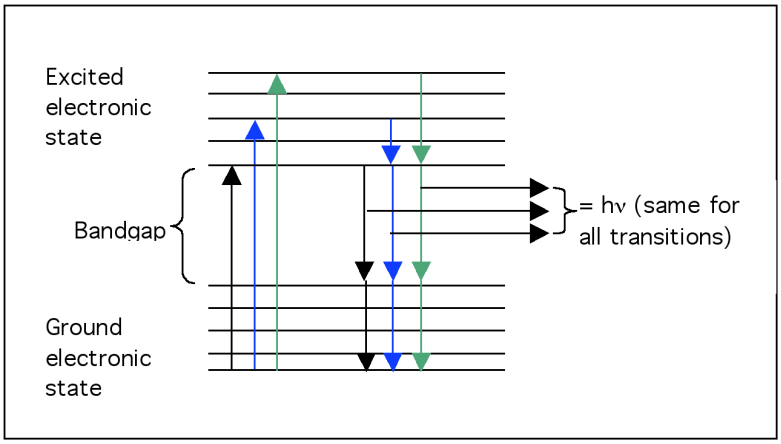

Fig 2.5 *Top Schematic:* Photonic band gap material that are periodic dielectric structures that forbid propagation of electromagnetic waves in a given frequency range (electron-hole pair in semiconductor). *Bottom Schematic:* Absorption of electron from a lower energy state (ground state) to a higher energy state and emission of photon from excited state (fluorescence).

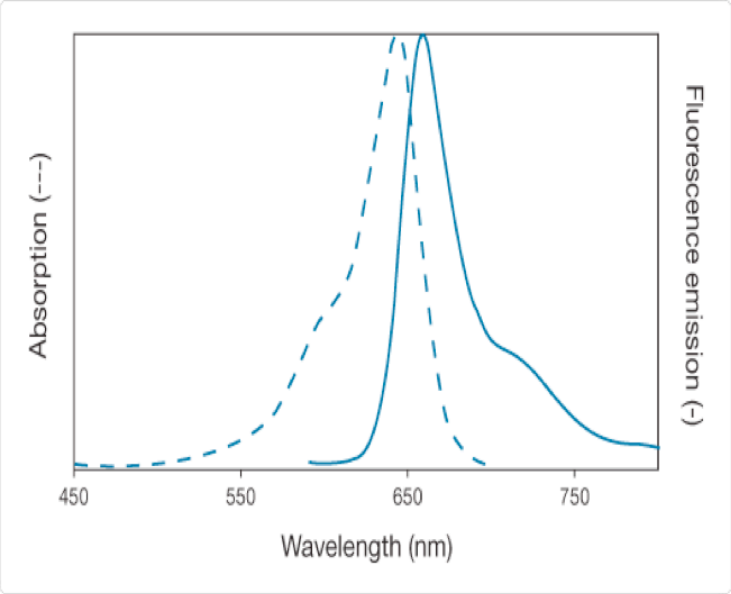

Fig 2.6. Foster Resonant Energy Transfer (FRET). Radiationless transter of energy that has to have at least 30% overlap between the emitting donating chromophore and the absorption of the accepting chromophore.

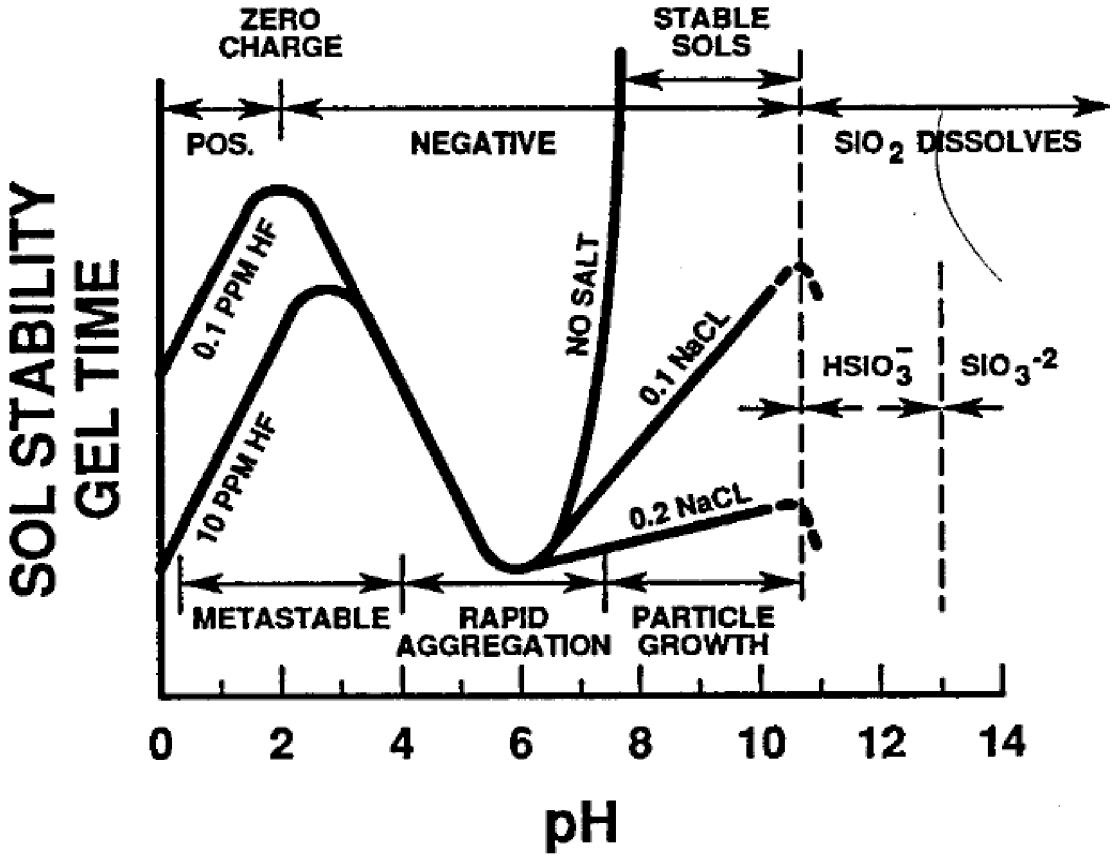

Fig 2.7. Graph by Iler representing the duration of stability gel time of a silica sol as a function of pH. Notice the metastable pH and rapid aggregation pH that were mainly used to manufacture encoded silica beads.

Chapter 3

A Batch Suspension Method for the Encapsulation of Quantum Dots in Silica Beads

3.1 Emulsion Design and Gelation Chemistry

In this chapter, a batch suspension process for the fabrication of silica microbeads encapsulated with quantum dots (QDs) is described. The method uses as its starting point the basic process of suspension polymerization for the fabrication of latex or polymer microbeads, as reviewed in Sec. 2.2.3, but alters the chemistry to gel silica in the form of beads rather than polymerize a pre-polymer to form particles. The suspension polymerization route in the fabrication of latex beads emulsifies (usually be a batch stirring operation) neat droplets of the prepolymer and a polymerization initiator (such as a free radical initiator) in a continuous phase immiscible with the prepolymer phase, and then polymerizes the droplets into beads by activating the initiator – either thermally or photochemically[22]. The emulsion is transformed into a suspension of latex beads, which are then collected by separating the beads form the continuous phase. Quantum dots can easily be encapsulated in the microbeads synthesized by this process by first dispersing the nanoparticles in the prepolymer so that they become distributed in the precursor droplets which form the dispersed phase of the emulsion. Dispersal required the surfaces of the QDs to be compatible with the polarity of the prepolymer, and retention of the QDs in the precursor droplets as they undergo polymerization requires that the surface coat of the QDs is not compatible with the continuous phase. In this way the QDs are retained in the droplets as they polymerize, at the concentration dispersed in the prepolymer solution. This insures that the spectral label derived from the composition of the QDs in each bead is the same for each bead in the batch, a necessary requirement for using the QD

encapsulated beads for labeling. The fact that the suspension route easily facilitates the incorporation of the quantum dots in the microbeads in a way that insures that the concentration of the QDs is the same in each bead is what makes this route attractive for the synthesis of encoded beads.

In the synthesis of silica microbeads by the emulsion/suspension route, the precursor droplets contain a silica precursor which is gelled to form the silica bead. Tetra-alkoxysilanes[89] are hydrophobic precursors that form silica by a two step process of hydrolysis[92] to silanol groups, and condensation by siloxane bridging to form silica, SiO_2[93]. The kinetics of the hydrolysis step is enhanced by an acid-catalyst while a base for high condensation rate and fast gelation is required. The rate of hydrolysis is directly dependent on the concentration of H^+ and hence the strength of the acid, ionization and dissociation (which are accelerated by solubility amongst other parameters) play a crucial role in the release of the electrophile, as well. This obviously allows us to take advantage of the behavior of opposite ends of the pH scale. Gelation time is fastest at intermideate pH- about 6 (fig 2.7)- but it can be accelerated by pH and catalytic mechanisms. Additionally, intermediate steps arise in the system depending on the type of solvent and catalyst used which slows down the reactions, known as reverse reactions[94].

To implement the formation of silica beads by an emulsion/suspension route, we utilize the tetra-alkoxysilane TEOS, tetraethoxyorthosilicate, as the precursor, and emulsify the neat hydrophobic liquid in an aqueous continuous phase in a batch operation by stirring. Hydrolysis of the silane in neat solution occurs via adsorption of water into the droplet, and subsequent diffusion through the droplet core. Acid hydrolysis with a contiuous aqueous phase at low pH accelerates the hydrolysis. Hydrolysis is the first step

in the two-step process. Once hydrolyzed, siloxane bridging of the silanols of the hydrolyzed species can begin. The transport of the water (and acid species) from the outside into the core of the droplet implies that the siloxane bridging and silica formation occurs from the droplet periphery inward so that in fact the gelation begins as a shell at the perimeter proceeding inward. Hydrolysis and reaction of the TEOS at the gelating shell boundary decreases the concentration of the TEOS at the inside of the shell facing the core. This creates a diffusive flux of TEOS from the core to the evolving shell. This gelation can be accelerated by raising the pH with a base[92, 95, 96]. Hence at intermediate stages in the gelation process a particle with a liquid core (TEOS) and a silica shell forms, and this suggests that this suspension gelation route can produce hollow as well as completely condensed particles. The formation of the shell limits the water transport into the core, and hence the complete gelation of the droplet can take an extended time. Hydrolysis of the TEOS produces alcohol (ethanol), and siloxane bridging liberates water. Quenching the gelation process can be accomplished by removing the base, and for full condensation of a completely gelled particle or of the shell of a hollow particle, the ethanol and water produced by the hydrolysis and siloxane bond formation have to be removed.

Encapsulation of hydrophobically modified quantum dots in fully gelled and hollow particles is accomplished by dispersing the nanoparticles into the neat TEOS solution. As the TEOS is hydrophobic, the nanoparticles can retreat into the TEOS core as the gelation proceeds. Alternatively, if the gelation process is rapid enough and networks around the nanocrystals, some of the crystals can become incorporated into the evolving gel in a spatially uniform way. Their disposition in the finally processed bead

after the gelation has been quenched is dependent on the extent of gelation. Particles consisting of shells encapsulating liquid TEOS retain some of the QDs in the liquid core; with time for beads suspended in an aqueous phase, the TEOS core fluid exchanges with the aqueous phase and the nanoparticles come out of solution since they cannot disperse in the aqueous phase. As will be demonstrated, the QDs become aggregated, and accumulate on the inside surface of the shell. Alternatively, if the beads are dried, then the TEOS/octylamine core eventually evaporates and the QDs one again aggregate on the inside surface of the shell. For the completely gelled particles, the nanoparticles are trapped in the silica gel matrix. The QDs can remain unaggregated in the matrix if the gelation matrix forms around the nanoparticles as mentioned previously. From the point of view of eliminating resonance energy transfer between mixtures of QDs for spectral encoding, the fully gelled particles have the most potential since they can remain unaggregated and attendant FRET with degradation of the spectral label is minimal. For hollow silica particles, the dispersal of the QDs in the (TEOS/Octylamine) fluid core of the hollow particles is unstable, and the QDs eventually aggregate on the inside surface of the shell (with attendant FRET) during the exchange of the TEOS interior with water or by evaporation.

An important issue in the encapsulation of the QDs in the silica beads by this emulsion/suspension route is the time of exposure of the nanoparticles to chemically damaging environments in the precursor droplets as the gelation proceeds. For a bead based microarray system where the QDs are sequestered in the silica matrix, stability of the nanoparticles in these systems is obviously of primary importance prior to and during the growth of the shell at the interface. This necessitates, in the case of silica which is

biologically friendly, that certain parameters be met, mainly the optimal control of the pH in the two step process for fastest gelation time of the solgel[94, 95, 97] and solvation of these hydrophobic nanoparticles in the droplet[54]. This requires that we have an accelerated process for silica growth both by the two-step process and catalyst.

The key is to find an accelerant that will provide a rather fast gelation within a limited diffusion time (potent catalyst) and one that is amphiphilic (can be partitioned into both oil and aqueous phases). To this extent octylamine was used as the gelation accelerating chemical[47, 48, 98]. Alkylamines have been used extensively to synthesize silica and other metaloxides[99]. Singh and Kosuge, and Chen et al separately synthesized hollow particles using octylamine as the structure-directing agent without the need to use an organic external phase to maintain the surface tension of the droplets. These experiments were carried out without any traditional alcohol[96] solvent and the thickness of the shell was controlled by the amount of TEOS used in the reaction. The initial process requires HCl where the hydrolysis rate is dominant followed by the addition of the octylamine and stirred for long period. Here it is believed that silicic acid, which at this pH range is positively charged, is attracted electrostatically to the protonated amine template. These authors followed the same procedure and recipe on a later paper but added a small molar ratio of ethanol[96] to lower the polarity of the solution and prevent smaller particle density, thus resulting in a more uniform size distribution. Cheng et al worked out a TEOS to octylamine ratio that when varied from 1-4 results in hollow to solid spheres, respectively[100]. Water content in the reaction vessel of the emulsion of utmost importance since hydrolysis of TEOS molecules sets off the first kinetic reaction, depending on the

pH scale that the water is set to, which determines the extent and nature of the silicate to be produced.

The spherical products obtained by octylamine templating produce a more uniform particle size distribution than other amines without necessitating an assisting platform other than its own liquid crystal (LC) phase[27], and with modifications to the molar ratios of H_20:Si (Rw) ratio, TEOS/OA (Rb), pH concentration (Ra) and the use of a solvating agent. Solvents are added to prevent liquid-liquid phase separation during the initial stages of the hydrolysis reaction (ternary-phase diagram) and these help control the increasing concentration of silicates and water being formed by the hydrolysis reactions that lead to gelation. In 1999, Antonelli[49] used the same approach to synthesize titanium isopropoxide with dodecylamine as the templating agent. Later Singh was the first to synthesize, using the same concept, silica hard spheres with several tens of micrometers in diameter as well as Brinker[101] did. By changing chemical compositions or mixing orders, Singh developed differing particle morphogenesis. The ability to use extreme sides of the pH scale to accentuate or separate either kinetic reaction is very useful in controlling the final product, and to, in the case of controlled dispersion methods such as flow focusing, maintain an electrostatically neutral environment to create the droplet, but ultimately for a particle based barcode the liquid phase must be condensed and the path for most material undergoing liquid-solid phase transitions is a gel.

Gelation enhancement has many parameters that can be tailored to refined specifications. As a function of pH, the maximum gelling rate for silicic acid- or silanols depending on the extent of hydrolysis- is around pH 3-4 and depending on the type of solvent and efficiency of catalyst is around pH 6. Kinetic hydrolysis of TEOS is fastest at

about pH 1.5 and condensation is best enhanced in an alkaline environment. Substantial research has been made towards using amines to synthesize metal oxides[99]. At these and other mild biological pHs Mizutani[102, 103]showed that, at pH 8.5, longer chain polyamines are significantly more effective at inducing silica precipitation from sodium silicate solutions than their monoamine counterparts. Primary amines react slower than secondary and tertiary amines[48, 103], octylamine[46, 48] was the best suited candidate as its amphiphilic properties provide the required solubility in both phases- lipophilic when not protonated and also highly hygroscopic when in contact with aqueous phase. This dual phase solubility makes it the ideal candidate to drive condensation in QD embedded silica droplets.

To use octylamine to accelerate the gelation process, the amine is dissolved in TEOS to form the hydrophobic phase that is then dispersed in the aqueous phase. The ratio of octylamine to TEOS in the dispersed phase is used to gel hollow and completely condensed particles. When the amine to TEOS ratio is large, there is not sufficient amount of TEOS to completely gel the particle. As the shell forms and gelation proceeds inward, the core is depleted of TEOS, and the particle evolves into a core shell structure in which a silica shell surrounds a liquid core of predominately octylamine. The QDs are either embedded in the shell or dispersed in the core. Further processing in which the amine is allowed to evaporate leads to a hollow particle with the QDs adhered to the inside surface of the shell. In the case of a low ratio of octlylamine to TEOS, the particles gel completely.

3.2 Experimental Section

3.2.1 Materials

Tetraethylorthosilane (TEOS) was obtained from Gelest Inc., octylamine 99+% from Acros, HCl 37% (ACS Reagent) from Sigma Aldrich. The quantum dot nanoparticles used were "Hops Yellow" with a spectral emission peak at 559 nm QD and "Maple Red-Orange" with a spectral emission peak at 616 nm. These are CdSe/ZnS core-shell nanoparticles with a hydrophobic TOPO covered coat from Evident Technologies, with the spectral emissions as characterized by the manufacturer. Deionized (DI) water with a resistivity close to 18 MΩ·cm was obtained using a Millipore system. All chemicals were used as is without further purification.

3.2.2 Experimental Procedure

An emulsion/suspension method following the procedures described by Cheng et al.[100] and discussed above was used to trap the QDs in the silica matrix. This methodology hinges on the use of proper pH control for both maximum kinetic hydrolysis of silica precursor and the use of a highly concentrated amount of octylamine for both the structure supporting LC phase and the pH required for condensation. The QDs as obtained from the manufacturer are suspended in toluene with spectral emission peaks at 559 nm and 616 nm. Here we used a ratio of 3:1 QDs emitting in the yellow region of the UV-vis and red emitting QDs, respectively. These are dispersed in the droplet phase. The total concentration for each type of QD was 6.12×10^{-7} M in the droplet phase. The hydrophobic droplet phase of the emulsion consists of and was prepared as follows: The QDs were dispersed in the mixture of TEOS (4.49 mL) and octylamine (4.54 mL) for 3 minutes in a 100 mL volume beaker with a magnetic stirrer at a 600 rpm rotation for hollow beads.

For preparation of the emulsion for hollow bead synthesis, the molar ratio of octyl

amine to TEOS is 1.36 to 1; TEOS (4.49 mL) and octylamine (4.54 mL) the total volume of this hydrophobic phase was 9.03 mL. A volume of 41.12 mL of 0.05 mol of concentrated HCl solution was added to the TEOS solution containing the QDs to form the emulsion, and the gelation reaction was allowed to proceed for 5 minutes while mechanically mixed. Separation of beads by suction was followed using 5 μm TMTP Millipore membrane filters. Air-drying proceeded for a few minutes before placement of sample in confocal light scanning microscopy (CLSM) for spectral emission analysis as described below. Particle size distribution was very broad as characterized by optical microscopy. The beads were stored in a plastic Petri dish.

For the synthesis of the solid microbeads, a solution was made with five times the volume of the TEOS used in the hollow beads synthesis to form solid beads. The synthesis method for the solid spheres is the same as the one described above for the hollow spheres that Cheng et al developed. The loading of QDs here was the same, 6.12 x 10^{-7} M at the 3:1 ratio as the hollow spheres.

3.2.3 Confocal Microscopy Characterization of the Emission Spectra of Embedded QDs in Beads.

Confocal light scanning microscopy (CLSM; Leica TCS SP2 AOBS, with an acoustic-optical beam splitter and a prism spectrophotometer detector) was used to characterize both the size of the beads and luminescence emanating from QDs both in the hydrophobic dispersed phase silica solution and the silica beads. The size of the beads does not allow for dynamic light scattering measurements as they are micron size. Spectral representation of the distribution of QDs in their respective environments was obtained as well as the ratio-metric barcodes. The background photoluminescence

spectrum (PL) of QDs in the appropriate loading concentration and in the beads was performed. Spectrofluorometry was done with CLSM.

3.3 Results and Discussions

The first set of results concern the microbeads which are completely gelled. These dichromatic loaded beads were dispersed in bulk monomer mixtures of the neat TEOS/octylamine silica solution and characterized using optical microscopy (Fig 3.1), CLSM (Fig 3.2) and scanning electron microscopy (SEM) (Fig 3.3). The SEM of the reprsentative microbead shows a particle approximately 30 um in diameter with a relative smooth surface. The optical microscopy of the collection of beads shows a broad size distribution ranging from about 25-50 um in diameter. This is characteristic of a size distribution that results from batch emulsification (fig 3.4). Silica is an optically transparent material and that is demonstrated with the optical micrograph. Fig 3.3, the confocal micrograph, shows the active emission of a group of silica beads encoded with the QDs, demonstrating that the QDs retain their photoluminescence (PL) property when embedded in the silica matrix. Importantly, in the picture, all beads show luminescence indicating that the QDs were present in all the precurser droplets. Fig 3.5 is a histogram of the beads in confocal micograph (fig 3.3) showing the particle distribution of 21 silica beads. The polydispersity can be seen to be very broad.

A magnified view of the fluorescence of a completely gelled bead prepared under identical conditions is given in the CLSM image of Figure 3.6. This detailed view shows a ‘patchy’ spatial photoluminescence, indicating a patchwork of higher luminescence. The formation of inclusions of QDs in the silica matrix of the microbead as evidenced in Figure 3.6 is considered with reference to their uniform dispersal in toluene where

confocal images of the toluene solution (not shown) show a uniform luminescence. The patchiness can be due to several reasons: Inclusions of the QDs can be due to the high viscosity of the new octylamine/TEOS precursor solution which makes their dispersal difficult, the change in the solvent polarity, and rapid internal inhomogeneous structuring of the silica matrix. The most straightforward explanation of this pattern is the latter, that the nanocrystals have aggregated inside the still liquid droplet into inclusions as they gel. It is believed that the inhomogeneity is due to differing kinetic rates of gelation leading to condensation of the silica matrix. The two rates exist due to a partial absorbance of moisture by the octylamine from the environment ionizing it and, thus when the octylamine/TEOS/QDs mixture is first stirred for the few minutes before adding the low pH aqueous solution, the hydrolysis of the TEOS by the absorbed moisture has a head start over the other parts of the oil droplet. With the presence of the octylamine and the hydrolyzing TEOS it creates inclusions due to the low solubility of the now polar molecules (ionized octylamine and prehydrolyzed TEOS) in the rest of the oil phase. In this circle of influence - the inclusions- where the kinetics of hydrolysis and condensation are off, the nanocrystals that happen to be placed there initially are now entrapped by the growing gel and ultimately the condensed matrix of the silica bead. This area where the kinetics was much faster than in the rest of the bead is restrictive to the nanocrystals due to their hydrophobic capping and they are confined by this environment to a much closer distance than in the first solid sphere without inclusions, as proof by their patchy areas showing increased PL signal.

The photoluminescence spectra of the solid beads (fig 3.4) provides additional insight into the disposition of the QDs in the matrix. In Fig. 3.4 is first presented the

spectra of the QD mixture as recorded in toluene which can be regarded as the PL of the unaggregated nanocrystals in a solvent which does not alter the luminescence properties of the nanocrystal. The PL data in Figure 3.4 has been normalized so that the area under the curves is unity. The spectra in the solid beads shows a blue shift and a broadening of the peaks, indicating decreased photoluminescence at the emission peaks. Yet Forster Resonance Energy transfer (FRET) from the smaller wavelength emitting QDs (559 nm) to the higher emitting QDs (616 nm) is not very evident. In fact, if, as detailed in Table 3.1 the spectra of the background and the bead spectra are fit to Gaussian distributions centered about each of the peaks in the emission spectra, and the area under the fits for each Gaussian computed, the ratio of the emission of the shorter wavelength emitting QDs to the longer wavelength emitting QDs is slightly less in the background than in the beads. As discussed earlier in Chapter 2, Forster Resonance Energy Transfer (FRET) is from the shorter emitters (donors) to the longer emitters (acceptors), so this small difference cannot be attributed to FRET. It is well known that the quantum yield (QY) of CdSe/ZnS nanocrystals decreases to some degree depending on the methodology and system used to encapsulate the QDs. The entire literature that deals with encapsulating QDs in silica matrix, whether it is by surface functionalization, coating or reverse emulsions, indicates that the QY indeed goes down. However the blue shifting of the emission of the QDs is more difficult to explain. As it is known, and the reason for why toluene was chosen as a solvating liquid for the hydrophobically capped QDs, is that it doesn't interact strongly with the nanocrystal surface where much of the trapped states are found which diminish the Photoluminescene (PL) of the QDs. When these solvency parameters are changed the PL of the nanocrystals could change in both intensity and

bandgap emission. Properties of the dielectric environment directly influence the power law emission that is identified in terms of a photoinduced ionization process that charges the QD. These can be a multiplicity of reasons depending on how the molecules of the sorrounding media interact with both the capping agents (TOPO and HDA) and when or if the surface of the nanocrystal is exposed its interaction with the trapped states that are dictated by the quantum confinement effect. When the potential of the media changes then the bandgap of the nanocrystal will shift to accommodate the new wavefunctions that are influencing its energy levels. The change of the PL spectra from the reference may more likely be due to these reasons rather than FRET. Various and more methodical experiments are required to unambiguously answer the question of the interaction and effects of the molecules in the solution consisting of TEOS and octylamine with the surface of the nanocrystal. It is observed that the shift of the PL of the embedded QDs in the beads is close to its original emission spectra and hints at the high kinetic reaction of both the hydrolysis step and condensation of the TEOS in this suspension method. This speedy reaction removes the shifting of the QDs bandgap leaving behind a signature very close to the original of the QDs. This PL only changes by a few nanometers and it ensures that little change has taken place on the surface of the nanocrystal. The diminishing QY is still existent but it is not a detriment to the fluorescence of the QDs spectra in each individual bead.

Transmission and confocal fluorescence spectra of hollow microbeads are shown in Figure 3.7a-c, and the PL for different regions of the hollow bead is given in Figure 3.8. These spectra are once again normalized using Gaussian fits as described earlier. The photoluminescence spectum of the hollow beads is significantly different from the solid

beads. In the latter case, the photoluminescence was distributed throughout the equatorial cross section as imaged in the micrograph. Patches of greater luminescence indicated aggregated regions. For the hollow spheres, the core of the bead is shown to be completely devoid of luminescence, indicating that there are relatively few QDs in the core. The core is surrounded by an annular region of high luminescence and this in turn is surrounded by a second annular region of reduced fluorescence. This distribution reflects the gelation process of the hollow beads, as was discussed mechanistically in the first section of this chapter. In the case of the synthesis of the hollow spheres, the gelation process that begins at the precursor drop periphery does not extend all the way into the center as it does for the solid beads. As a result the core remains fluid-like, containing the unreacted TEOS and octylamine. Some QDs have been trapped in the silica shell, as they are trapped in the entirety of the solid bead. However, the remainder of the QDs is situated in the fluid core. The beads after gelation are suspended in an aqueous solution, and the TEOS/octylamine core exchanges with the large reservoir of aqueous solution. As a result, the QDs in the hydrophobic core fall out of solution as the core changes to water since the hydrophobic QDs are not compatible with the more polar aqueous environment. The only place for the QDs to locate after no longer being able to be dispersed in the core is as the aqueous/annular shell interface, and this explains the high luminescence of this region as is clear from Fig. 3.6b. This dropping out of solution of the QDs and their relocation at the shell/aqueous core interface is also supported by the luminescence spectrum taken in the region of interest of the hollow part of the bead, i.e. the bright annular region between the core and the shell. This region shows very little luminescence of the shorter wavelength emitting QDs relative to the longer wavelength

QDs, as also indicated by the ratio of areas of the two peaks (Table 3.1) for luminescence measured in the region of interest corresponding to the bright annular space. Between the shell and the dark core. QDs which have fallen out of the core as its polarity changes become situated on the inside surface of the shell where they aggregate, giving rise to FRET which accounts for the reduced emission of the shorter wavelength emitting QDs. The ratio of the areas under the emission spectra for these two QDs for the area of interest corresponding to the shell resembles that of the solid bead, providing further support that the gelation of the hollow shells proceeds as in the solid beads from the periphery to the core center, with QDs incorporated into the evolving silica matrix and the gelation front moves inward. It is observed that the shift of the PL of the embedded QDs in the beads is close to its original emission spectra and hints at the high kinetic reaction of both the hydrolysis step and condensation of the TEOS in this suspension method. It is noteworthy to point out the hollowness of some of the beads in the 1:1.36 molar ratio of TEOS to OA. . In summary, these hollow particles demonstrate a rather large resonant energy transfer at the region of hollow topography. This can be attributed to the crashing out of the QDs as the solvent evaporated and there was no matrix developed to sustain the QDs individually, as the CLSM and optical micrographs show the inhomogeneity both physically and spectrally. Table 3.1 quantitatively shows the normalized areas of solid bead and all the hollow sphere areas under the curves. In these two beads the relative unchanged PL emission shown as a total of the areas under the peaks shows there is not much change in the total signature of the beads even when there is a limited amount of morphological change. However, as will be explained below, when there is extreme inclusions of the QDs in the silica matrix the Gaussian curves are lost

and the original barcode is lost as the signal from the donating QDs (the smaller wavelength emitting nanocrystal) it almost disappears.

To emphasize the effect that solvency has by way of preventing ionization or hydrolysis of either the octylamine and TEOS fig 3.9 shows a 'very patchy' solid bead that was synthesized the same was as the other solid beads. As can be seen from the CLSM there is extreme inclusions of the nanocrystals inside this bead leading to great changes to the PL spectra of the various regions in this particle. The changes were so drastic that normalization of the data for the peaks of the areas of the bead was not practical. For reference, a graph showing an area of the bead where there seemed not to be a great deal of PL emission (fig 3.10) is presented though, note, not normalized. This suggests an even larger amount of moisture was absorbed by the octylamine as suggested by the extremely bounded PL areas. To note, a reference to chapter 4, fig 4.8 here is now made. The spectra in both cases look alike but the resons for why there are inclusions in the bead in chapter 4 is different than here and will be discussed in greater detail.

The resonant energy transfer can also be noticed at the edges of the solid beads by the higher PL intensity in those areas. This of course, is an effect of the longer contact of the TEOS/ OA with the pH 1.5 aqueous solution. The faster effect of hydrolysis at the initial pH combined with the high solubility of OA in water, which raises the pH to a level that enhances the condensation kinetics, confluence to trap the QDs at the edges in a tighter matrix thus reducing their spacing and causing resonant energy transfer. It is unknown to the author as to why in the solid beads a continuous homogeneous ring of resonant energy transfer, as shown in the hollow spheres, is not form since the entire surface of the beads are in contact with the initially low pH aqueous solution. It is

assumed that the lower amount of TEOS in the synthesis of the hollow beads creates a diffusion- limited condensation of the partially hydrolyzed TEOS forming the matrix and the faster ionization and diffusion of the octylamine out of the beads leaves behind a depleted region as there is not enough material to catalyze. While the reaction continues for the 5 minutes that is required to create the solidification of the silica there is a limit of the amount of the octylamine that diffuses out due to its limited solubility. This amount of octylamine that has been ionized, it is argued by Kosuge, and Cheng et al., that provides the structure-directing system to create spheres. However, an averaged PL of the entire bead resembles the original PL spectra in the background.

Additionally, the SEM pictures of the silica beads shows that a rather smooth surface is obtain from this synthesis. A smooth surface indicates a molecular level reaction and it portents to present itself as a method for creating lipobeads.

3.4 Conclusion

Retaining PL spectra that does not change for the encapsulated QDs in the silica matrix is only one of the necessary requirements for optical use of these beads. The optical transparency and maintenance of the spectral code paves the road to abilitate the use of these QDs as tracers for indexing of each individual bead. Nonetheless the application of encapsulating multiple quantum dots in a silica matrix without the need to chemically change the QDs to place them in the silica is proven here and also as a facile way of making these beads. Such an entity has been heralded as the application needed to overcome the notorious impediment when it comes to creating a barcode. A lipobead based array requires that a multitude of codes be created to deal with the onerous amount of information needed to establish a methodical analysis of interactions with this

surrogate cell membrane. However the large population dispersion is a great obstacle to use these beads in technologies now ubiquitous with assaying methods, and the requirement is to create a population distribution tight enough to advance the notion of a lipobead based array. Additionally, the solubility of the capping agents of the nanocrystals is a key factor to determine whether the encoding inside the beads will result in a working barcode.

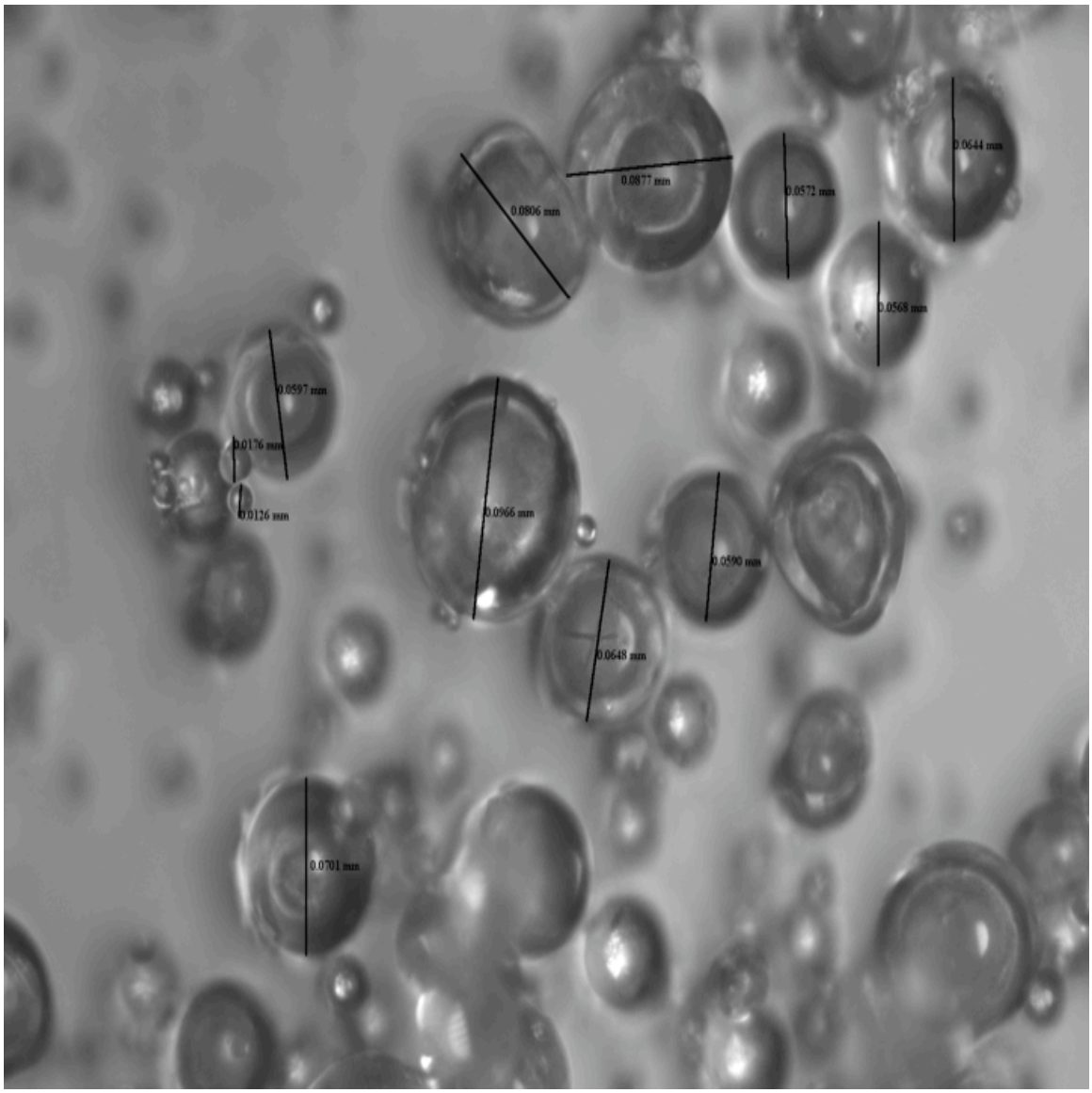

Figure 3.1. Optical micrograph of silica beads. Notice that silica is an optically transparent material. 4:1 TEOS/Octylamine molar ratio 4:1 TEOS/Octylamine molar ratio emulsion/suspension beads.beads. Notice large polydispersity due to emulsion method.

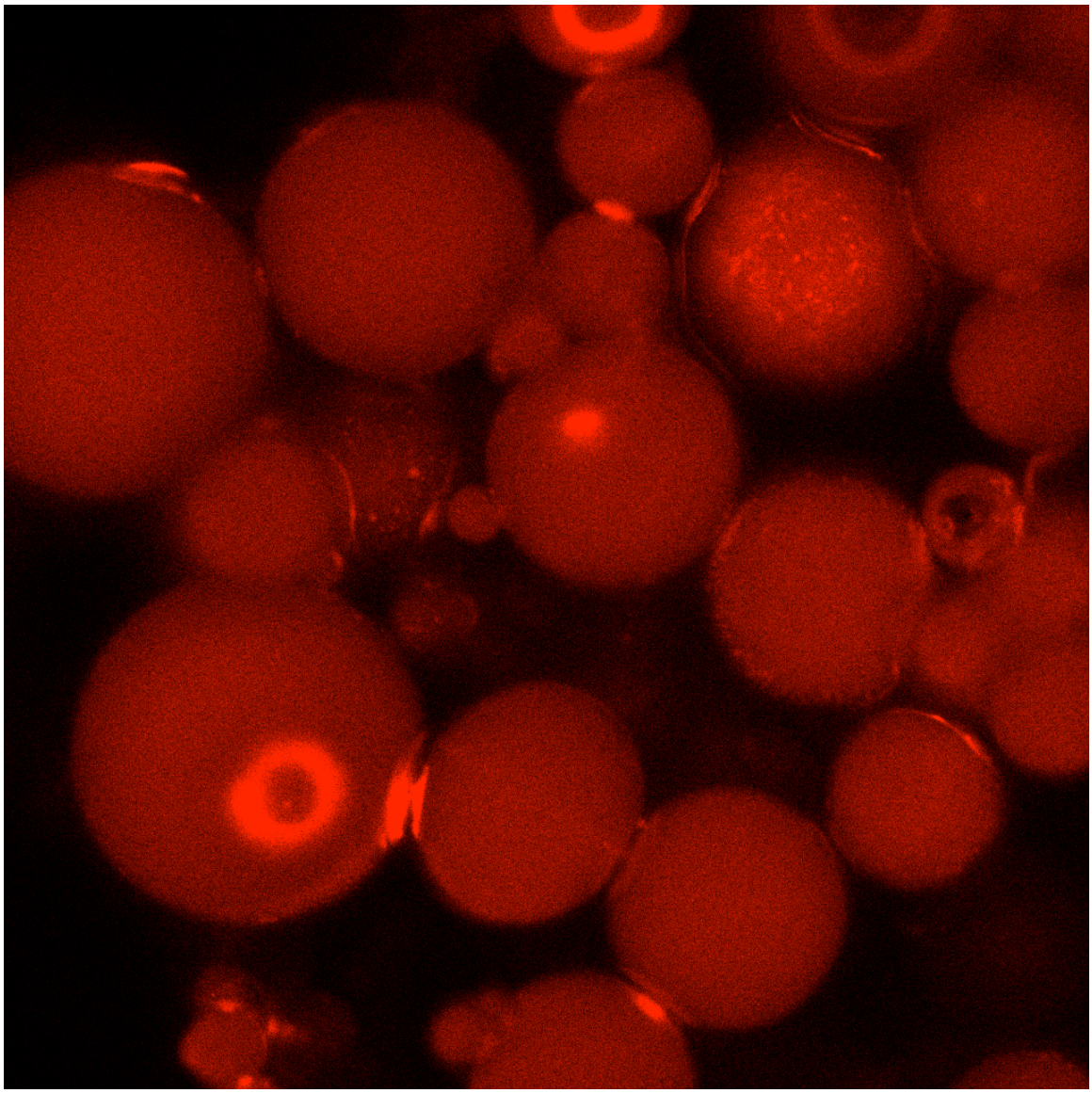

Figure 3.2. CLSM micrograph PL Emission of Emulsion/Suspension 3:1 560/620 nm QDs solid silica beads. Under 10x magnification. Note that all the silica beads show PL.

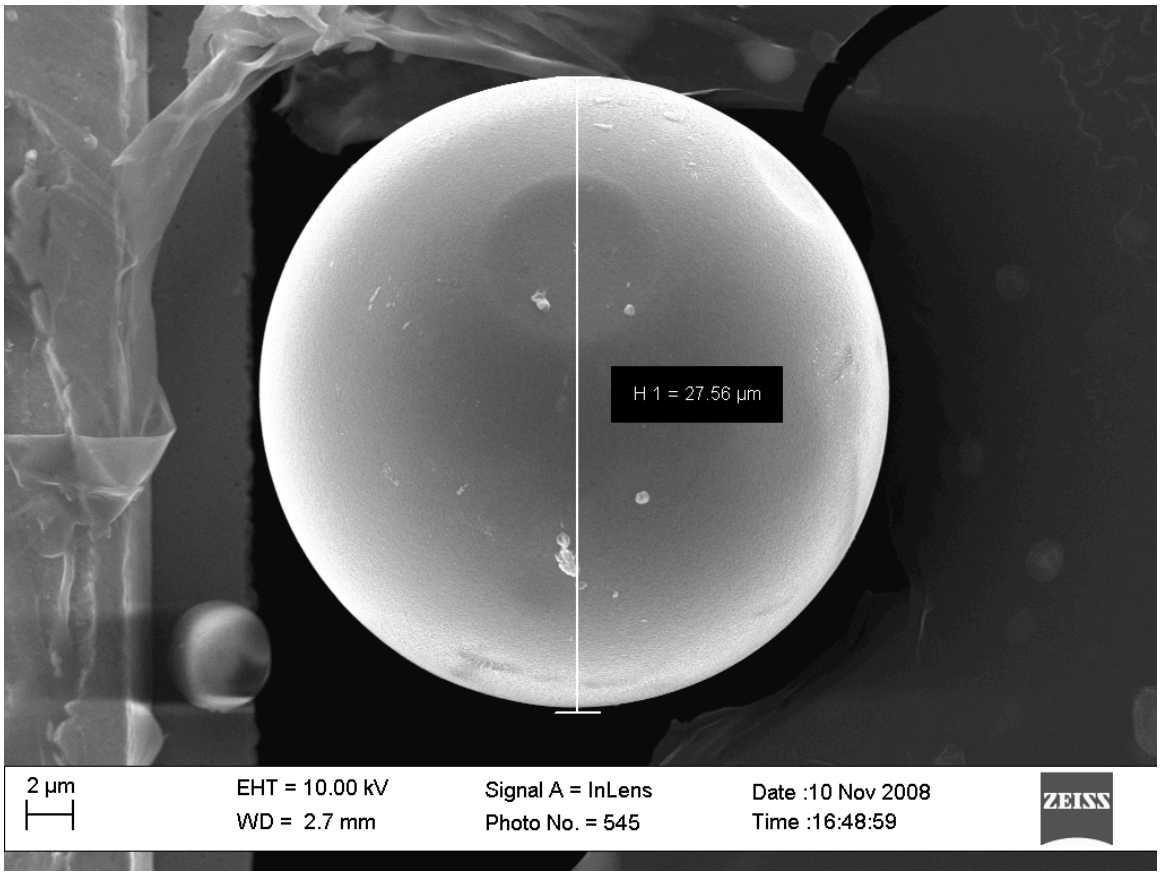

Figure 3.3. SEM micrograph of Suspension Silica Bead. Notice the smooth edges that the bead displays.

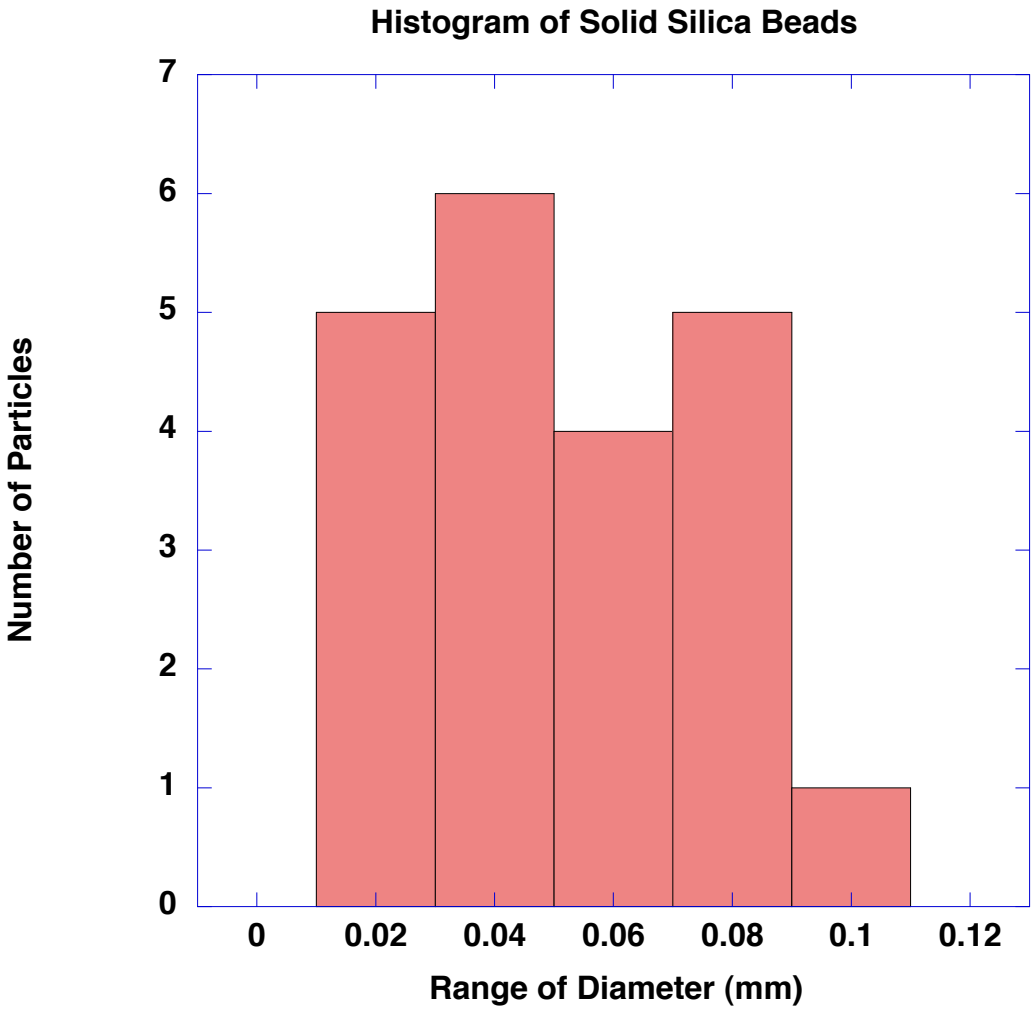

Fig 3.4. Histogram of Particle size of Solid Silica Beads prepared with 4:1 TEOS/Octylamine. Total count of particles was 21.

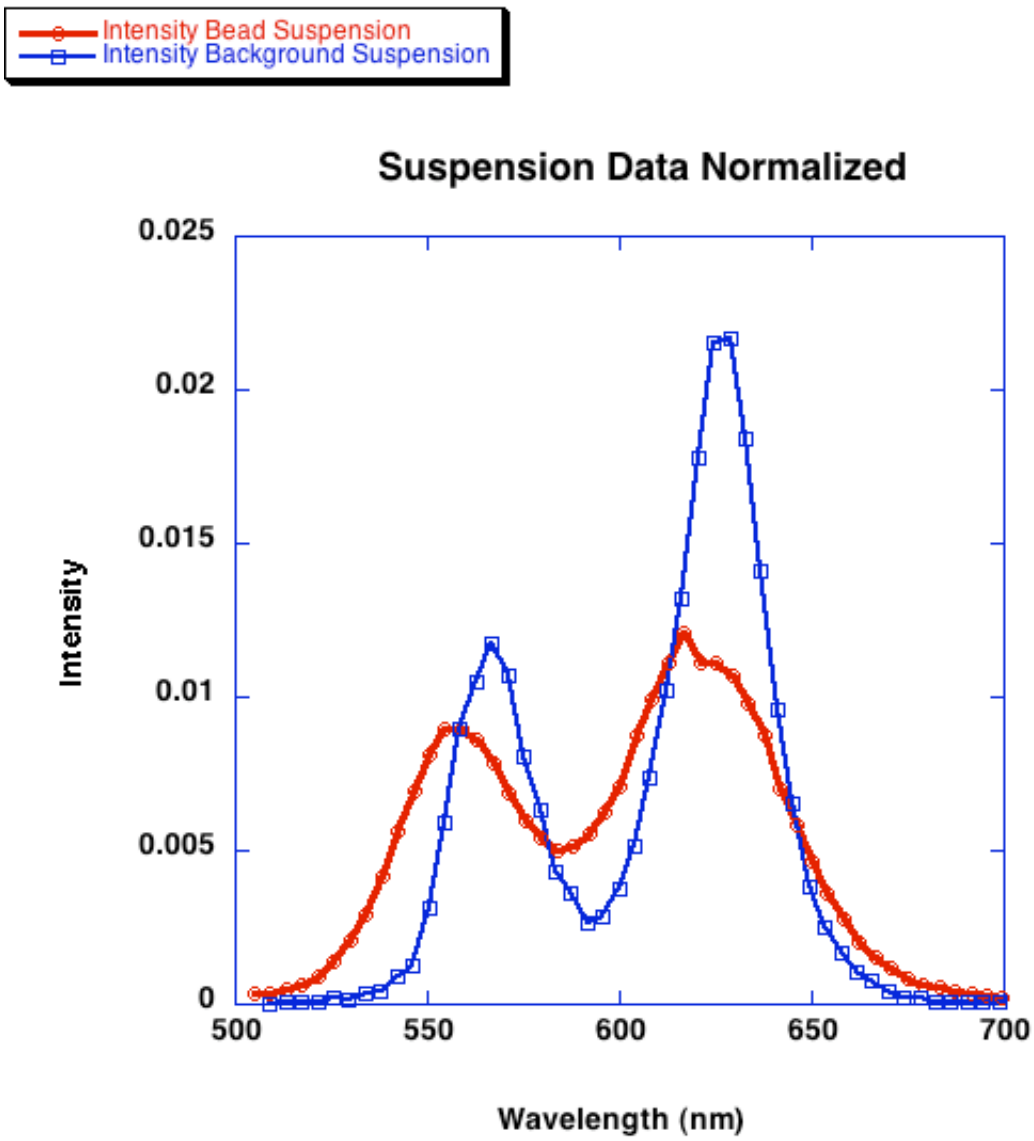

Figure 3.5. PL emission of Suspension of Silica Bead and background. Notice the PL inside the silica bead retains the original spectra. There is a blue shift due to the direct synthesis of TEOS in the presence of QDs.

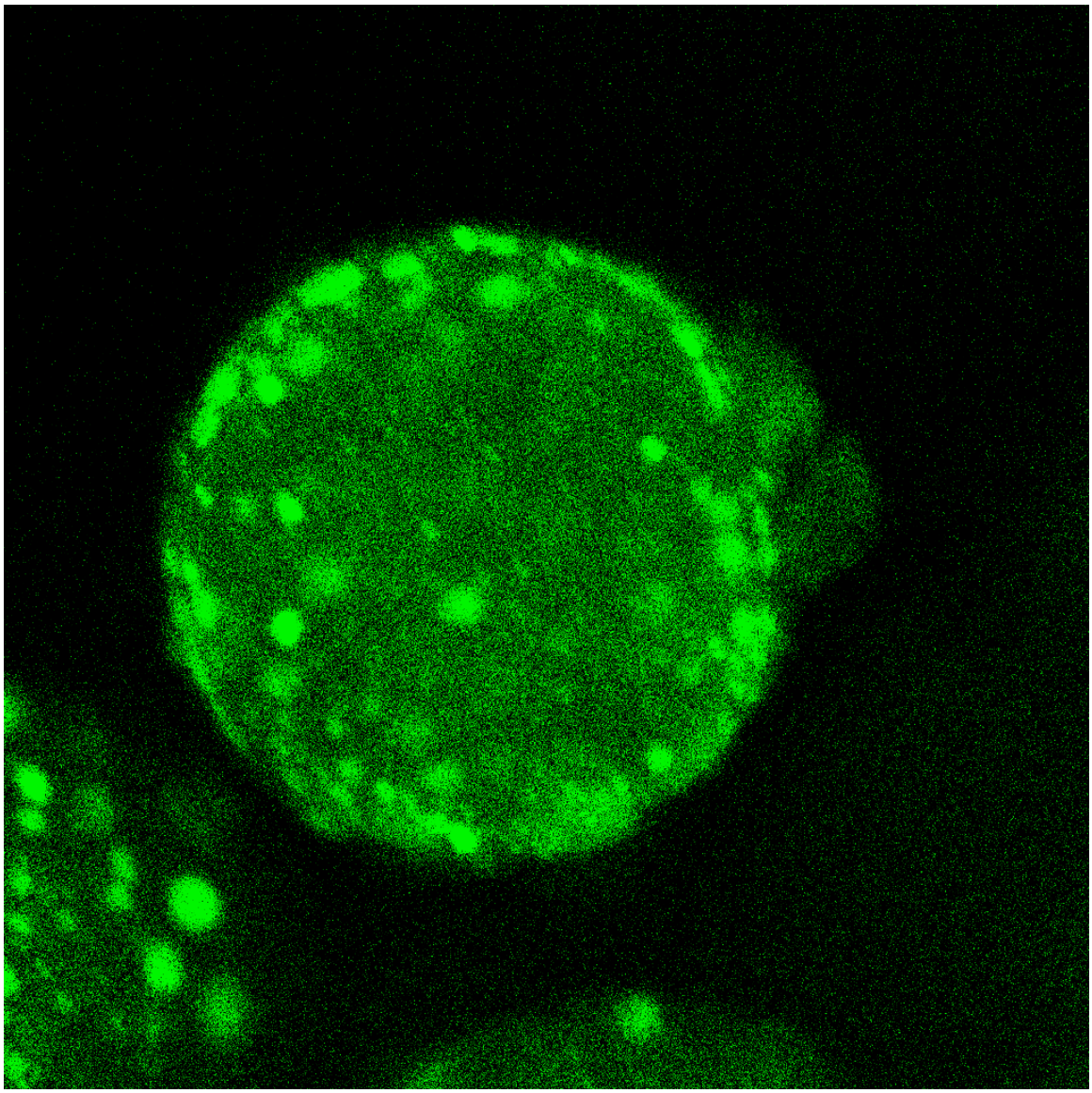

Figure 3.6. CLSM of "Patchy' PL Emission of Solid (4:1 TEOS/Octylamine molar ratio) Suspension Silica Bead. Notice the inclusions throughout the bead. Here the inclusions are not limited to the edges.

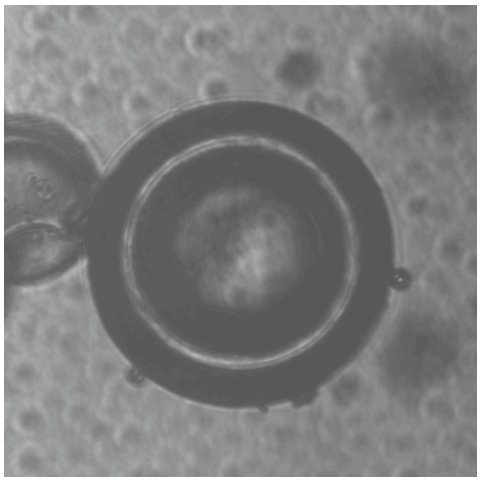

Figure 3.7a. CLSM Transmission micrograph of hollow sphere. 1:1.36 TEOS/Octylamine molar ratio.

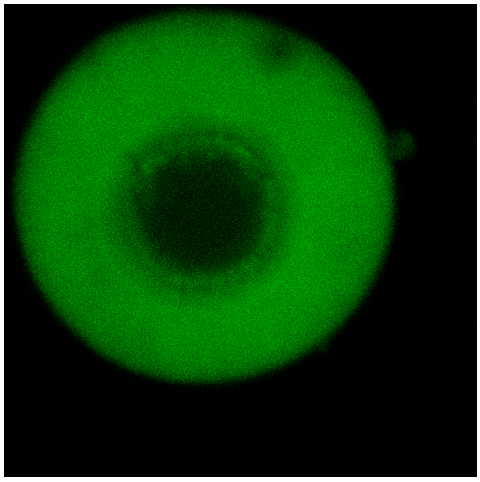

Figure 3.7b. CLSM micrograph PL emission at 560 nm of hollow of sphere.

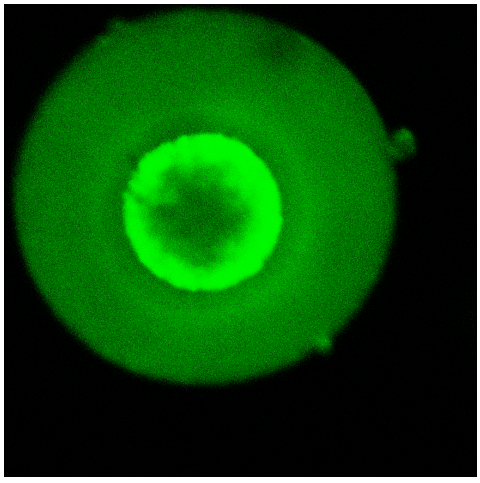

Figure 3.7c. CLSM micrograph PL emission at 620 nm of hollow of sphere.

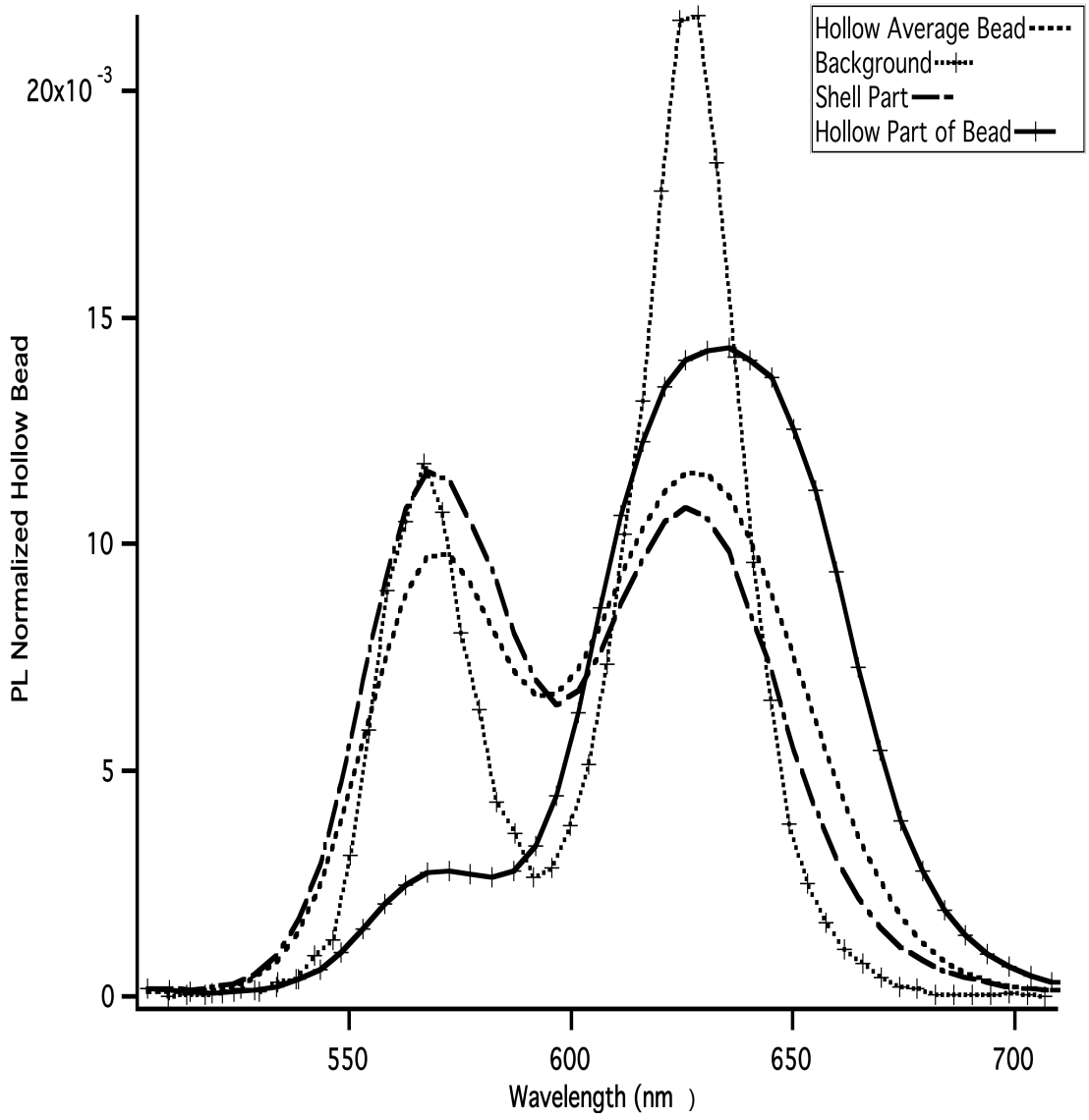

Figure 3.8. PL Emissions of hollow sphere and the 3 parts of interest in the bead. The shell and the overall average of the bead retain the shape of the background signature spectra, however, the PL of the hollow area of the bead varies considerably from the others.

Beads	Area 1	Area 2	Total Area
Background	0.31095	0.63284	0.94379
Solid	0.34282	0.57233	0.91515
Hollow Entire Bead	0.33183	0.66817	1.00000
Hollow Part	0.06427	0.93565	0.99992
Hollow Shell Part	0.441	0.558	0.999
Patchy 2 Beads	0.067489	0.9325	0.9999
Patchy 2 Clear Area	0.01974	0.97937	0.9911
Patchy Clustered Area	0.3247	1.6459	*1.96*

Table 3.1. Normalized areas under the curves of the solid bead, hollow and patchy Silica beads. They all are very close to 1 except when the

FRET distorts the peaks where it is no longer a Gaussian as seen by the Patchy Clustered Area.

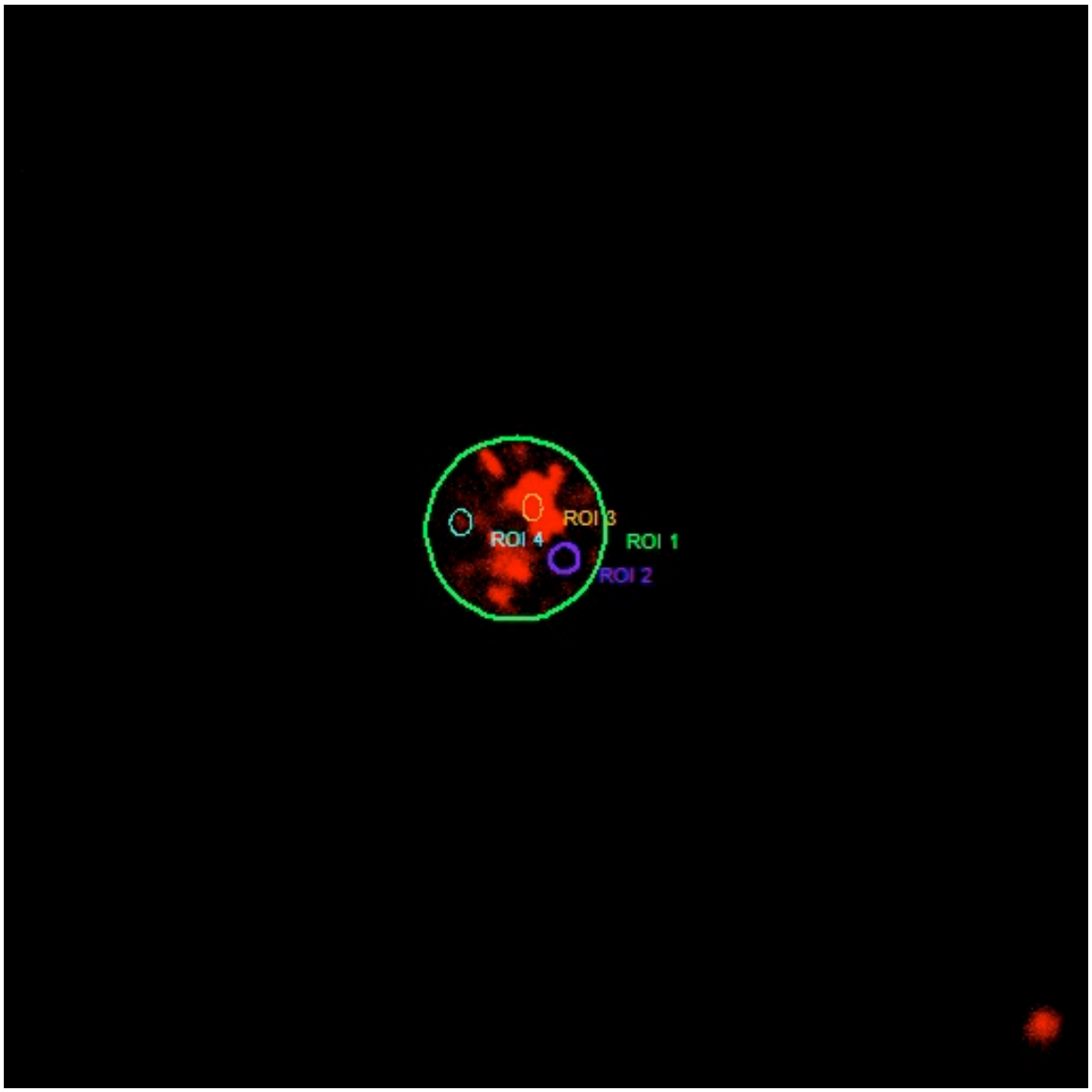

Fig 3.9. CLSM of “very” patchy particles. Notice the inclusions that aggregates are more pronounced than the previous patchy bead.

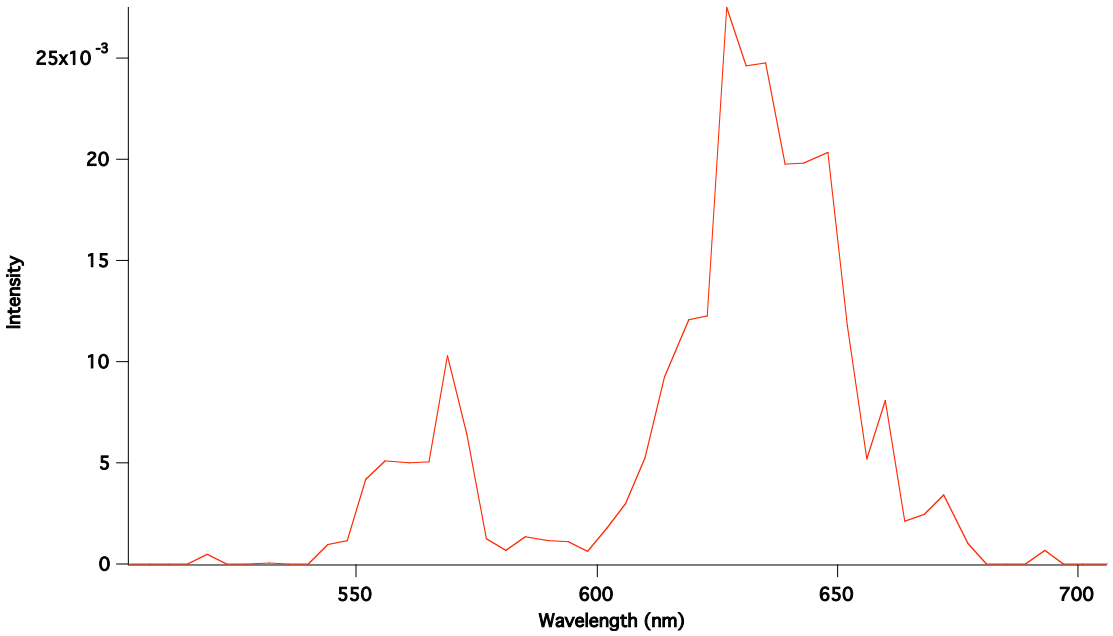

Figure 3.10. PL of 'very' patcy bead. The area of interest was the purple area in figure 3.5. It is not a small area but the signal to noise ratio is really large as there are very few nanocrystals in that area as well as FRET.

Chapter 4

Microfluidic Generation of Silica Beads with Encapsulated Quantum Dots

4.1 The Advantages of the Microfluidic Production of Particles

In this chapter, we employ the same general concept as in Chapter 3 of making spectrally encoded microbeads by gelling precursor silica droplets laden with quantum dots, but use microfluidic flow-focusing to create the precursor silica droplets. The intent of this chapter is to develop an additional method for the manufacture of QD encoded microbeads which improves on the properties of the microbeads fabricated in the previous chapter, and thereby furthers the development of a legitimate and more functional bead based array. To summarize again, the encoded beads for a bead-based microarray are required to have three key properties: (1) the beads should be approximately 10-100 microns in size to miniaturize the screening, and to be compatible with flow cytometers and wafer micro-arrays. The size distribution of the beads should be very narrow so that the spectral label is not distorted. (2) The beads should be encoded with a scheme that allows for a large encoding capacity. (3) The beads should be made of a material that allows for easy probe conjugation. In the previous chapter, emulsion droplets of (hydrophobic) tetra-alkoxysilanes (particularly tetra-ethoxysilanes, TEOS) with dispersed hydrophobic QDs in water were formed by the batch stirring of the TEOS into water. The TEOS droplets then condensed into silica beads by transport of water from the outside continuous aqueous phase into the droplet interior. Water transport into the TEOS droplets hydrolyzed the TEOS into silanols, allowing for gelation through the formation of siloxane linkages and matrix formation. The QDs became incorporated into the matrix, as they cannot escape the droplet due to their poor water solubility. In this

droplet emulsification/gelation or suspension polymerization method, the beads formed properly encapsulated the QDs to form a barcode, but the size distribution of the microbeads was wide due to the fact that the stirring method used to produce the pre-cursor emulsion droplets retained a wide size distribution.

Here we describe the process in which, by the use of a microfluidic flow-focusing device, an emulsion of uniformally sized precursor silica droplets are formed in an immiscible continuous phase, and subsequently gelled into silica particles. In the production of the emulsion by microfluidic flow-focusing, the silica precursor liquid and the continuous phase are brought together from separate inlets into a two dimensional core-outer fluid flow arrangement at an orifice, with the precursor in the core and the continuous phase in the outer region nearest the wall. (See Figures 4.1 and 4.2 for a schematic of the microfluidic cell.) As this core-inner fluid flow passes through the orifice, the continuous phase stretches and breaks the precursor liquid into droplets of uniform size which move through the channel downstream of the orifice as a train of droplets. Their individual production, undertaken in a repeatable manner due to the constancy of the flow conditions, insures the production of droplets with a monodisperse size with a variation of typically less than five percent. The droplets then move single file downstream from the orifice. In microfluidic cells made using soft lithography techniques (as undertaken here), the orifice and channels are rectangular in cross section with constant heights. Typically, the orifice is 50 μm in width and 100 μm in height, and the channels approximately 200 μm in width and 100 μm height. Relative to the QD encoded microbeads prepared from emulsion droplets formed by stirring in a batch process, this microfluidic based approach not only encapsulates QDs into a silica matrix

formed as a bead, but fulfills the requirement of monodispersity in the bead size distribution. The microfluidic method has been used to produce solid polymer particles by thermally or photo polymerizing the pre-polymer monomer droplets, either downstream of the orifice or when collected in a receptacle.

4.2 Emulsion Design and Gelation Methods in the Microfluidic Production of Silica Particles

The application of microfluidic flow focusing to the production of silica particles is more involved because of the complexities of the silica gelling process, and, as we describe in the following, only two studies have attempted to form silica particles by this route. To implement a microfluidic flow-focusing route for silica bead production, these past investigations as well as this study use a water-in-oil emulsion in contrast to the oil-in-water emulsion aused previously. As was the case in the previous chapter, that the stability of the nanoparticles in this system is obviously of primary importance prior to growth of a shell at the interface and this necessitates mainly control of pH for fastest gelation time of the sol-gel and solvation of these hydrophobic nanoparticles in the droplet. The silica precursor is solubilized in an aqueous solution alongside the QDs and formed microfluidically as an emulsion of water droplets in an oil. The droplets containing the silica precursor are then gelled downstream to form silica beads, with the amount of silica in the precursor aqueous droplet sufficient. This design contrasts with the previous chapter where the silica precursor droplets are hydrophobic tetraalkoxysilanes (TEOS, an oil) dispersed in water. The reason that water droplets are made in oil rather than the TEOS droplets in water is because in the latter system silica formation begins as the TEOS droplets contact the aqueous phase. In the microfluidic

production of the droplets by flow focusing, the two phases are first brought together into a core-annular geometry prior to the production of the droplets; this flow regime in the case of the hydrophobic TEOS as the core phase and water as the annular phase would immediately begin to form a shell of silica at the interface and the uniform snap-off production of droplets in the orifice would not be possible. Aqueous silica precursor droplets in oil can be formulated (as described below) to not immediately gel, and hence are more suitable to the flow focusing production of droplets. There are three central issues to the chemistry and the required engineering of this system which differs from the batch oil-in-water emulsification procedure method described ion Chapter 3.

The first issue concerns the incorporation of the QDs. Since the system for creating the bead is now aqueous based, this polar solvent now becomes the vestibule for retaining the QDs in the droplet until they can be trapped in the silica bead. Functionalization of the surface of the QDs is now mandatory to keep the nanocrystals from precipitating out of the droplet into the continuous oil phase. In fact the continuous oil phase serves to keep the QDs sequestered in the droplet so that the nanocrystal concentrations in the droplet/microbead remain unchanged from the initial loading in the solution from which the droplets are created. The surface functionalization of the nanocrystals must be such that the chemical moities attached to the nanocrystal surface impart aqueous solubility to the nanocrystals, and are coordinated sufficiently strongly with the surface so that the groups remain fixed to the surface during the processing steps. In this study, QDs functionalized with polyethylene glycol moities are used to increase the aqueous solubility.

The second issue concerns the stability of the aqueous dispersed phase of the emulsion. To render normally aqueous insoluble silica precursors such as tetra-alkoxysilanes (e.g. TEOS) soluble in water, the alkoxides can be hydrolyzed. Hydrolysis of the tetra-alkoxysilanes yields hydroxyl groups (silanols) which provide water solubility. Acid catalyzed hydrolysis insures the most rapid rate of hydrolysis, and hence a aqueous silica precursor solution can be prepared by dissolving the tetra-alkyl silane in a low pH solution. However, once hydrolyzed to silanols, the silanol groups can begin to condense by forming siloxane linkages, and the precursor solution begins to gel before it can be emulsified by flow focusing. Hence the pre-hydrolyzed solution should be stable against gelation for extended times. This can be by fixing the pH of the pre-hydrolyzed solution so that it is at the isoelectric point (IEP) (fig 2.7) where the gelation time of the solgel is the longest. This stable solution point, where the silica molecules interact extremely slowly, is at about pH 2, when the charges on the silanol and siloxane surfaces are neutralized by the acid. Pre-hydrolyzing silica and maintaining it for the duration of the necessary droplet production time requires both rapid hydrolysis and high solubility of TEOS in the solution. In this manner the recipe to adhere to this engineering process requires a substantial amount of alcohol (ethanol) and catalyst. While the catalyst concentration keeps the solution at the proper pH from gelling, the alcohol in the system allows for uniform solubility of the solute to produce a stable and immicible droplet as well as ease of evaporation to drive gelation and finally condensation when the proper sequential steps are taken for post collection of particles (see below).

The third issue concerns the sol-gel reaction required to transform the hydrolyzed alkoxide droplets into a silica gel particle. To form a gel, the hydrolyzed alkoxides need

to react, and this can be accelerated by removal of the ethanol and water to concentrate the alkoxides (usually by thermal evaporation), and force the silanol groups of the hydrolyzed alkoxide to form siloxane linkages. Because water is produced when the silanols react, removing the water drives the reaction kinetics towards the formation of the product siloxanes.

In this study this sol-gel transformation of the inorganic oxide is utilized, but a template in the solution is also used to organize the internal structure of the silica gel (the pore sizes and their arrangement) into a prescribed mesoporous structure. As described below, the results of previous studies has shown that, aside from the control of the gel structure, templated silicaas sol-gel processed here, is more mechanically stable than silica formed without the template. Templates used for sol-gel processing are the crystalline phased of amphiphilic species such as surfactant molecules or block co-polymers. Amphiphies contain hydrophilic (polar) and hydrophobic (nonpolar) moieties which are separated from one another in the molecule or polymer (e.g. surfactants which commonly consist of a linear hydrocarbon chain and a polar head group (hydroxyl, ethoxylate, quaternary ammonium cation)). At low concentrations in an hydrophilic solvent such as a mixture of water and alcohol (ethanol), the amphiphilic templates are singly dispersed and solvated, but as their concentration increases the amphiphiles aggregate into structures which shield the nonpolar group from the hydrophilic solvent. Examples of these structures at low concentrations include spherical and cylindrical micelles where the nonpolar part of the amphiphile is arranged in the core of the structure and the polar groups on the outside, and a lamella structures in which the nonpolar and polar groups form sheets. These aggregates are dispersed in solution, but at higher

concentrations lyotropic liquid crystalline mesophases can form such as hexagonally packed cylindrical micelles (hexagonal liquid crystals), lamellar liquid crystals and bicontinuous cubic phases in which hydrophobic and hydrophilic domains are interconnected in a structure in which each is continuous. The phase diagram of the amphiphile describes the emergence of these aggregates as a function of concentration. The precursor solution of the droplet contains both the hydrolyzed alkoxide and the amphiphile template at a concentration in which it is unaggregated. The evaporative removal of the alcohol and the water concentrates the silica precursor, and also drives the self-assembly of the template into aggregate structures. As these aggregate structures form, the silanol groups of the hydrolyzed alkoxides, hydrogen bond to the polar surfaces of the aggregate, thereby templating an the arrangement of the silica precursor molecules. Their localization on the template drives the initial reaction of the alkoxides, and silica surfaces coat the polar surfaces of the aggregate structure. Further siloxane linkages form from these templated structures, and essentially fill in or occupy the alcohol/water space between the hydrophobic cores of the aggregates. Since this templating occurs only as the precursors become relatively concentrated, the aggregate structures forming the template are the lyotropic liquid crystal phases which emerge at the higher concentrations of amphiphiles. The final structure of the gel that emerges consists of the remaining hydrophobic cores of the liquid crystal fixed in a silica gel matrix. Calcination of the gel removes the hydrophobic cores and condenses the silica of remaining water, leaving a mesoporous solid material – a silica fossil of the amphiphile template - in which the pore structure reflects the liquid crystalline spatial structure of the amphiphile template that forms upon evaporation. This silica condensation route, which

uses the evaporation of solvent to both induce the self assembly of amphiphilic templating structures as well as the sol-gel transformation of silica precursors on these structures, is termed evaporative induced self-assembly (EISA)[105], and is a direct method for the fabrication of nanostructured silica materials.

The templating of mesoporous silica structures using the lyotropic liquid crystalline phases of an amphiphile was first demonstated by Kresge[106] using long chain alkyl ammonium surfactants (e.g. cetyl trimethyl ammonium bromide), under strong hydrothermal processing conditions to form powders with the pore structure of the powder material having diameters between 2-10 nm. In further research, Brinker demonstrated, again using long chain alkyl ammonium surfactants, that thin films of solutions of the silica precursor with the surfactant template which were formed by dip coating on a solid substrate can be transformed into mesoporous silica films by evaporative induced self-assembly under milder evaporative conditions. These studies noted a reduced tensile stress when the silica monolith is prepared with a template, than without the template, leading to more mechanically stable structures. In this regard, further studies demonstrated that the use of nonionic block copolymers as amphiphile templates rather than the alkyl ion surfactants resulted in materials with porous structures with superior mechanical stability. Brinker's studies also indicated that the formation of the liquid crystalline phase is influenced by interactions of the solution with the solid substrate: As the amphiphile becomes concentrated, the liquid crystalline phase becomes nucleated at the solution/solid interface where interactions of the amphiphiles with the molecules at the substrate interface first organize the amphiphiles. These incipient

structures are themselves the templates for the liquid crystal phase, and its structural orientation relative to the substrate.

The use of evaporative self-assembly to form mesoporous silica microbeads from droplets of a silica alkoxide precursor dispersed in an oil phase was first studied in a batch process by Andersson et al.[107] who termed the process emulsion and solvent evaporation (ESE). In their study hydrolyzed TEOS in water and alcohol was emulsified in an oil (hexadecane) by stirring, and the emulsion was then heated under vacuum to gel the particles. The water and alcohol are required to diffuse through the oil phase and then evaporate into air at the air/oil interface of the emulsion. Hexadecane is used as the continuous phase because of the relatively high solubility of water and alcohol in this oil relative to other oils. Andersson et al used the nonionic triblock copolymer P-104 to template the silica formed in the microdroplet, taking advantage of the superior mechanical stability of mesoporous silica formed from this template relative to the ionic surfactants. The use of flow focusing in a microfluidic device to create the pre-hydrolyzed droplets and narrow their size distribution was subsequently considered by Weitz et al. These authors used the same P-104 template in the precursor solution as that of Andersson et al, but with more alcohol to accelerate the evaporation process. They formed the pre-hydrolyzed silica droplets in hexadecane oil using flow focusing and collected the emulsion (prior to gelation) in a receptacle. Weitz et al then heated the emulsion to form the beads as part of the off-chip or post-production phase of the particle formation process.

In the study of Weitz et al, the gelation of the droplets by the heating of the emulsion (under vacuum) in an off-chip receptacle into which the emulsion is collected

from the output of the microfluidic cell requires continual stirring of the droplets in the receptacle to prevent coalescence (which would lead to a loss in monodispersity) or settling at the bottom (which would cause the droplets to spread on the surface and lose their spherecity). The stirring has to be undertaken for a time period (usually a few hours) necessary to remove the water and alcohol by evaporation through the oil. This can prove challenging because as the droplets evaporate their density increases and they have an increasing tendency to settle to the bottom of the receptacle. Note that the off-chip collection breaks the stable flow regime in the microfluidic cell in which the droplets move single file through the channels, maintaining a separation distance sufficient to prevent coalescence and a flow speed that insures that they do not settle to the bottom of the channel. If gelation of the droplets can be undertaken on the chip in this flow arrangement (i.e. allow the water and alcohol to evaporate into the surrounding oil as they moved through the cell), the coalescence and settling in the off-chip collection can be avoided. Once the particles are sufficiently gelled, they can then be collected in a receptacle without coalescence or deformation upon settling. This task is however difficult, because in the microfluidic cell, the droplet velocities are relatively fast (a few centimeters/sec.) and unless the chip contains an extended channel course for the droplets, it is diffcult to arrange for them to spend enough time in the cell to gel the particles by evaporation

In an effort to gel the silica precursor droplets as they move single file through the microfluidic cell, Lee et al channeled the train of droplets in the microfluidic cell into an extended length of polyethylene tubing (a few meters) with a relatively large internal diameter (350 μm), much larger than the height and width of the microchannels. The

larger diameter reduced the train velocity and, taken together with the long length of tubing, allowed sufficient diffusion of the water and alcohol into the surrounding oil to gel the droplets at the end of the tubing. Lee et al also channeled more oil into the droplet train, downstream of the flow-focusing orifice, but on the chip to increase the distance of separation between the droplets so that when the train entered the larger tubing the droplets remained sufficiently separated.

Here an alternative procedure for gelation is studied in the context of microfluidic droplet production which allows the droplets to gel on the chip, and avoids the off-chip processing of Weitz et al and Lee et al. In this procedure, we use the same general chemical composition as Weitz and Lee of a precursor droplet solution of prehydrolyzed TEOS and the P-104 triblock copolymer template, and create the droplets using flow focusing as they have done. As was discussed in the previous chapter, the kinetics of the hydrolysis step is enhanced by an acidic catalyst, while a basic one is required for high condensation rate and fast gelation, is required. This obviously allows us to take advantage of the behavior of opposite ends of the pH scale. The idea here is to introduce octylamine, a base, into the acidified aqueous droplets of the prehydrolyzed silica and triblock copolymer template after they have been formed at the flow focusing orifice, so as to increase the pH inside the droplet and initiate gelation. In our flow regime, the precursor droplets are first introduced at the flow focusing point into a mineral oil phase which is completely immiscible with the aqueous prehydrolyzed TEOS droplet phase. We use for the continuous phase a mineral oil, rather since hexadecane, since we do not depend on concentrating the prehydrolyzed alkoxide to initiate the gelation, and therefore do not require the initial removal of the water and alcohol. Two different approaches are

devised for the introduction of the octlyamine into the precursor droplets (Figures 4.1 and 4.2). These are described below.

In the first, Figure 4.1, the octlyamine is introduced downstream of the orifice through two side arm channels which intersect with the flow. These conduits channel the flow of a 1:1 (by volume) mixture of octlyamine and mineral oil (into which the octylamine is soluble), at a controlled flow rate, into the main stream consisting of the moving train of precursor droplets in mineral oil. The octylamine/mineral oil mixture originally flows as a thin distinct layer on the inside surface of the channel (a sidewall film) whose thickness is controlled by the flow rate of the mixture. As the octylamine diffuses into the main mineral oil stream suspending the droplets from this thin layer, this distinct layer disappears and merges with the suspending mineral oil in the mainstream. More importantly by diffusion in the symmetric flow cell normal to the direction of the flow and convection driven in the direction of the uniaxial laminar flow, the octlyamine in the mainstream mineral oil gradually reaches the droplets where it raises the pH and initiates the gelling process. The gelation process catalyzed by the increase in the pH is allowed to proceed in the droplet over an extended time as the droplet moves through a serpentine or sidewinding channel (Figure 4.1) which increases its passage lifetime in the cell. The gelation in this stage is occurring without removal of the water and alcohol but proceeds because of the catalyst so that upon exit the droplets are to a sufficient degree mechanically stable so as to be able to be collected in a receptacle. The droplets are collected in a empty receptacle so the mineral oil continuous phase alone suspends the gelled particles. After collection, an small excess of a 0.03 M ammonium hydroxide solution[108] is poured onto the collected particles to completely condense the gelled silica

beads. In essence this is an accelerated process for silica growth to a condensation state accentuated both by the two-step process in the initial prehydrolysis of TEOS and the use of a catalyst with a final step to expedite and facilitate the final product.

In the second approach, the flow rate of the octylamine/mineral oil is kept fixed, but one arm of the microfluidic cell is blocked off (Figure 4.2) so that the octylamine/mineral oil layer develops with a larger thickness on one side of the conduit. The train of precursor droplets in this case collides with the layer, allowing direct transport of octlyamine into the droplet. More importantly, this direct contact allows the direct transport of water and alcohol out of the droplet and into the octylamine/mineral oil layer since the water and alcohol are soluble in this mixture. Thus in the asymmetric flow cell (where one channel is blocked off) rapid mass transfer diffusion of the aqueous content of the droplet into the more polar octylamine solvent occurs. Although, the fluid introduced downstream from the orifice is a mixture of mineral oil and octylamine, the large volume of the catalyst changes the polarity of this fluid. Gelation time is fastest at intermediate pH- about 6- but it can be accelerated by increasing the pH. That is what the octylamine accomplishes as the droplet moves down the side winding (serpentine) channels. The time scale for the contact of the continous phase with the dispersed phase in a flow-focusing device is rather short as the interphases are continuously refreshed in the moving liquids as well as the diffusion time of a surfactant into a droplet. However, the effectiveness of the catalyst to condense the silica is kinetically faster than the moving phases and as a consequence clogging of the cell occurs at the orifice of the device due to the extreme efficiency of the octylamine. These directly contacted droplets immediately condense inside the channel. As will be explained, while the rapid condensation causes

the gelled droplets to be crenated, they do not require any further processing (e.g. treatment with ammonium hydroxide) to complete the formation of the gelled particles.

When placed down stream from the orifice, the octylamine is in an oil soluble form as there is no polar liquid contact until it diffuses out into the continuous phase and comes into contact with the dispersed phase therefore it was required for continued production of droplets to introduce the catalyst away from the orifice. The degree of solidification of the silica droplets depended on whether the device had symmetric flow introduction of the catalyst or not. Even when the concentration of the catalyst was absorbed into the droplet during a symmetric introduction of the catalyst flow it was rather quick and if the flow was introduced asymmetrically a large area of the droplet came into contact with the catalyst mixture and a sudden, drastic change in the topography and shape of the now condensed beads occurred. A similar effect, but not as rapid occurs when the percentage of catalyst introduced was greater than 15 percent of the continuous flow rate. This is obviously due to the higher concentration of the catalyst changing the liquid phase to a more gelled state and the change in polarity of the continuous phase to allow diffusion of the ethanol, which is more soluble in mineral oil than water would be.

4.3 Experimental Section

4.3.1 Materials

Tetraethylorthosilane (TEOS) was obtained from Gelest Inc., octylamine (99+% from Acros), HCl 37% (ACS Reagent) from Sigma Aldrich, P104 (Pluronic, triblock polymer) from BASF, ethanol from Sigma Aldrich, mineral oil (viscosity about 250 cp) from Sigma Aldrich, Span 85 (Sorbitan trioleate) from Acros. Quantum dots with peaks

in their spectral emission at 562 nm and 612 nm were obtained from eBioscience, Ca. These are CdSe/ZnS core-shell nanoparticles with a hydrophilic coat of polyethylene glycol (pegelated QDs) with the spectral emissions as characterized by the manufacturer. Deionized (DI) water 18 MΩcm resistivity was obtained using a Millipore system. For the manufacture of the microfluidic cells, Sylgard 184 elastomer base and curing agent was purchased from Dow Corning. The negative tone SU8-2050 photoresist and developer was purchased from Microchem. Silicon wafers were obtained from Silicon Quest Int. Chemicals were used as received.

4.3.2 Experimental Procedure

Prehydrolized TEOS solution was made following the recipe and protocol of Carroll et al[87]. Briefly, a combination of TEOS, ethanol, and a pH 2.0 HCl solution was first mixed and stirred for a half hour before being mixed with a solution of water and P104 triblock polymer. A couple of milliliters of the mixture of these two solutions were used for the generation of the droplets- the dispersed phase. While a solution of mineral oil containing anywhere between 3-6 wt% Span 85 was used for the continuous phase. For the preparation of the silica beads with QDs embedded in them, the only other procedure that was done was to mechanically dissolve the two different types of emitting QDs in the P104 solution for about a half hour before mixing it with the prehydrolized silica solution. The QDs, obtained from eBiosciences, emitted upon excitation at approximately 562 and 616 nm (as documented by the manufacturer). These as obtained from the manufacturer were dispersed in an aqueous solution, and were dissolved in the precursor solution first by dispersing in the P104/water solution. This solution was later combined with the prehydrolyzed TEOS/water/ethanol solution. The QDs were dispersed

at a molar ratio of 3:1, and the total concentration for each type of QD was 6.12 x 10^{-7} M. As mentioned above, the QDs were functionalized with a surface coat of polyethylene glycol to increase their aqueous solubility.

Fabrication of a mold via soft lithography and microfluidic devices were done following the usual protocols[109, 110]. Microchannels were drawn in Adobe Illustrator CS3 software and were printed on a transparency paper using a 20000 dpi resolution laser printer. Master molds are created by coating a 100 μm thick SU8-2050 photoresist layer on a test grade silicon wafer. The prepared transparency paper (mask) is attached to a glass slab to ensure a flat contact between the mask and the silicon wafer. The mask is then placed on top of the wafer and the combination is exposed to a collimated deep UV light (AOI, λ=350nm). Subsequent baking and development of the resist forms the master mold on the silicon surface. To make microchannels, PDMS elastomer base is mixed with a 10:1 weight ratio of curing agent and the mixture is poured on the prepared master mold. After curing in an air-convection oven at 65^{o}C, microchannels are cut and peeled off from the mold. To generate hydrophilic surfaces and to bond microchannels to another surface, we oxidize the PDMS surface in air plasma (Harrick Scientific). Prior to bonding, the microscope slide is first coated with a thin film of PDMS in order to ensure that all microchannel walls have the same wetting characteristics. Exposure to the plasma renders the PDMS surfaces temporarily hydrophilic so the microchannels are postbaked at 65°C for several hours to ensure that the surface reverts to a hydrophobic condition. The fluids are introduced into the microchannel device through flexible tubing and the flow rates are controlled separately by syringe pumps (Harvard Pumps PHD 2000). The flow rates of the continuous phase and dispersed were Q_o=0.24 mL/hr and Q_i= 0.03

mL/hr, respectively and in this work the external flow rate is always larger than the dispersed flow. Larger or smaller droplets can be tailored according to the flow rate ratio of the two solutions. At the aforementioned flow rates, the drop formation was visualized by an inverted microscope (Nikon Eclipse 600POL, upright) and a high-speed camera (FASTCAM 1024 PCI). Downstream from the orifice where the droplets are generated a solution of either 100% octylamine or a 50/50 per volume octyalmine/mineral oil mixture was introduced and the use of symmetric arms designed as part of the microfluidic device was tailored for this purpose. The gelled particle train exits the microfluidic cell via an extended length of Teflon tubing 350 μm in diameter and 45 cm in length.

The flow rate of the octylamine solution was restricted to no more than 20%Q_o. Video was taken between 1,000-2,000 frames per second. Collection of droplets was accomplished by coating the surfaces of a 20 mL scintillation vial with Rainx. The actual media of droplet collection was the mineral oil that poured out of the collection tube while awaiting droplets to be delivered form the device. After collection, the droplets were subjected to a 0.03 M solution of ammonium hydroxide and let stand for at least 2 hrs before being prepared to be placed in SEM. For the droplets processed by direct contact with the octylamine no other process was required for solidification of droplets.

4.3.3 Confocal Microscopy Characterization of the Spectral Emission of QDs Embedded in the Beads

Confocal light scanning microscopy (CLSM; Leica TCS SP2 AOBS, with an acoustic-optical beam splitter and a prism spectrophotometer detector) was used to characterize both the size of the beads and luminescence emanating from QDs both in the prehydrolyzed silica solution and the beads. The size of the beads does not allow for

dynamic light scattering measurements. Spectral representation of the distribution of QDs in their respective environments was obtained. Spectrofluorometry was done with (CLSM).

4.4 Results and Discussions

4.4.1 Hydrodynamics of the Flow Focusing

When dealing with microfluidic flow focusing (MFFD), the fluid mechanics dictates a low Reynolds number associated with the characteristic length of the channels which in this case are 200 μm x100 μm in width and height, respectively. For flow through a straight pipe with a circular cross-section, Reynolds numbers of less than 2300 are generally considered to be of a laminar type. In these long, narrow geometries flows are predominantly uniaxial which means that the entire fluid moves parallel to the walls of the device. Using PDMS as the material for the channels imparts smooth walls and allows for smooth speed and flow profiles, and along with the dimensionless Reynolds number at low values there is an absence of the non-linearities created by the inertial term of the Navier-Stokes equation. Hence, Reynolds number is a measure of the relative importance of the convective and diffusive transport of momentum[111]. At low Reynolds number inertial forces are absent and vice versa is true, so the dominant forces are the viscous forces in MFFD system.

Typical of microfluidics, the stretching and breakup of the core fluid at the orifice is a balance between viscous stresses and capillary pressure or interfacial tension forces as these forces control the break up process and the size of the droplets. The capillary number describes the ratio of viscous to capillary forces. The capillary number is defined by the ratio of the fluid's velocity and viscosity over the interfacial tension. Size

population, and the break-up flow regime are determined by a combination of the capillary number (Ca) and the viscous drag that the dispersed phase is acted upon as determined by the flow rate ratio of the inner to outer fluid. The importance of this is where the droplets break with respect to the orifice. Contraction of the inner fluid upstream at the orifice stretches (squeezes) it into a thin filament inside it. The extra pressure applied upstream needed to squeeze the fluids through orifice leads to pinch-off. Downstream of the orifice the volume of the fluid increases and decelerates the flow leading to expansion and produces, by feeding more volume into the bulb of what has now become a droplet, a neck that develops at the base and a near spherical droplet pinches off by interfacial tension. As the production of the droplets continues, increasing the flow rate increases the capillary number providing an increase in frequency of the droplet generation as to satisfy the conservation of mass of the dispersed phase[1, 112]. This in turn allows for precisely controlled droplet size.

This dictates the hydrodynamic regime where the capillary instabilities affect the dispersed phase filament to breakup. The dispersed phase finger either retracts after pinch off or remains displaced in the orifice or beyond it. In the first instance it is called the geometrically mediated regime (droplet size is larger than orifice almost as large as downstream channel dimension), the second is within the orifice or down stream of the orifice, known as the dripping (small range of operation, no proposed scaling relation to size droplet and it is shear driven) or jetting regimes (determined by high Ca number while keeping flow rates constant), respectively[113, 114]. Dripping regime produces nearly monodispersed droplets while the jetting produces sizes that are aligned with the highest capillary wave that creates instability in the aqueous filament created by the viscous

effects of the moving external phase. Also highly monodispersed droplets are generated but the size is still determined by the capillary number and flow rate ratio (see Figures 4.3a and 4.3b for flow regimes).

Scaling arguments made by both Garstecki et al.[112], and corroborated by Anna's[1, 115] work on a more in-depth experimental work accounting for more operational parameters in a MFFD, suggested that droplet volume should be inversely proportional to the flow rate of the continuous phase and in conjunction to its viscosity. As opposed to the view that Zhou et al.[113], reinforced by previous work done by Stone and Leal[116], where the external phase was quiescent however, had in their simulations show that 'the drop size also depends strongly on the diameter of the downstream collection tube. Therefore, the pinch-off of the drop is not entirely determined by the capillary instability. Collection tube here means the downstream channel post orifice. In our work the downstream collection tube, which essentially is an extension of the closed system microchannel, does not appear to have any effect on the droplet production as it constituted of a serpentine channel followed by a 45 cm long Teflon tube, 350 μm in diameter. The only effect that was observed was the extra pressure created by the tube that prolonged the onset of the droplet formation and it also required that the octylamine flow rate downstream be turned off, after having been pressurized, or providing minimal flow until the regime and drop formation developed and stabilized. This usually takes a few minutes. The one issue with droplet production in the jetting regime was that of wetting the bottom of the cell by the aqueous solution. If the solution was used after some aging, thus evaporation of solvents and/or precipitation of the silica with P104 occurred, wetting of the bottom surface occurred and production was restricted to a short time.

This solution contained a rather large amount of P104, a tri block polymer. As the wetting increased the aqueous finger or filament elongated orders of magnitude than the interphase created by the squeezing of the two immiscible liquids. And its behavior resembled that of the Rayleigh-Plateau instability causing large population distributions in addition to satellite droplets that were caused by the viscous drag of the continuous phase of the settled aqueous finger.

4.4.2 Silica Droplets Gelled By Octylamine Introduced Into The Precursor Droplets By Diffusion Through The Continuous Phase in A Symmetric Cell

The first set of results describe the particles produced in which octylamine is introduced symmetrically in the cell, and diffuses through the mineral oil into the precursor silica droplets to initiate the gelation. Complete gelation is achieved by collecting the partially gelled particles and then immersing them in 0.03 M ammonium hydoxide. Figure 4.4a, taken as a frame from the fast video recording, shows the production of the droplets at the flow-focusing orifice, and the formation of the optically distinct octylamine layer along the sidewalls of the channel. The droplet formation is seen to proceed through the break-up of a long layer of the precursor liquid. The flow rate of the octylamine (as a 1:1 mixture with mineral oil) through the sidearm is 15% of the mineral oil continuous phase flow rate. This layer is also shown to merge with the main continuous phase after the first elbow of the serpentine part of the cell. The droplet train, suspended in the continuous mineral oil phase is also evident in the figure. Note that as the train moves through the channel where it encounters the side channels for the octyl amine introduction the continuous phase widens into these channels which causes a slowdown in the droplet train and decrease in the distance between droplets. Under the

pproper flow rates, the droplets do not coalesce at this juncture, and as the train moves downstream the continuous phase narrows due to the introduction of the thin layer of octylamine and the droplets increase their separation distance. Figure 4.4b provides a second frame from this flow regime of the movement of the silica droplet train through the serpentine channel. The droplets remain apart, which insures that their monodisperse size distribution is retained.

Figure 4.5 is an SEM micrograph of silica particles obtained from the flow regime shown in Figure 4.4a (a ratio of the flow rate of a 1:1 mixture of octylamine and mineral oil to the flow rate of the continuous phase of 15%). The corresponding optical micrographs are given in Figures 4.6a and 4.6b (for a flow rate of the octylamine of .10 the continuous mineral oil flow rate). As these figures show, the particle size distribution is rather tight showing that the regime was one that produced monodispersed beads and, as a matter of making the point, solid. The solidification of the silica droplet is one of the advantages of this process whereby the final synthesis of the silica beads does not require the extra steps taken by Carroll et al. and Lee et al.[88] In this system the external oil phase was exchanged from hexadecane to mineral oil, a proper spherical shape is retained though the amount of ethanol in the solution was doubled, alcohol is a better solvent for both the P104 and TEOS than water. This required that an extra surfactant with an HLB= 5.5 (Hydrophile Lipophile Balance) with more affinity to ethanolic solutions be used to stabilize the drops. This retains a spherical contour of the drops, where the surface tension is high, to beads an extremely low solubility of the solvents into the continuous phase is required. Heating at 65°C-70°C aided the evaporation of the ethanol but it was

neither instrumental nor necessary, as the 0.03 M ammonium solution proved to be enough to completely solidify the beads that had been collected.

It was observed that a large amount of the molar concentration of the octylamine that is flowed in the 'arms' of the microchannels changes the morphology of the drops. The phase transition of a liquid material to a solid is through the gelling phase, as was discussed earlier, and as such the density of the material increases. If there is an overly generous amount of the surfactant causing gelation in the droplets multiple issues also were observed to occur. Mainly that crenation sets in rather rapidly, even before the drops exit the microfluidic device. The corrugation of the drops is seen at octylamine flow rates of 20%Q_o and higher amounts increase the extent of fringed edges (Figures 4.7a and 4.7b). Insolubility of the contents of the drop with the external phase is essential and pains are taken to retain this. When too much octylamine diffuses into the continuous phase it changes the polarity of the media and partial solubilities change allowing the compatibility with polar liquids. In the Section 4.4.4 a system where there is total crenated particles is discussed.

The access to more octylamine in the mineral oil allows for the extraction of the ethanol whose volume composes 50% of the initial droplet content and probably some of the water as well. Once the octylamine molecules have been ionized by the aqueous phase there is total diffusion into the drop, and as the acid is still available they are neutralized until an adequate concentration enters the droplet to start driving the pH up. The droplets have about 17 minutes residence time in which diffusion of the octylamine into the droplet to start gelation can start taking place. During this time the interfacial tension starts to change and gradual solidification of the aqueous content is highly

desirable. The octylamine surfactant starts to change the energetics of this interface and more favorable mass transfer of contents occurs. Most of the ethanol is evaporated or extracted out of the drops and the original particle size is diminished by the same percentage of ethanol lost. Most of the ethanol is evaporated or extracted out of the drops and the original particle size is diminished by the same percentage of ethanol lost. Fig 4.8b demonstrates the deformation of the beads that were synthesized with 20%Q_o of octylamine.

Surfactant concentration also plays a central role in the regime in which droplet break up takes place[117]. Experiments[118] were done where the concentration of surfactant was varied to understand the physical tendencies that it caused in the development of a consistent trend of dispersion production in the system, however, the system in this case was an asymmetric T-shape microfluidic system. Here Dreyfuss et al. studied the patterns in which the increment of surfactant affected the stability of the development of the droplet regime and found that as the surfactant concentration increased the capillary forces start to dominate the system over the viscous forces showing the physical reason between apparent decorrelation of the patterns in the flow. Partial wetting of walls, due to low surfactant coverage of the PDMS, was seen and anchoring of the droplets in the microchannels was found. In our experiment the use of 6 wt% Span 85 dispersed in the mineral oil, which is twice the amount most authors have reported in their experiments, was utilized more to thermodynamically stabilize the droplets while exiting the device of a 200 μm channel into a tube with inner diameter of 350 μm where it is most difficult to retain individual droplets as the separation throughout the serpentine channels is maintained from the moment of droplet production in the orifice. The excess amount of

Span 85 did not alter the regime of the droplet production at all. The entrainment of the droplets is of utmost importance in this process as the amount of octylamine that diffuses into the dispersed phase starts to raise the pH of the individual aqueous drops and the onset of gelation begins. This also proved extremely helpful in the collection process, as the scintillation vial in which the drops were collected did not have need of any liquid to keep the particles separated. The amount of Span 85, a highly hydrophobic surfactant, was enough to allow handling the particles in this manner, without need to stir or heat to evaporate the solvents inside the droplets. The droplets were gelled by the diffusion of the octylamine into the drops. Once this phase change begins, the probability of agglomeration occurring is high- a notoriously difficult system to deal with in gelation processes and materials- mainly at the larger area of the punch hole, where the opening between the device and the tube feeding is located, due to the flow velocity diminishing but also where some particles begin to drag along the bottom surface (Figure 4.7b). The continued path along the inside of the collection tube, which we estimated to be around 16 min. at the external flow rate, is also cause for caution as this can also cause aggregation. But as the SEM and optical micrographs show, the beads maintained their spherical shape throughout the entire process. This shows that the amount of the octylamine flowed into the main channel was significant enough to drive gelation and assist in the elimination of overly complicated post-processing requirements, but at the same time not to cause any polymorphism in the droplets before they became beads. Lee et al. speculated on a mechanism that this "distinctive surface morphology is due to the diffusion of the oil-soluble precursor solution (ethanol, tetraethylorthosilicate (TEOS), and P104, a Pluronic block copolymer) into the oil phase and subsequent polymerization

of inorganic silica precursors in the interfacial subphase upon further diffusion of ethanol into the oil phase". The SEM micrograph shows a smooth surface on the silica beads just as the suspension method did, although both systems were considerably different from an emulsification and stability processing point.

4.4.3 Photoluminescence Spectra of Quantum Dots Incorporated in the Silica Beads Gelled By the Diffusion of Octylamine Into the Precursor Droplets

Quantum dots, as obtained from eBiosciences, that have been functionalized with a polyethylene oxide surface coat and fluoresce at wavelengths of 562 and 616 nm (as communicated from the manufacturer) were dissolved in a 3:1 molar ratio, first in the aqueous/alcohol block copolymer solution before combination with the prehydrolyzed TEOS solution. A reference photoluminescence spectrum (PL) was taken for this solution by placing the solution in a glass enclosure, and recording the emission spectra using a confocal microscope. The spectra shown in Figure 4.8 shows peak emission wavelengths at 574 nm and 639 nm respectively, which is a rather high blue shift relative to the manufacturer's specification. This spectra was recorded approximately 2 hrs after preparation of the solution; a spectra taken immediately after preparation (not shown) indicated a greater integrated intensity under the 574 peak and less area under the 639 nm peak. This indicates that the QDs in the solution have begun to aggregate, as the decrease in the 574 nm peak relative to the 639 nm peak indicates fluorescence resonance energy transfer from the 574 nm to the 639 nm QDs.

Figure 4.8 also records the PL spectra of the QDs incorporated into the silica beads; here the integrated intensities indicate less aggregation and resonance energy transfer than in the reference spectrum taken in the P104/aqueous mixture. We see also

that the intensity and emission wavelength of the 616 nm QD returns to normal. One conjecture is that in the reference, the P104 triblock copolymer mixture does not solvate well the QDs. When the complete solution is made by the addition of the hydrolyzed TEOS, the block co-polymer is diluted allowing a better solvation of the QDs. In addition, the gelation can act to retain the separation of the QDs. These may be the reasons why there is less resonance energy transfer in the beads (and hence less aggregation) then in the reference solution. Nevertheless, the signature emission profile of these QDs in their native aqueous solution is not obtained.

The manufacturer, eBioscience provides a table (Table 4.1) of the stability of the QDs in a changing content of a mixture of water and ethanol, increasing up to 90% ethanol content. The conclusion of the table is that up to 10% ethanol had no effect on the solubility of the QDs. The tests on which the table is based were only optical and physical characterization and could not verify the state of the surface functional molecules. The prehydrolyzed silica solution contains 50% ethanol after the hydrolysis of the entire TEOS content. According to the table there is supposed to be slight aggregation at this amount of ethanol in the solution, but perhaps not enough to show that amount of FRET. The procedure called for the QDs to sit in the solvent for an hour; it takes a little longer to set up and start droplet production. Perhaps in this time interval the QDs precipitated to a larger extent. The other component that could cause surface instability in the nanocrystals is the amount of HCl used to bring the pH to 2. Possible cleavage of the PEG leaving behind the organic chain exposed to the polar solvents can cause more agglomeration of the QDs and enhance the change in PL of the two individual QDs as referenced by Foster. Further experiments to ascertain true conditions for the insolubility

of the QDs are required. Perhaps a different protocol to solvate the QDs in the prehydrolyzed solution is needed.

4.4.4 Silica Particle Production With Octylamine Introduced Into the Precursor Droplets by Direct Contact in the Asymmetric Microfluidic Cell

In this section particles formed from the gelation of the silica precursor droplets by direct contact with the octylamine catalyst phase will be discussed (see the cell design of Figure 4.2). We noted in the previous section the availability of octylamine in the continuous phase where a large quantity of it by diffusion can change the polarity of the media and allow for a rapid transfer of the droplet solvents out of the drops and into the mineral oil. This causes crenation in the beads (Figure 4.7), and this behavior can be accelerated if the droplets make direct contact with the octylamine layer introduced downstream of the flow focusing point. In the asymmetric flow one of the channel 'arms' through which the octylamine is fed, is clogged (Figure 4.2). When the droplets make their way through that part of the channel an additional force is introduced that speeds up their velocity thus pushing them forward but as only one channel is providing the entire flow rate being introduced the drops are pushed in that direction as they reach the first elbow. At the first elbow, as the octylamine solution has not yet diffused into the mineral oil, a distinct layer exists asymmetrically on the sidewall of the channel with the unblocked side arm. At the first elbow, the droplets collide with this layer and octylamine can directly transfer into the droplet, and alcohol and water out of the droplet. Water is particularly able to move out into this liquid as octylamine is highly hygroscopic and the catastrophic change in solubility leads the droplets to crenate rather profusely and extremely fast.

The loss of the solvents in the droplets changes the morphology of the drops as this loss reduces the volume of the drop but at the same time the catalyst reacts violently as it has all the available components to solidify the silica. The mass loss to the octylamine phase is kinetically fast and the drop cannot accommodate a new interface, the loss of volume and the solidification of the silica concomitantly force the creation of an interface that is corrugated (see Figs. 4.9 and 4.10). Once these particles have taken their new shape and are traveling down the serpentine channels it is very difficult to prevent clogging of the cell. The particles are extremely hard and they tumble rather than flow, and as there is a slowing down of the flow at the punch hole, clogging is most likely. These crenated particles were not embedded with QDs.

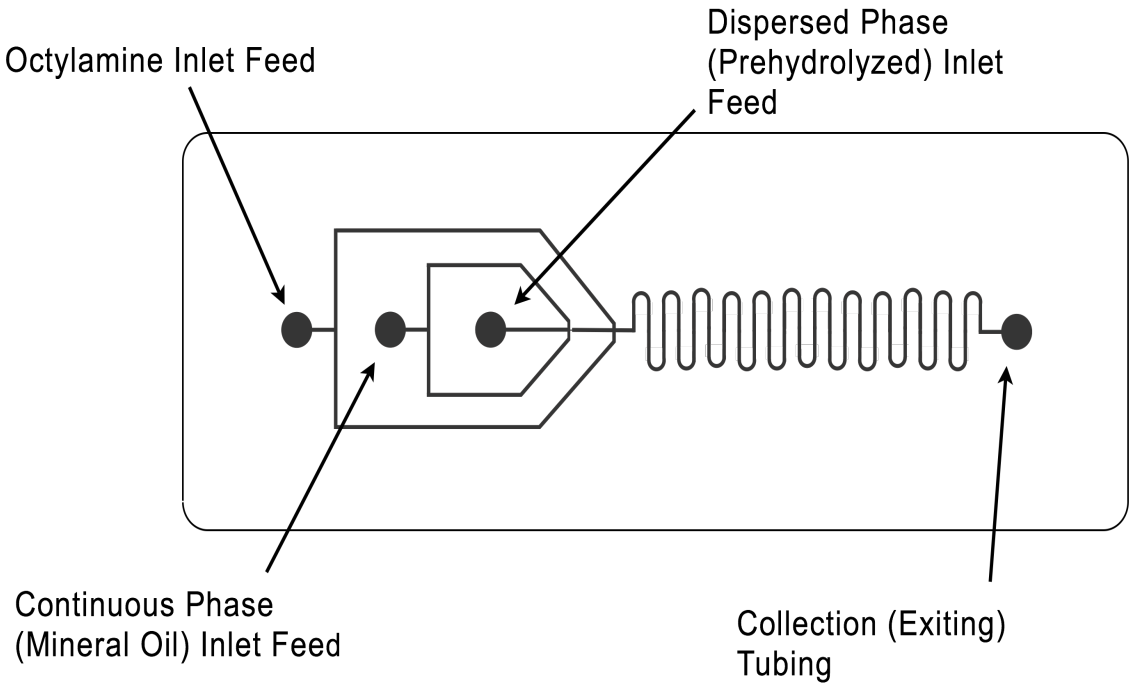

Figure 4.1 Microfluidic cell for the production of precursor droplets by flow focusing, the introduction of the octylamine downstream of the droplet production orifice and the serpentine part of the fluidic cell to allow a longer residence time of the droplets in the cell so that the droplets can gel.

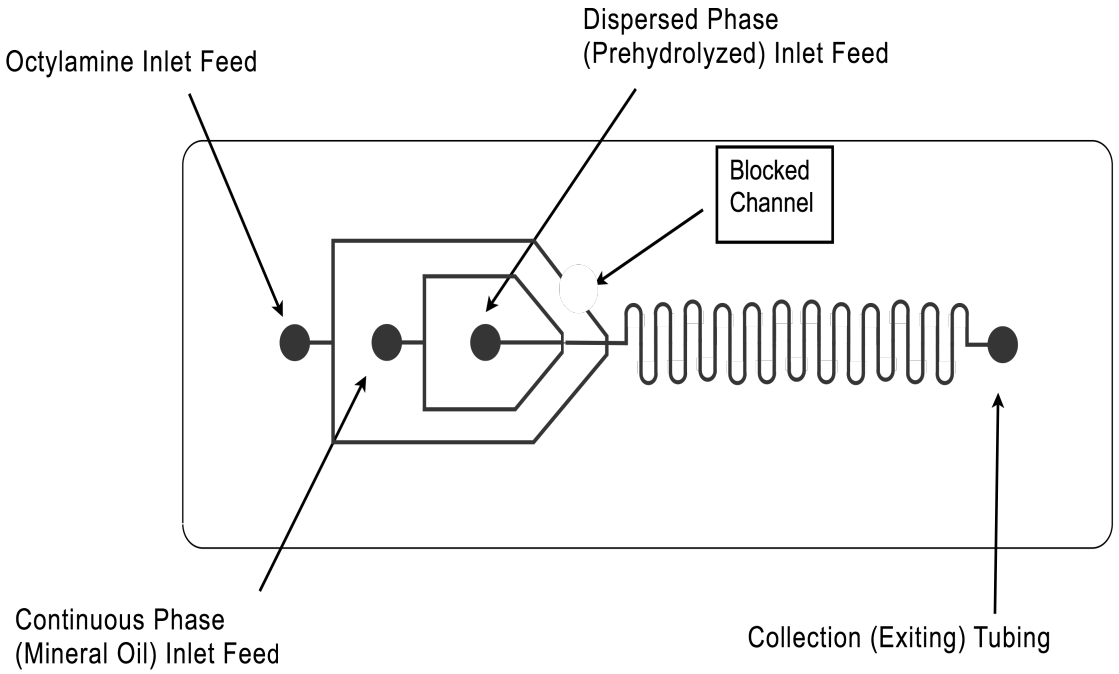

Figure 4.2 Asymmetric Microfluidic cell for the production of precursor droplets by flow focusing, the introduction of the octylamine downstream of the droplet production orifice through only one arm to facilitate direct contact of the droplets with the octylamine and the serpentine part of the fluidic cell for allowing the droplets to gel by extending the passage time.

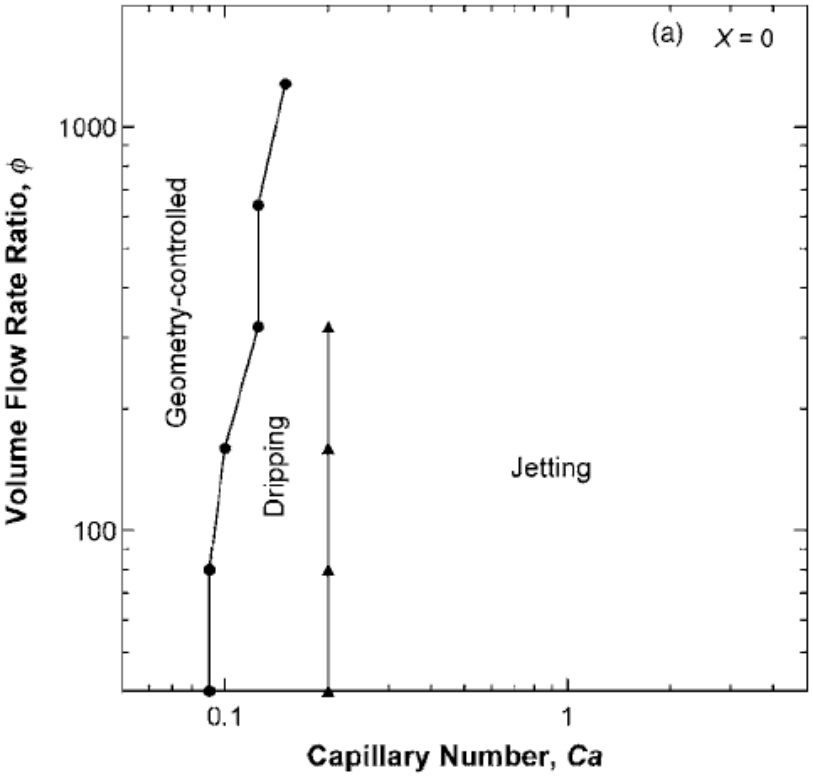

Figure 4.3a. Flow Regimes without surfactant

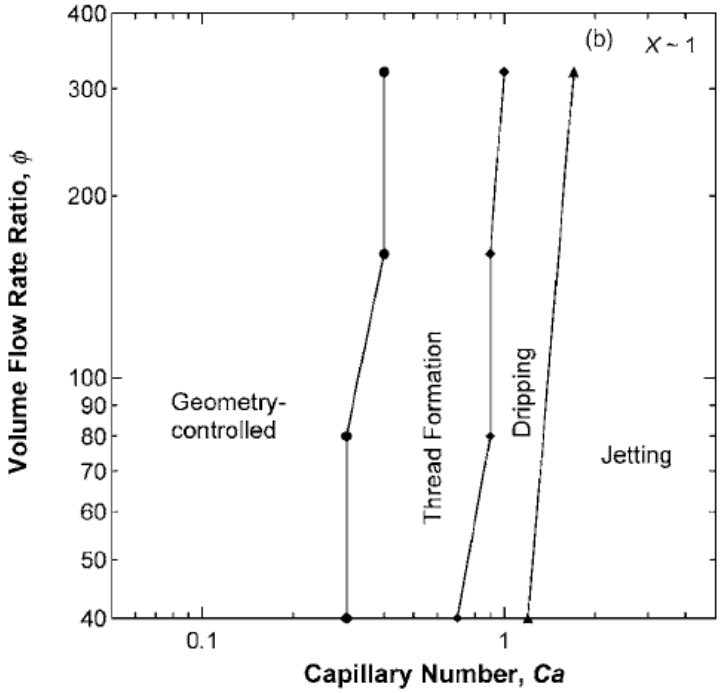

Figure 4.3b. Flow Regimes with surfactant[1]

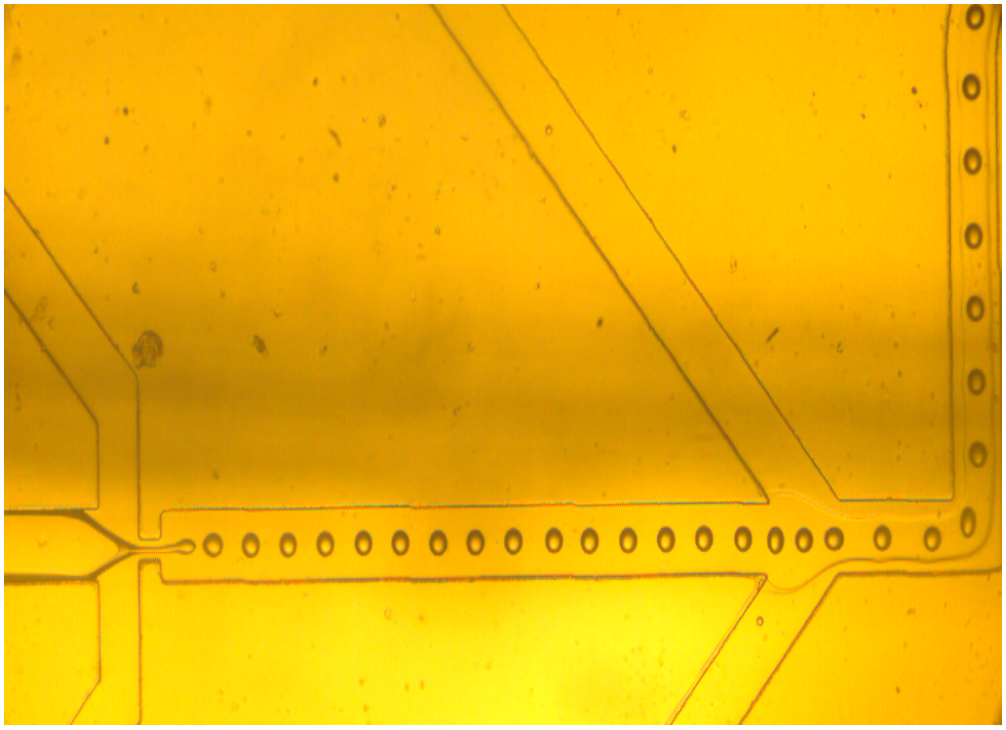

Figure 4.4a. MFFD showing production of droplets and downstream feeding of calalyst. Note the interphase at the arms where the octylamine solution meets the continuous phase.

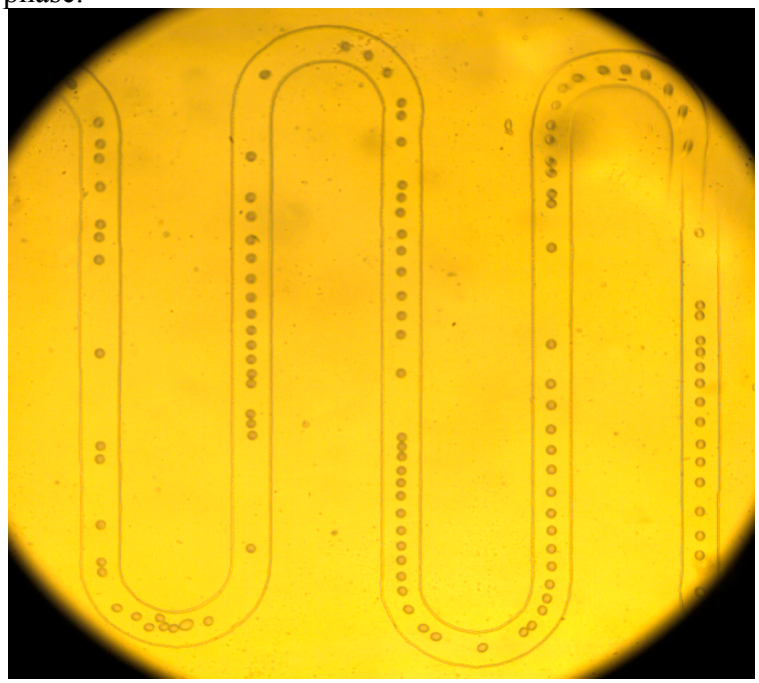

Figure 4.4b. MFFD showing the downstream serpentine channel where the droplet train remains intact.

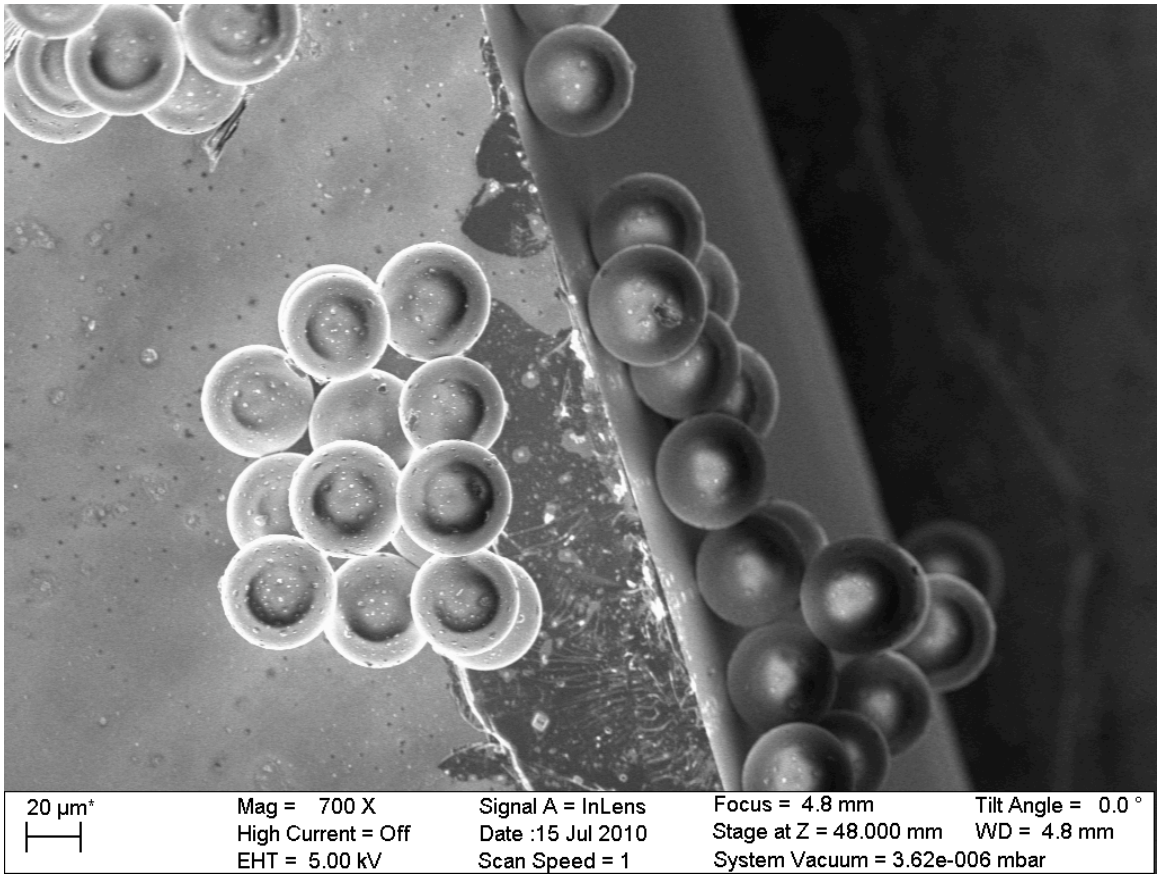

Figure 4.5. SEM micrograph of silica particles made with 15%Qo octylamine. Treated with 0.03M Amonnium hydroxide solution for 2 hrs and then aliquoted onto Silicon wafer for SEM sampling. Notice the tight size distribution of the particles and the size is much less than the initial droplets generated due to the extraction of the aqueous solvent.

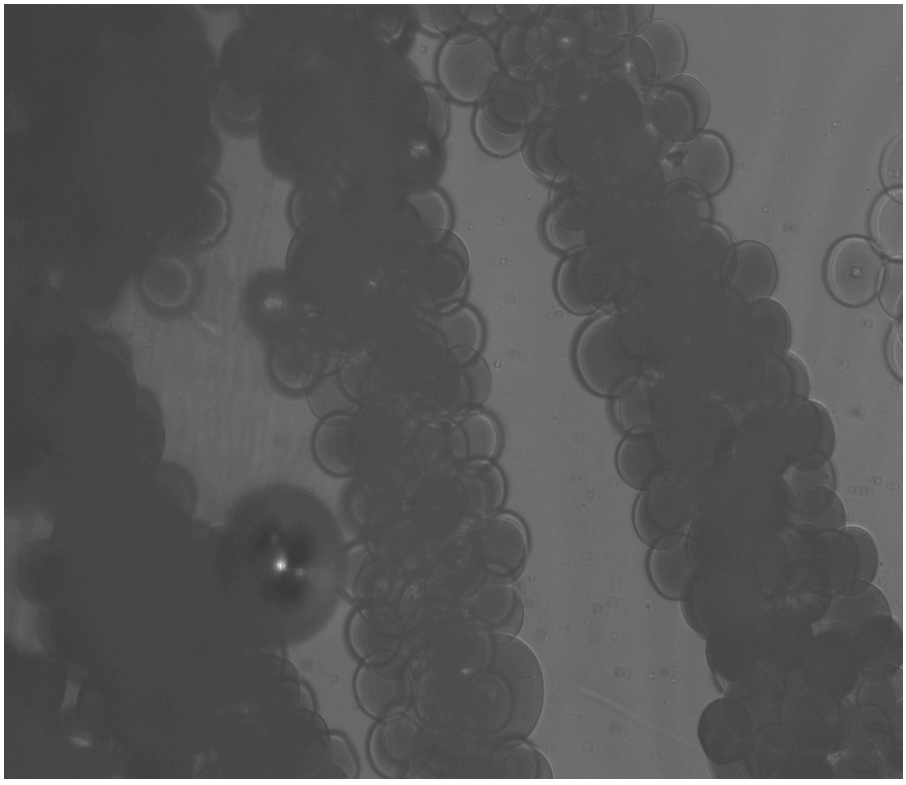

Figure 4.6a. Optical micrograph of particles made with the octylamine flow rate of 15%Q_o.

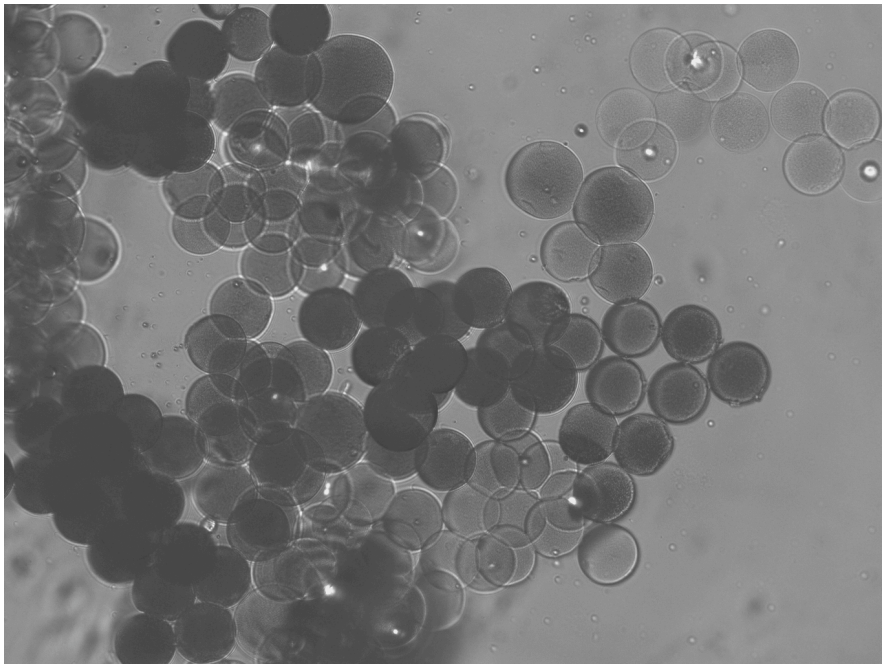

Figure 4.6b. Optical micrograph of particles made with the octylamine flow rate of 10% Q_o.

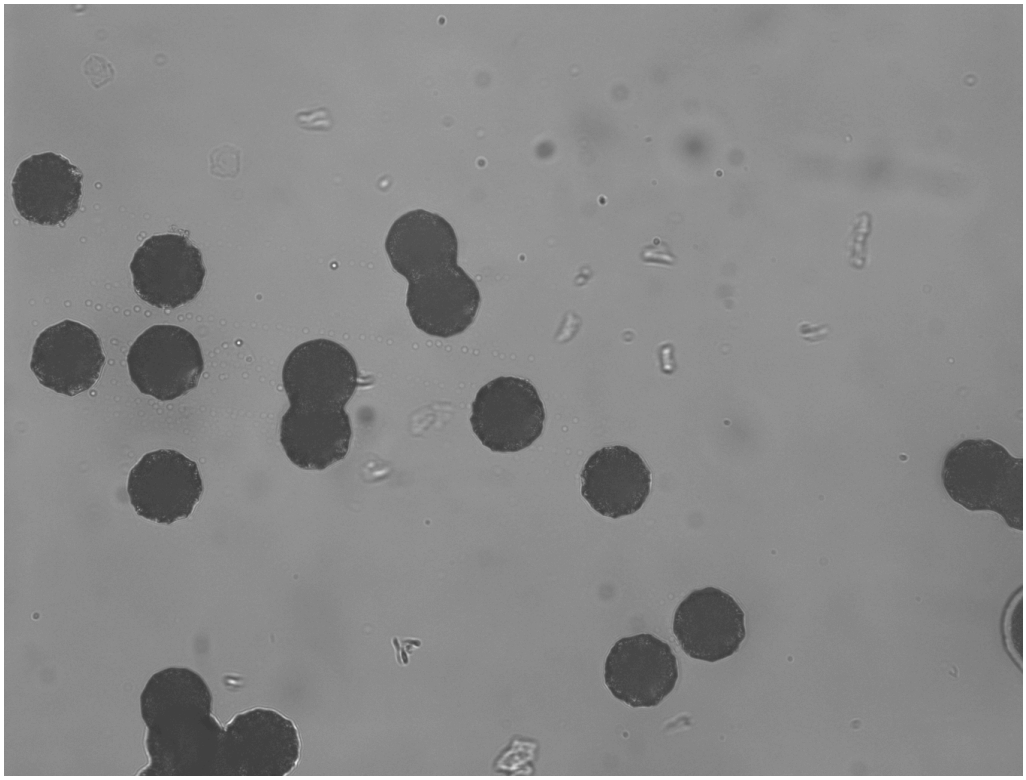

Fig 4.7a. Silica particles synthesized with an octylamine flow rate equal to 20%Qo.

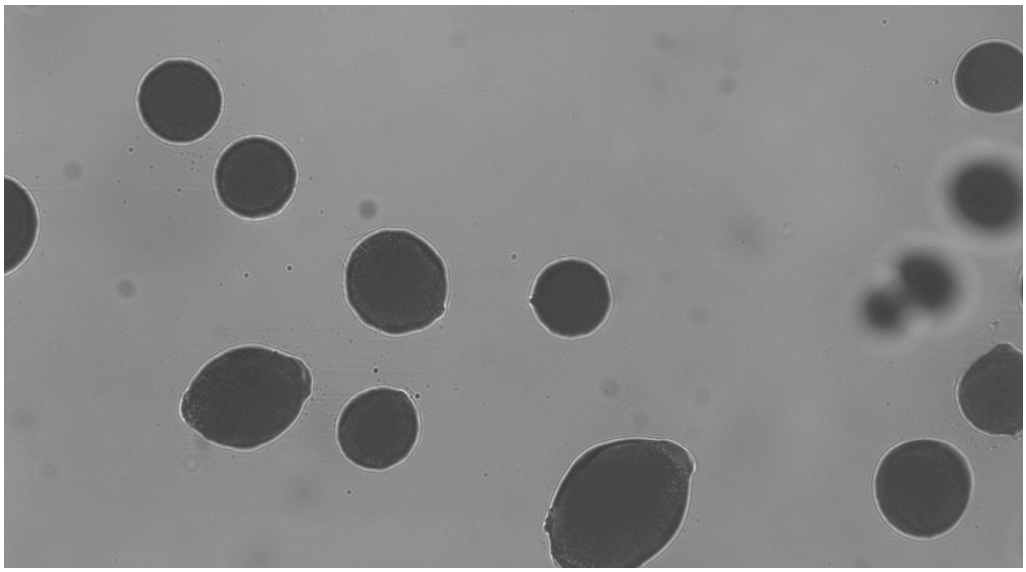

Figure 4.7b. Silica particles synthesized with an octylamine flow rate equal to 20%Qo, were dragged along bottom of MFFD.

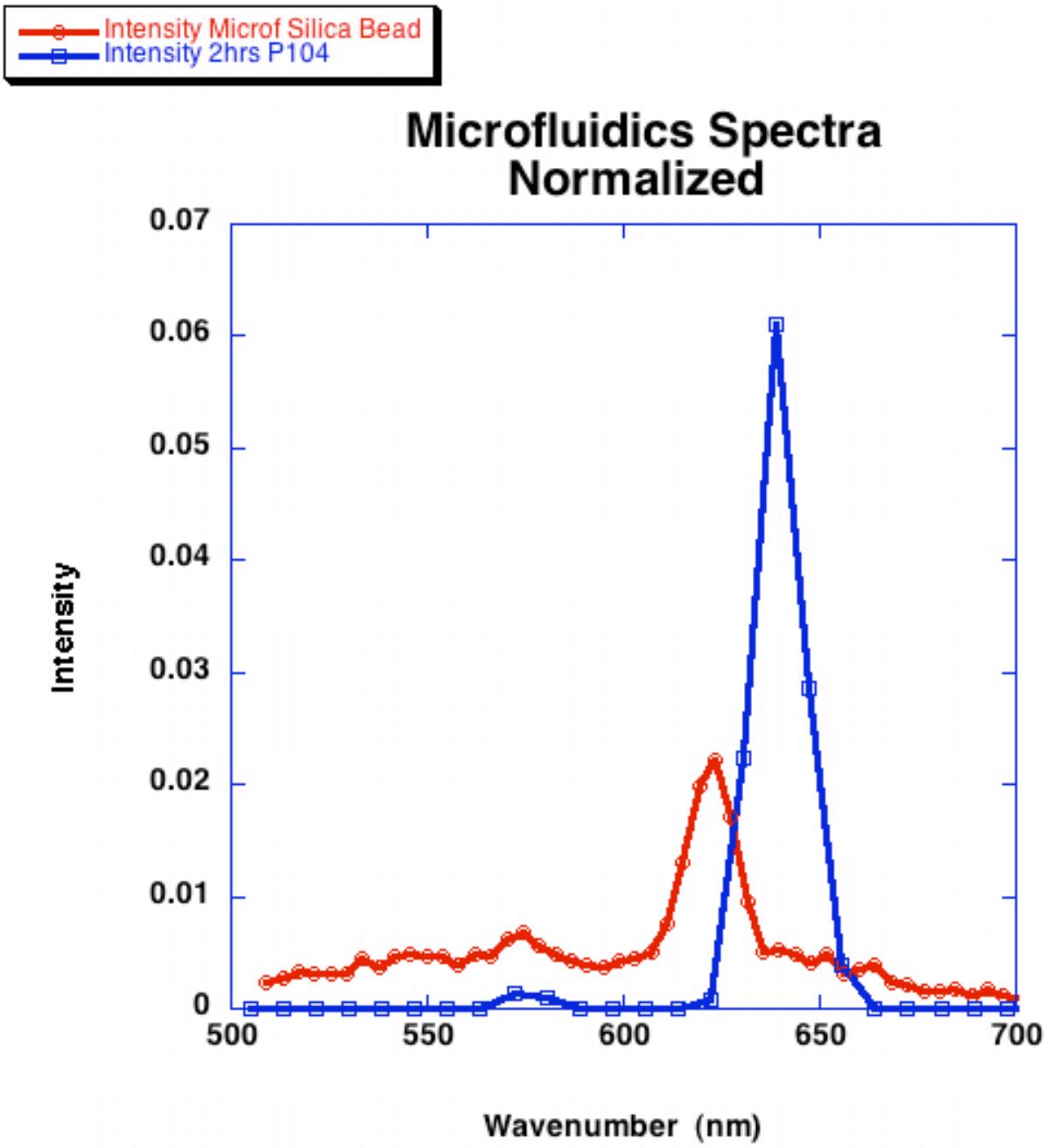

Figure 4.8. Normalized PL of both background of in 560 nm and 620 nm QDs (squares) and in silica bead (circles).

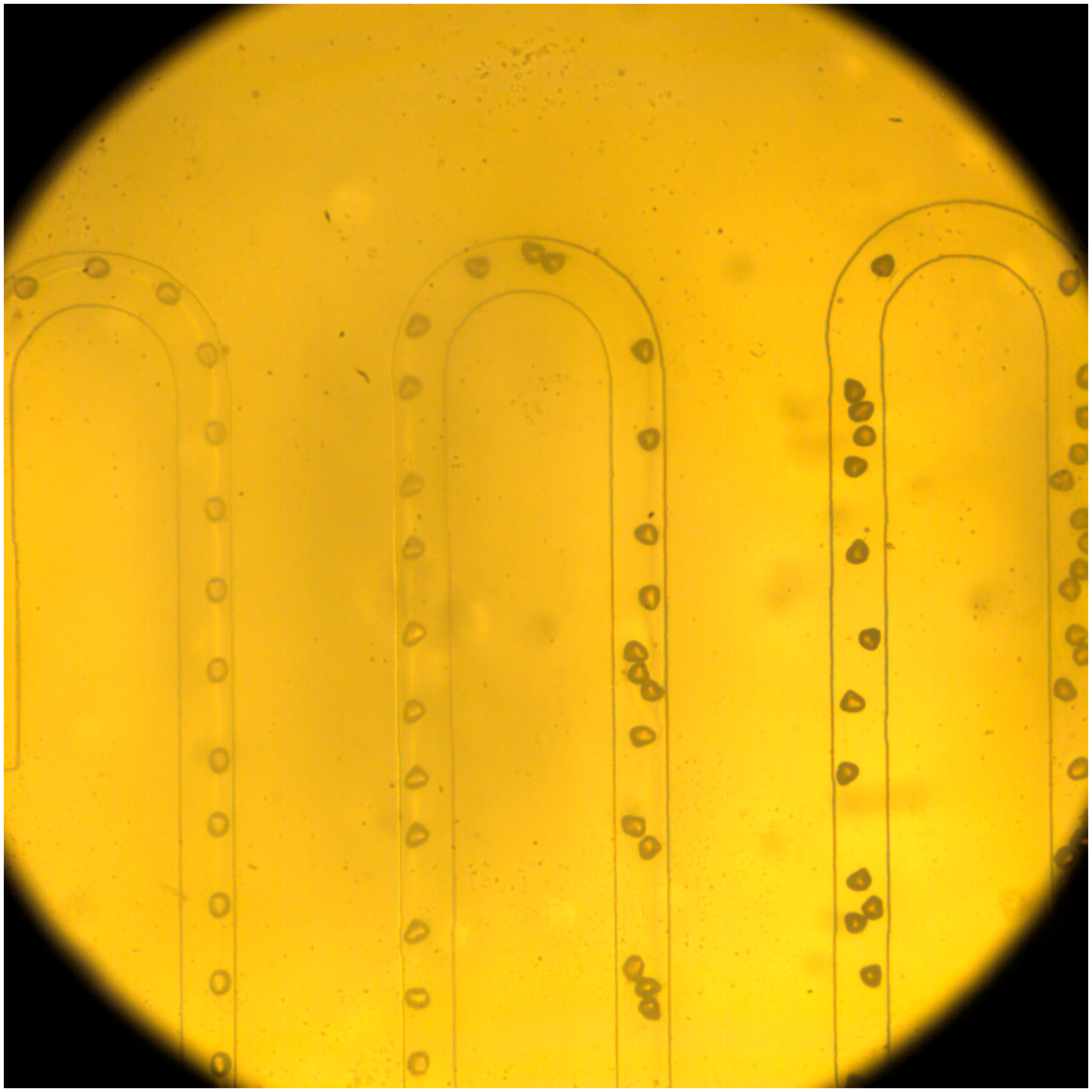

Figure 4.9. Micrograph of downstream view of particles in an asymmetric MFFD that were in direct contact with the octylamine solution. Notice at the left of the picture where the droplets are still spherical and to the right where they started to crenate.

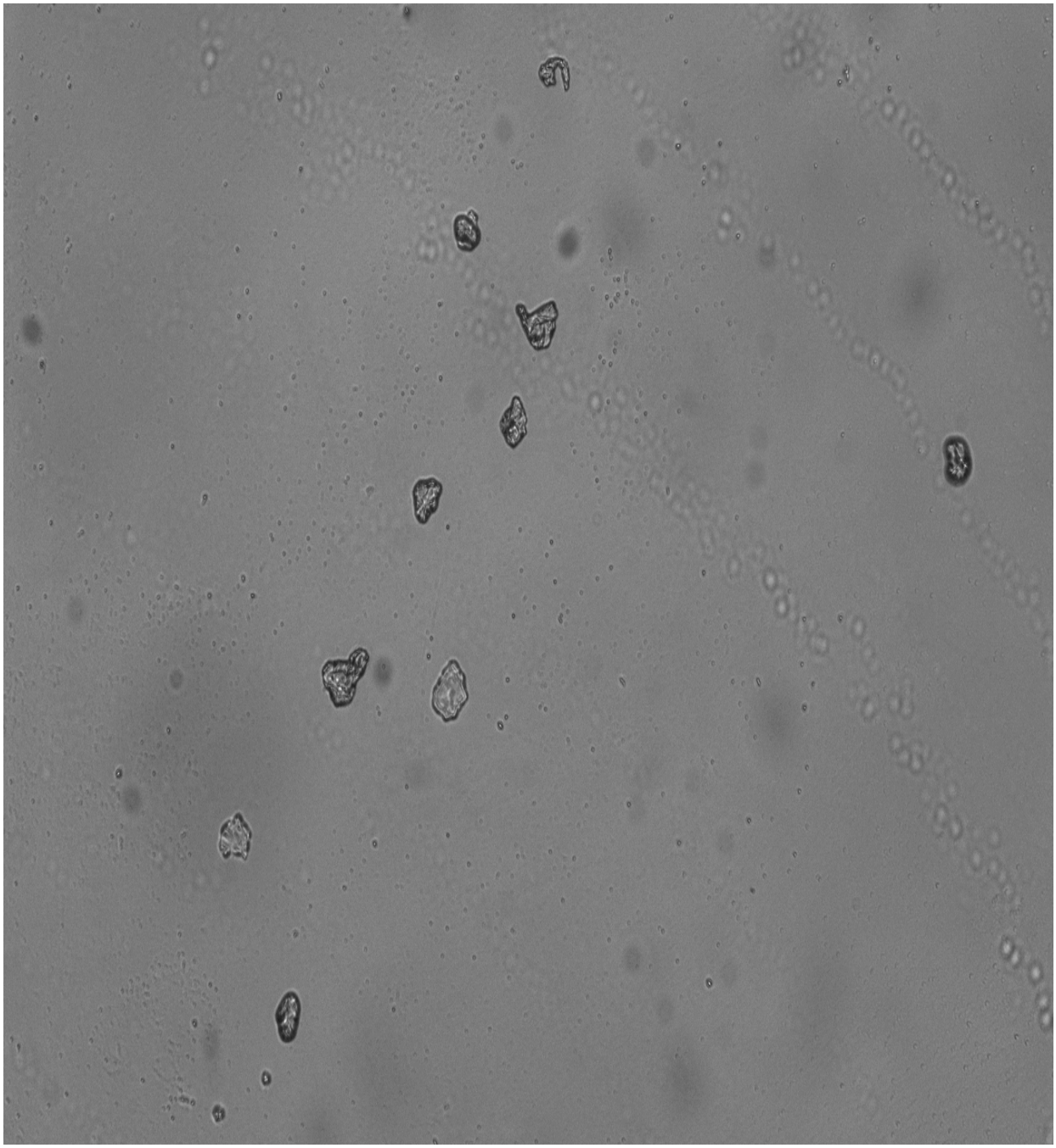

Figure 4.10. Silica particles produced with asymmetric MFFD. Notice the large extent that particles crenate when exposed to direct contact with the octylamine solution.

Solvent	Emission Wavelength	Aggregation
H2O	605	No
10% EtOH in H2O	605	No
50% EtOH in H2O	606	Slight
90% EtOH in H2O	N/A	Complete Aggregation

Table 4.1. eBioscience stability of Pegelated QDs in different contents of water and ethanol.

Bibliography

1. Anna, S. L.; Mayer, H. C., Microscale tipstreaming in a microfluidic flow focusing device. *Physics of Fluids* **2006,** 18, (12).
2. Walter, G.; Bussow, K.; Cahill, D.; Lueking, A.; Lehrach, H., Protein arrays for gene expression and molecular interaction screening. *Current Opinion in Microbiology* **2000,** 3, (3), 298-302.
3. Kodadek, T., Protein Microarrays: Prospects and Problems. *Chemistry and Biology* **2001,** 8, 105-115.
4. Lal, S.; Christopherson, R.; Remedios, C. d., Antibody Arrays: An Embryonic But Rapidly Growing Technology. *DDT* **2002,** 7, S143-S149.
5. Yeo, D.; Panicker, R.; Tan, L.; Yao, S., Strategies for Immobilization of Biomolecules in a Microarray. *Combinatorial Chemistry and High Throughput Screening* **2004,** 7, 213-221.
6. Trau, M.; Battersby, B. J., Novel Colloidal Materials for High-Throuput Screening Applications in Drug Discovery and Genomics. *Advanced Materials* **2001,** 13, 975-979.
7. Bronwyn J. Battersby, G. A. L. a. M. T., Optical encoding of microbeads or gene screening: alternatives to microarrays. *DDT* **2001,** 6, (12), S19-S26.
8. Nolan, J. P.; Sklar, L. A., Suspension array technology: evolution of the flat-array paradigm. *Trends in Biotechnology* **2002,** 20, (1), 9-12.
9. Landfester, K., Polyreactions in miniemulsions. *Macromolecular Rapid Communications* **2001,** 22, (12), 896-936.
10. Taylor, G. I., The Formation of Emulsions in Definable Fields of Flow. *Proceedings of the Royal Society of London. Series A, Containing Papers of a Mathematical and Physical Character* 1934**,** Vol. 146, (No. 858. (Oct. 1, 1934)), 501-523.
11. Katharina Landfester, N. B., Franca Tiarks, and Markus Antonietti, Miniemulsion Polymerization with Cationic and Nonionic Surfactants:
A Very Efficient Use of Surfactants for Heterophase Polymerization. *Macromolecules* 1999**,** 32, 2678-2683.
12. Paul D. T. Huibers, V. S. L., Alan R. Katritzky,; Dinesh O. Shah, a. M. K., Prediction of Critical Micelle Concentration Using a
Quantitative Structure-Property Relationship Approach.
1. Nonionic Surfactants. *Langmuir* **1996,** 12, 1462-1470.
13. Andreas Hannisdal, M.-H. E., Pal V. Hemmingsen, Johan Sjoblom, Particle-stabilized emulsions: Effect of heavy crude oil components
pre-adsorbed onto stabilizing solids. *Colloids and Surfaces A: Physicochem. Eng. Aspects* **2006,** 276 45–58.
14. Christoffer Johans, P. L. a. K. K., Electrodeposition at polarisable liquid-liquid interfaces: The role of interfacial tension on nucleation kinetics. *Physical Chemistry Chemical Physics* **2002,** 4, 1067-1071.
15. Binks, B. P.; Lumsdon, S. O., Influence of Particle Wettability on the Type and Stability
of Surfactant-Free Emulsions. *Langmuir* **2000,** 16, 8622-8631.

16. N. Bechthold, F. T., M. Willert, K. Landfester, M. Antonietti, Miniemulsion Polymerization: Applications and New Materials. *Macromol. Symp.* **2000,** 151, 549–555
17. Shah, Polymerization of Oil-in- Water Microemulsions: Polymerization of Styrene and Methyl Methacrylate. *Journal of Polymer Science: Polymer Letter Edition* **1984,** 22, 31-38.
18. Nina Andersson, B. K., Robert Corkery, and Peter Alberius, Combined Emulsion and Solvent Evaporation (ESE) Synthesis Route
to Well-Ordered Mesoporous Materials. *Langmuir* **2007,** 23, 1459-1464.
19. L. M. Gan, C. H. C., J. H. Lim, K. C. Lee, and L. H. Gan, Styrene polymerization in ternary microemulsions: effects of water-soluble and oil-soluble initiators. *Colloid & Polymer Science* **1994,** 272, 1082-1089.
20. NINHAM, D. J. M. A. B. W., Micelles, Vesicles and Microemulsions. *Journal of the Chemical Society Faraday Trans. 2* **1981,** 77, 601-629.
21. J. E. Puig, V. H. P. e.-L., M. P&ez-Gonz~lez, E. R. Macias, B. E. Rodriguez, and E. W. Kaler, Comparison of oil-soluble and water-soluble initiation of styrene polymerization in a three-component microemulsion. *Colloid & Polymer Science* **1993**, 114-123.
22. Aaron Olsen, H.-C. L., Marios Hatzopoulos, Jeroen S. van Duijneveldt, and; Vincent, B., Synthesis of Amphoteric Polystyrene Particles Using Mixed Initiators. *Langmuir* **2008,** 24, 3801-3806.
23. Sheng-Wen Zhang, S.-X. Z., Yu-Ming Weng, and Li-Min Wu, Synthesis of Silanol-Functionalized Latex Nanoparticles through Miniemulsion Copolymerization of Styrene and ç-Methacryloxypropyltrimethoxysilane. *Langmuir* **2006,** 22, 4674-4679.
24. Fumiyoshi Ikkai, S. I., Eiki Adachi, Mitsutoshi Nakajima, New method of producing mono-sized polymer gel particles using microchannel emulsification and UV irradiation. *Colloid & Polymer Science* **2005,** 283, 1149-1153.
25. Vincent, B. N. a. B., Stability of Various Silicone Oil/Water Emulsion Films as a Function of Surfactant and Salt Concentration. *Langmuir* **1994,** 10, 2493-2494.
26. Peter J. Dowding, B. V., Suspension polymerisation to form polymer beads. *Colloids and Surfaces A: Physiochem. Eng. Aspects* **2000,** 161, 259-269.
27. H.N. Singh, C. D. P. a. S. K., Water Solubilization in Microemulsions Containing Amines
as Cosurfactant. *Journal of American Oil Chemsit's Society* **1973,** 1, 69-73.
28. Chengzhong Yu, B. T., Jie Fan, Galen D. Stucky, and Dongyuan Zhao, Synthesis of Siliceous Hollow Spheres with Ultra Large Mesopore Wall Structures by
Reverse Emulsion Templating. *Chemistry Letters* **2002**, 62-63.
29. Alivisatos, P., The Use of Nanocrystals in Biological Detection. *Nature Biotechnolgy* **2004,** 22, 47.
30. Battersby, B. J.; Bryant, D.; Meutermans, W.; Matthews, D.; Smythe, M. L.; Trau, M., Toward Larger Chemical Libraries: Encoding with Fluorescent Colloids in Combinatorial Chemistry. *Journal of the American Chemical Society* **2000,** 122, (9), 2138-2139.
31. Fournier-Bidoz, S.; Jennings, T. L.; Klostranec, J. M.; Fung, W.; Rhee, A.; Li, D.; Chan, W. C. W., Facile and rapid one-step mass preparation of quantum-dot barcodes. *Angewandte Chemie-International Edition* **2008,** 47, (30), 5577-5581.

32. Gao, X.; Nie, S., Doping Mesoporous Materials with Multicolor Quantum Dots. *Journal of Physical Chemistry B* **2003,** 107, 11575-11578.
33. Ishii, S.; Ueji, R.; Nakanishi, S.; Yoshida, Y.; Nagata, H.; Itoh, T.; Ishikawa, M.; Biju, V., Fabrication of a quantum dot-polymer matrix by layer-by-layer conjugation. *Journal of Photochemistry and Photobiology a-Chemistry* **2006,** 183, (3), 285-291.
34. Joumaa, N.; Lansalot, M.; Theretz, A.; Elaissari, A.; Sukhanova, A.; Artemyev, M.; Nabiev, I.; Cohen, J. H. M., Synthesis of Quantum Dot-Tagged Submicrometer Polystyrene Particles by Miniemulsion Polymerization. *Langmuir* **2006,** 22, (4), 1810-1816.
35. Juan Li, X.-W. Z., Yuan-Jin Zhaoa and Zhong-Ze Gu, Quantum-dot-coated encoded silica colloidal crystals beads for multiplex coding. *Chemical Communication* **2009**, 2329-2331.
36. Nie, X. G. a. S., Qauntum Dot-Encoded Beads. In *Methods in Molecular Biology*, Wright, J. R. a. D. W., Ed. Humana Press Inc. : Totowa Vol. 303, pp 61-71.
37. Nie, X. G. a. S., Doping Mesoporous Materials with Multicolor Quantum Dots. *Journal of Physical Chemistry B* **2003,** 107, 11575-11578.
38. Nie, X. G. a. S., Quantum Dot-Encoded Mesoporous Beads with High Brightness and Uniformity: Rapid Readout Using Flow Cytometry. *Analytical Chemistry* **2004,** 76, 2406-2410.
39. Vaidya, S. V.; Gilchrist, M. L.; Maldarelli, C.; Couzis, A., Spectral bar coding of polystyrene microbeads using multicolored quantum dots. *Analytical Chemistry* **2007,** 79, 8520-8530.
40. Yuan-Cheng Cao, Z.-L. H., Tian-Cai Liu, Hai-Qiao Wang, Xiao-Xia Zhu,; Zhan Wang, Y.-D. Z., Man-Xi Liu, Qing-Ming Luo, Preparation of silica encapsulated quantum dot encoded beads for multiplex assay and its properties. *Analytical Biochemistry* **2006,** 351, 193-200.
41. Jonathan S. Owen, J. P., Paul-Emile Trudeau, and A. Paul Alivisatos, Reaction Chemistry and Ligand Exchange at Cadmium-Selenide Nanocrystal Surfaces. *Journal of the American Chemical Society* **2008,** 130, 12279-12281.
42. Hao Zhang, D. W., and Helmuth Mohwald, Ligand-Selective Aqueous Synthesis of One-Dimensional CdTe Nanostructures. *Angew. Chem. Int. Ed.* **2006,** 45, 748-751.
43. Guodong Sui, J. O., Xiaojun Ji, Kerim M. Gattás-Asfura,; Roger M. Leblanc, a. M. M., Surface Chemistry Studies of Quantum Dots (QDs) Modified with Surfactants. *Journal of Cluster Science* **2003,** 14, (2), 123-133.
44. Guodong Sui, J. O., Xiaojun Ji, Kerim M. Gattás-Asfura,; Roger M. Leblanc, a. M. M., Surface Chemistry Studies of Quantum Dots (QDs) Modified with Surfactants. *Journal of Cluster Science* **2003,** 14, (2), 123-133.
45. Thomas Pons, H. T. U., Igor L. Medintz, and Hedi Mattoussi, Hydrodynamic Dimensions, Electrophoretic Mobility, and Stability of Hydrophilic Quantum Dots. *Journal of Physical Chemistry B* **2006,** 110, 20308-20316.
46. David B. Robinson, J. L. R., Christina A. Bauer and Blake A. Simmons, Dependence of amine-accelerated silicate condensation on amine structure. *Journal of Materials Chemistry* **2007,** 17, 2113-2119.
47. K. Kosuge, P. S. S., Mesoporous silica spheres via 1-alkylamine templating soute. M*icroporous and Mesoporous Materials 2***001,** 44-45, 139-145.

48. Katya M. Delak, a. N. S., Amine-Catalyzed Biomimetic Hydrolysis and Condensation of Organosilicate. C*hemistry of Materials 2***005,** 17, 3221-3227.
49. Antonelli, D. M., Synthesis of phosphorus-free mesoporous titania via templating with amine surfactants. M*icroporous and Mesoporous Materials 1***999,** 30, 315-319.
50. Thorsen, T. Microfluidic Technologies for High-Throughput Screening Applications. California Institute of Technology, Pasadena 2003.
51. Grondahl, L.; Battersby, B. J.; Bryant, D.; Trau, M., Encoding Combinatorial Libraries: A Novel Application of Fluorescent Silica Colloids. L*angmuir 2***000,** 16, (25), 9709-9715.
52. Tushar R. Sathe, A. A., and Shuming Nie, Mesoporous Silica Beads Embedded with Semiconductor Quantum Dots and Iron Oxide Nanocrystals: Dual-Function Microcarriers for Optical Encoding and Magnetic Separation. A*nalytical Chemistry 2***006,** 78, 5627-5632.
53. Bawendi, M., Incorporation of Luminescent Nanocrystals into monodisperse Core-Shell Silica Microspheres. A*dvanced Materials 2***004,** 16, (23-24).
54. Daniele Gerion, F. P., Shara C. Williams, Wolfgang J. Parak,; Daniela Zanchet, S. W., and A. Paul Alivisatos, Synthesis and Properties of Biocompatible Water-Soluble Silica-Coated CdSe/ZnS Semiconductor Quantum Dots. J*ournal of Physical Chemistry B 2***001,** 105, 8861-8871.
55. Deniz, A. A.; Laurence, T. A.; Dahan, M.; Chemla, D. S.; Schultz, P. G.; Weiss, S., Ratiometric Single-Molecule Studies of Freely Diffusing Biomolecules. A*nnual Review of Physical Chemistry 2***001,** 52, (1), 233.
56. Brus, L., Electronic Wave Functions in Semiconductor Clusters: Experiment and Theory. J*ournal of Physical Chemsitry 1***986,** 90, 2555-560.
57. Herron, Y. W. a. N., Nanometer-Sized Semiconductor Clusters: Materials Synthesis, Quantum Size Effects, and Photophysical Properties. J*ournal of Physical Chemistry 1***991,** 95, 525-532.
58. Kortan, A. R. R. H., R. L.Opila, M. G.; Bawendi, M. L.; Steigerwald, P. J. Carroll, Louis E. Brus, Nucleation and growth of cadmium selendie on zinc sulfide quantum crystallite seeds, and vice versa, in inverse micelle media. J*ournal of the American Chemical Society 1***990,** 112, (4), 1327-1332.
59. R. Rosetti, L. E. B., Electron-hole recombination emission as a prove of surface chemistry in a aqueous CdS colloids. J*ournal of the American Chemical Society 1***982,** 86, 4470-4472.
60. B. O. Dabbousi, J. R.-V., F. V. Mikulec, J. R. Heine, H. Mattoussi, R. Ober,; K. F. Jensen, a. M. G. B., (CdSe)ZnS Core-Shell Quantum Dots: Synthesis and Characterization of a Size Series of Highly Luminescent Nanocrystallites. J*ournal of Physical Chemistry B 1***997,** 101, 9463-9475.
61. Sungjee Kim, B. F., Hans-Ju¨rgen Eisler, and Moungi Bawendi, Type-II Quantum Dots: CdTe/CdSe(Core/Shell) and CdSe/ZnTe(Core/Shell) Heterostructures. J*ournal of the American Chemical Society 2***003,** 125, 11466-11467.
62. Schmid, G., N*anoparticles : From theory to application.* Wiley-VCH Verlag GmbH & Co. KGaA: Weinheim, 2004.

63. Zhihong Nie, J. I. P., † Wei Li,† Stefan A. F. Bon,‡ and Eugenia Kumacheva, An "Inside-Out" Microfluidic Approach to Monodisperse Emulsions Stabilized by Solid Particles. J*ournal of the American Chemical Society 2***008,** 130, 16508-16509.
64. Mulvaney, T. N. a. P., Single Quantum Dots in Spherical Silica Particles. A*ngew. Chem. Int. Ed. 2***004,** 43, 5393-5396.
65. Cosgrove, T.; Roberts, C.; Choi, Y.; Schmidt, R. G.; Gordon, G. V.; Goodwin, A. J.; Kretschmer, A., Relaxation studies of high molecular weight poly(dimethylsiloxane)s blended with polysilicate nanoparticles. L*angmuir 2***002,** 18, (26), 10075-10079.
66. Cosgrove, T.; Roberts, C.; Garasanin, T.; Schmidt, R. G.; Gordon, G. V., NMR spin-spin relaxation studies of silicate-filled low molecular weight poly(dimethylsiloxane)s. L*angmuir 2***002,** 18, (26), 10080-10085.
67. Carles Curutchet, A. F., Alex Zunger, and Gregory D. Scholes, Examining Forster Energy Transfer for Semiconductor Nanocrystalline Quantum Dot Donors and Acceptors. T*he Journal of Physical Chemistry C 2***008,** 112, 13336-133341.
68. Roi Baer; Rabani, a. E., Theory of resonance energy transfer involving nanocrystals: The role of high multipoles
. T*HE JOURNAL OF CHEMICAL PHYSICS 2***008,** (128), 184710.
69. Tan, L. W. a. W., Multicolor FRET Silica Nanoparticles by Single Wavelength Excitation
. N*ano Letters 2***006,** 6, (1), 84-88.
70. Yang, X.; Zhong, Y., Encapsulation of Quantum Nanodots in Polystyrene and Silica Micro-Nanoparticles. L*angmuir 2***004,** 20, 6071-6073.
71. Graf, C.; Dembski, S.; Hofmann, A.; Ruhl, E., A General Method for the Controlled Embedding of Nanoparticles in Silica Colloids. L*angmuir 2***006,** 22, (13), 5604-5610.
72. Manoranjan Pattanaik, S. K. B., Adsorption behaviour of polyvinyl pyrrolidone on oxide surfaces. M*aterials Letters 2***000,** 44, 352-360.
73. Caruso, F., Nanoengineering of Particle Surfaces. A*dvanced Materials 2***001,** 13, 11.
74. Yang, W. T., D.; Renneberg, R.; Yu, N.T.; Caruso, F.; , Layer by Layer Construction of Noverl Biofunctional Fluorescent Microparticles for Immunoassay Applications. J*ournal of Colloid and Interface Science 2***001,** 234, 356.
75. Michael I. Goller, T. M. O., Declan O.H. Teare, Brian Vincent, Inorganic "silicone oil" microgels. C*olloids and Surfaces A: Physiochem. Eng. Aspects 1***997,** (123-124), 183-193.
76. Koole, R., Matti M. van Schooneveld, Jan Hilhorst, Celso de Mello Donegá,; Dannis C. Hart, A. v. B., Daniel Vanmaekelbergh, and; Meijerink, A., On the Incorporation Mechanism of Hydrophobic Quantum Dots in Silica Spheres by a Reverse Microemulsion Method. C*hemistry of Materials 2***008,** 20, 2503-2512.
77. Anna, S. L.; Bontoux, N.; Stone, H. A., Formation of dispersions using "flow focusing" in microchannels. A*pplied Physics Letters 2***003,** 82, (3), 364-366.
78. Shengqing Xu, Z. N., Minseok Seo, Patrick Lewis, Eugenia Kumacheva, Howard A. Stone,; Piotr Garstecki, D. B. W., Irina Gitlin, and George M. Whitesides, Generation of Monodisperse Particles by Using Microfluidics: Control over Size, Shape, and Composition. A*ngew. Chem. Int. Ed. 2***005,** 44, 724-728.

79. Zhihong Nie, S. X., Minseok Seo, Patrick C. Lewis, and; Kumacheva*, E., Polymer Particles with Various Shapes and Morphologies
Produced in Continuous Microfluidic Reactors. J*ournal of the American Chemical Society 2***005,** 127, 8058-8063.
80. Wei Li, Z. N., Hong Zhang, Chantal Paquet, Minseok Seo, Piotr Garstecki, and Eugenia Kumacheva, Screening of the Effect of Surface Energy of Microchannels on Microfluidic Emulsification. L*angmuir 2***007,** 23, (15), 8010-8014.
81. Hong Zhang, E. T., Raheem Peerani, Zhihong Nie,; Ruby May A. Sullan, G. C. W., and Eugenia Kumacheva, Microfluidic Production of Biopolymer
Microcapsules with Controlled Morphology. J*ournal of the American Chemical Society 2***008,** 128, (37), 12205-12210.
82. Wei Li, H. H. P., Zhihong Nie, Brendan MacDonald, Axel Guenther, and Eugenia Kumacheva, Multi-Step Microfluidic Polymerization Reactions
Conducted in Droplets: The Internal Trigger Approach. J*ournal of the American Chemical Society 2***009,** 130, (30), 9935-9941.
83. Minseok Seo, Z. N., Shengqing Xu, Michelle Mok, Patrick C. Lewis, Robert Graham, and Eugenia Kumacheva, Continuous Microfluidic Reactors for Polymer Particles. L*angmuir 2***005,** 21, 11614-11622.
84. Patrick C. Lewis, R. R. G., Zhihong Nie, Shengqing Xu, Minseok Seo, and Eugenia Kumacheva, Continuous Synthesis of Copolymer Particles in Microfluidic Reactors. M*acromolecules 2***005,** 38, (10), 4536-4538.
85. Zhihong Nie, W. L., Minseok Seo, Shengqing Xu, and Eugenia Kumacheva, Janus and Ternary Particles Generated by Microfluidic
Synthesis: Design, Synthesis, and Self-Assembly. J*ournal of the American Chemical Society 2***006,** 128, (29), 9408-9412.
86. Stanislav Dubinsky, H. Z., Zhihong Nie, Ilya Gourevich,; Dan Voicu, M. D., and Eugenia Kumacheva, Microfluidic Synthesis of Macroporous Copolymer Particles. M*acromolecules 2***008,** 41, (10), 3555-3561.
87. Carroll, N. J. R., S. B.; Derbins, E.; Mendez, S.; Weitz, D. A.; Petsev, D. N., Droplet-Based Microfluidics for Emulsion and Solvent Evaporation Synthesis of Monodisperse Mesoporous silica Microspheres. L*angmuir 2***008,** 24, 658-661.
88. Lee, I. Y. Y., Z. Cheng, H.-K. Jeong,, Generation of Monodisperse Mesoporous Silica Microspheres with Controllable Size and Surface Morphology in a Microfluidic Device. *Advanced Functional Materials 2***008,** 18, 4014-4021.
89. Iler, R. K., T*he Chemistry of Silica.* John Wiley and Sons: New York, 1979.
90. Brinker, C. J.; Scherer, G. W., S*ol-Gel Science The Physics and Chemistry of Sol-Gel Processing.* Academic Press Inc.: San Diego, 1990; p 908.
91. Daniel Mark, S. H., Roland Zengerle, Jens Ducree, Goran T. Vladisavljevi, Manufacture of chitosan microbeads using centrifugally driven flow
of gel-forming solutions through a polymeric micronozzle. J*ournal of Colloid and Interface Science 2***009,** 336, 634-641.
92. BERNARDS, A. H. B. a. T. N. M., THE DEPENDENCE OF THE GELATION TIME ON THE HYDROLYSIS TIME
IN A TWO-STEP SiO 2 SOL-GEL PROCESS. J*ournal of Non-Crystalline Solids 1***988,** 105, 207-213.

93. T.N.M. Bernards, M. J. v. B. a. A. H. B., Hydrolysis-condensation processes of the tetra-alkoxysilanes
TPOS, TEOS and TMOS in some alcoholic solvents. J*ournal of Non-Crystalline Solids 1***991,** 134, 1-13.
94. Mackenzie, E. J. A. P. a. J. D., SOL-GEL PROCESSING OF SILICA
II. The role of the catlyst. J*ournal of Non-Crystalline Solids 1***986,** 87, 185-198.
95. C.J. BRINKER, K. D. K., D.W. SCHAEFER and C.S. ASHLEY, SOL-GEL TRANSITION IN SIMPLE SILICATES J*ournal of Non-Crystalline Solids 1***982,** 48, 47-64.
96. I. Artaki, T. W. Z. a. J. J., Solvent Effects on the condensation stage of the sol-gel process. J*ournal of Non-Crystalline Solids 1***986,** 81, 381-395.
97. M.J. van Bommel, T. N. M. B., E.W.J.L. Oomen and A.H. Boonstra, The influence of cross-linking on gel formation. J*ournal of Non-Crystalline Solids 1***992,** 147-148, 80-84.
98. Shiquan Liu, J. R., Xueye Sui, Pegie Cool, Etienne F. Vansant,; Gustaaf Van Tendeloo, X. C., Preparation of hollow silica spheres with different mesostructures. J*ournal of Non-Crystalline Solids 2***008,** 354, 826-830.
99. Gao, X. S. a. L., Synthesis, Characterization, and Optical Properties of Well-Defined
N-Doped, Hollow Silica/Titania Hybrid Microspheres. L*angmuir 2***007,** 23, 11850-11856.
100. Xin Cheng a, S. L. a., b,*, Lingchao Lu a, Xueye Sui a, Vera Meynen b,; Pegie Cool b, E. F. V. b., Jianzhuang Jiang, Fast fabrication of hollow silica spheres with thermally stable nanoporous shells. M*icroporous and Mesoporous Materials 2***007,** 98, 41-46.
101. Qisheng Huo, J. F., Ferdi Schuthand ; Stucky, G. D., Preparation of Hard Mesoporous Silica
Spheres. C*hemistry of Materials 1***997,** 9, 14-17.
102. Mizutani, T., Nagase, H., Fujiwara, N. & Ogoshi, H. , Silicic acid polymerization catalyzed by amines and polyamines. . *Bull. Chem. Soc. Jpn 1***998,** 71, 2017–2022
103. Angren, P. L., M.; Rosenholm, J.B., Kinetics of Cosurfactant-Surfactant-Silicate Phase Behavior. 2. Short-Chain Amines. L*angmuir 2***000,** 16, 8809-8813.
104. Abey Issac and Christian von Borczyskowski, F. C., Correlation between photoluminescence intermittency of CdSe quantum dots
and self-trapped states in dielectric media. P*HYSICAL REVIEW B 2***005,** 71, 161302.
105. Brinker, C. J., Lu, Y., Sellinger, A., H. Fan, Evaporation-Induced Self-Assembly: Nanostructures Made Easy. A*dvanced Materials 1***999,** 11, (7), 579-585.
106. Kresge, C.; Leonowicz, M.; W, R.; Vartuli, C.; Bec, J., N*ature 1***992,** 359, 710.
107. Andersson, N. B. K., Robert Corkery, and Peter Alberius, Combined Emulsion and Solvent Evaporation (ESE) Synthesis Route to Well-Ordered Mesoporous Materials . L*angmuir* **2007,** 23 (3), 1459-1464.
108. Yague, C. M. M., Valeria Grazu, Manuel Arruebo, Jesus Santamarıa, Synthesis and stealthing study of bare and PEGylated silica micro- and
nanoparticles as potential drug-delivery vectors. C*hemical Engineering Journal 2***008,** 137 45–53.

109. McDonald, J. C.; Duffy, D. C.; Anderson, J. R.; Chiu, D. T.; Wu, H. K.; Schueller, O. J. A.; Whitesides, G. M., Fabrication of microfluidic systems in poly(dimethylsiloxane). E*lectrophoresis 2***000,** 21, (1), 27-40.
110. McDonald, J. C.; Whitesides, G. M., Poly(dimethylsiloxane) as a material for fabricating microfluidic devices. A*ccounts of Chemical Research 2***002,** 35, (7), 491-499.
111. Deen, W. D., A*nalysis of Transport Phenomena.* Oxford Unversity Press New York, 1998.
112. Garstecki, P. S., H.A. and George M. Whitesides, Mechanism for Flow-Rate Controlled Breakup in Confined Geometries: A Route to Monodisperse Emulsions. P*hysical Review Letters 2***005,** 94, (164501).
113. Zhou, C. Y., P.; Feng, J.J., Formation of simple and compound drops in microfluidic devices. P*hysics of Fluids 2***006,** 18, 092105-1-18.
114. De Menech, M. G., P.; JOUSSE, F.; STONE, A. H. A., Transition from squeezing to dripping in a microfluidic T-shaped junction
. J*ournal of Fluid Mechanics 2***008,** 595, 141–161.
115. Wingki Lee, L. M. W., and Shelley L. Anna, Role of geometry and fluid properties in droplet and thread formation processes in planar flow focusing. P*hysics of Fluids 2***009,** 21, 032103-1-032103-14.
116. STONE, H. A. a. L., L.G., relaxation and breakup of an initially extended drop in an otherwise quiescent fluid. J*ournal of Fluid Mechanics 1***989,** 198, 399.
117. Hansen, S. P., G.W.; Meijer, H.E.H, The effect of surfactant on the stability of a fluid filament embedded in a viscous fluid. j*ournal of fluid mechanics 1***999,** 382, 331-349.
118. Dreyfus, R. P. T., and HerveWillaime, Ordered and Disordered Patterns in Two-Phase Flows in Microchannels. P*HYSICAL REVIEW LETTERS 2***003,** 90, (14), 144505-1-4.